

# **Settlement Analysis of Reinforced Granular Beds near Bridge Abutments**

M.Rajashekhar

A Dissertation Submitted to  
Indian Institute of Technology Hyderabad  
In Partial Fulfillment of the Requirements for  
The Degree of Master of Technology



भारतीय प्रौद्योगिकी संस्थान हैदराबाद  
Indian Institute of Technology Hyderabad

Department of Civil Engineering

December, 2015

## Declaration

I declare that this written submission represents my ideas in my own words, and where others ideas or words have been included, I have adequately cited and referenced the original sources. I also declare that I have adhered to all principles of academic honesty and integrity and have not misrepresented or fabricated or falsified any idea/data/fact/source in my submission. I understand that any violation of the above will be a cause for disciplinary action by the Institute and can also evoke penal action from the sources that have thus not been properly cited, or from whom proper permission has not been taken when needed.

*M. Rajashekhar*

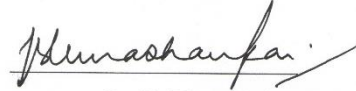
(Signature)

M.Rajashekhar

CE13M0001

## Approval Sheet

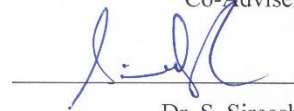
This thesis entitled "Settlement Analysis of Reinforced Granular Beds near Bridge Abutments" by M.Rajashekhar is approved for the degree of Master of Technology from IIT Hyderabad.



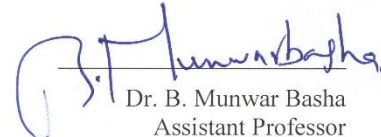
Dr. B. Umashankar  
Assistant Professor and Head  
Department of Civil Engineering  
Indian Institute of Technology Hyderabad  
Advisor

---

Prof. M. R. Madhav  
Visiting Professor  
Department of Civil Engineering  
Indian Institute of Technology Hyderabad  
Co-Advisor



Dr. S. Sireesh  
Associate Professor  
Department of Civil Engineering  
Indian Institute of Technology Hyderabad  
Examiner



Dr. B. Munwar Basha  
Assistant Professor  
Department of Civil Engineering  
Indian Institute of Technology Hyderabad  
Examiner



Dr. Raja Banerjee  
Associate Professor and Head  
Department of Mechanical & Aerospace Engineering  
Indian Institute of Technology Hyderabad  
Examiner

## **Acknowledgements**

My sincere gratitude to my advisor Dr. B. Umashankar and co-advisor Prof. M. R. Madhav for their continuous support, help and motivation. I would like to thank all the faculty members of Civil Engineering Department.

I am very grateful to all my family members for their valuable support in my entire life.

My heartfelt thanks to my friends Preethi Sekar, Hari Prasad, Sasanka Mouli, Raviteja, Sahith, Saranya, Aranya, Chandu, and my juniors and my classmates Thejesh, Sahithi, Troy and for being supportive all through the days. A deepest thanks to my friends Jyothi, Prashanth, Rajini, Shiva, Teja who supported me personally and motivated towards my goal.

Last but not the least, thanks to the lab assistants Suresh, Ravi, Vajra Simha Reddy for their help during my experimental work.



Dedicated to  
**My Family and Teachers**

## **Abstract**

An approach slab is constructed to provide a smooth transition between the bridge deck and the existing roadway pavement. The differential settlement between the bridge deck and the approach slab leads to the formation of a “Bump” at the end of the bridge. This is mainly due to difference support systems for the bridge deck and the slab. A detailed literature review had been done on the causes and the mitigation techniques available.

In the present study experimental investigations had been done using a large scale testing. Influence of various parameters effecting the differential settlement at bridge approach slab was studied. Parameters such as optimum thickness of granular sub-base layer, length of reinforcement, initial depth of reinforcement, and edge distance of wheel load from an edge of abutment were analyzed in the present study. Optimum values for above parameters had been proposed.

Numerical modelling studied was conducted using finite difference program FLAC3D. This study aims in analyzing two layered soil system with unreinforced and reinforced conditions. Parametric studies on thickness of top layer, stiffness of reinforcement, stiffness of two soil layers, initial depth of reinforcement and spacing between reinforcement layers over the load carrying capacity of circular footing was analyzed in the present study.

# Contents

|  |    |
|--|----|
| 1. Introduction .....  | 10 |
| 1.1 Overview.....  | 10 |
| 1.1.1 Differential settlement (bump) between bridge approaches and bridge deck ..... | 10 |
| 1.1.2 Bump Tolerance.....  | 12 |
| 1.2 Objective of the study .....   | 12 |
| 1.3 Organization of thesis .....   | 13 |
| 2. Causes and Mitigation techniques for Bump .....                                   | 14 |
| 2.1 Mechanisms Causing the Bump .....  | 14 |
| 2.1.1 Consolidation settlement of foundation soil .....                              | 15 |
| 2.1.1.1 Initial Consolidation .....  | 15 |
| 2.1.1.2 Primary Consolidation .....  | 16 |
| 2.1.1.3 Secondary Consolidation .....  | 16 |
| 2.1.2 Poor Compaction and Consolidation of Backfill Material .....                   | 16 |
| 2.1.3 Poor Drainage and Soil Erosion.....  | 16 |
| 2.1.4 Traffic Volume .....   | 18 |
| 2.1.5 Age of the Approach Slab.....  | 18 |
| 2.1.6 Approach Slab Design .....   | 18 |
| 2.1.7 Skewness of the Bridge.....  | 19 |
| 2.1.8 Seasonal Temperature Variations .....  | 20 |
| 2.2 Mitigation Techniques to Alleviate Bump.....                                     | 21 |
| 2.2.1 Improvement of Foundation Soil.....  | 21 |
| 2.2.1.1 Vertical Drains .....  | 21 |
| 2.2.1.2 Stone Columns.....   | 21 |
| 2.2.1.3 Deep Soil Mixing Columns .....   | 23 |
| 2.2.1.4 Compaction Piles .....   | 24 |
| 2.2.2 Improvement of approach embankment/backfill material .....                     | 25 |
| 2.2.2.1 Use of Geosynthetic Reinforcement in backfill/foundation soil .....          | 25 |
| Effect of Shear Reduction.....   | 25 |
| Confinement Effect.....  | 26 |
| Membrane Effect .....  | 27 |
| Anchorage Effect .....   | 27 |
| 2.2.2.2 Mechanically Stabilized Earth (MSE) Wall .....                               | 28 |

|   |    |
|---|----|
| 2.2.2.3 Geosynthetic Reinforced Soils (GRS) .....                                   | 29 |
| 2.3 Geosynthetic Reinforced Granular Fills .....                                    | 32 |
| 2.3.1 Numerical studies on Reinforced Granular Fills .....                          | 32 |
| 2.3.2 Experimental or Prototype Studies on Reinforced Granular Fills .....          | 34 |
| 3. Experimental Investigation .....   | 38 |
| 3.1 Laboratory Testing Setup.....   | 38 |
| 3.1.1 Reaction frame .....  | 38 |
| 3.1.2 Loading system .....  | 39 |
| 3.1.3 Soil chamber .....  | 39 |
| 3.1.4 Compactor.....  | 40 |
| 3.2 Instrumentation .....   | 41 |
| 3.3 Sample preparation .....  | 42 |
| 3.4 Materials Properties .....  | 43 |
| 3.4.1 Sand .....  | 43 |
| 3.4.1.1 Gradation analysis.....   | 43 |
| 3.4.1.2 Shear parameters of sand .....  | 43 |
| 3.4.1.3 Elastic modulus of sand .....   | 47 |
| 3.4.2 Granular Sub Base (GSB).....  | 54 |
| <10 .....   | 54 |
| 3.4.3 Reinforcement (Geogrid).....  | 54 |
| 3.5 Results and Discussions.....  | 55 |
| 3.5.1 Optimum thickness of Granular Sub-base layer ( $H_1$ ) .....                  | 55 |
| 3.5.2 Optimum length of reinforcement ( $l_g$ ) .....                               | 58 |
| 3.5.3 Optimum depth of reinforcement ( $d_i$ ).....                                 | 61 |
| 3.5.4 Effect of edge distance of wheel load from edge of an abutment ( $d_e$ )..... | 63 |
| 3.6 Special Recommendations .....   | 69 |
| 4. Modeling in FLAC 2D .....  | 71 |
| 4.1 Problem definition .....  | 71 |
| 4.2 FLAC – an overview.....   | 71 |
| 4.3 Finite difference program .....   | 72 |
| 4.4 Material Models .....   | 73 |
| 4.4.1 Mohr-Coulomb Model.....   | 73 |
| 4.4.2 Reinforcement model.....  | 74 |

|  |     |
|--|-----|
| 4.5 Validation study using FLAC <sup>3D</sup> .....  | 76  |
| 4.5.1 Homogeneous soil system - Unreinforced condition.....  | 77  |
| 4.5.2 Homogeneous soil system – Single layer of reinforcement .....  | 81  |
| 4.5.3 Homogeneous soil system – Two layers of reinforcement.....   | 85  |
| 4.5.4 Two layered soil system – Unreinforced condition .....   | 87  |
| 4.5.5 Two layered soil system – Single layer of reinforcement .....  | 89  |
| 4.5.5.1 Effect of initial depth of reinforcement & Effect of reinforcement.....                              | 89  |
| 4.5.5.2 Effect of stiffness of top layer with single layer of reinforcement in two layered soil system ..... | 91  |
| 4.5.6 Two layered soil system – Two layers of reinforcement.....   | 94  |
| 4.5.6.1 Effect of spacing between reinforcement layers .....   | 94  |
| 4.5.6.2 Effect of stiffness of reinforcement .....   | 96  |
| 4.6 Results and Discussions.....   | 97  |
| 4.6.1 Effect of stiffness of bottom layer .....  | 97  |
| 4.6.2 Effect of stiffness of top layer.....  | 98  |
| 4.6.3 Effect of thickness of top layer .....   | 99  |
| 4.6.4 Effect of angle of internal friction ( $\phi_2$ ) of bottom layer.....                                 | 101 |
| 5. Conclusions .....   | 102 |
| References.....  | 104 |

# Chapter 1

## Introduction

A bridge approach slab is a portion of roadway which follows immediately from the bridge abutments. An approach slab is a reinforced concrete structure constructed to provide a smooth transition between the bridge deck and the pavement. But as the time passes, a rough transition will develop in some approach slabs due to differential settlement between approach slab and bridge abutment. This leads to occurrence of “*bump*” in roadways (Briaud et al. 1997). Reinforced soil system can be used to support bridge and its approaching roadways which have potential to reduce the construction cost and time, and to provide a smooth riding for traffic by eliminating “bump” at bridge and approach slab interface. This report provides the causes for differential settlement between the bridge deck and the approach slab, followed by a review and discussion on the current practices used to eliminate “bump”, and the effectiveness of the proposed geogrid reinforced granular fills to reduce the differential settlements.

### 1.1 Overview

#### 1.1.1 Differential settlement (bump) between bridge approaches and bridge deck

An abrupt change in grade often occurs at bridge approaches. This is mainly due to different support systems for the bridge deck and the roadway fill; the bridge deck is supported on the abutment resting on deep pile foundations made of concrete and roadway fill on an earthen embankment or a natural soil subgrade (Figure 1.1). In order to reduce this problem, bridge approaches are usually constructed with reinforced concrete slabs connecting the bridge deck with the adjacent paved roadway. The primary function of this approach slab is to provide a smooth transition between the bridge deck and the existing roadway pavement. However, differential settlement (approach slab settlement) at the end of the bridge, referred to as ‘bump’, is inevitable at the intersection of bridge deck and the roadway (Figure 1.2). This uneven transition may cause distraction to drivers of fast moving vehicles over this uncontrolled section, and pose discomfort to the passengers. This

differential settlement is a complex issue which has to be dealt by both the design and construction teams together.

The bump will not only create discomfort to the passengers, but also adds huge maintenance costs to the transportation agencies and at the very least to the vehicles. In the United States, Department of Transportation (DOT) agencies have been spending considerable amounts of their maintenance budget in repairing the sections to mitigate the bumps every year. Bridge approach settlement was reported to induce damage to 25% of the bridges nationwide (approximately 150,000 bridges) with an estimated annual maintenance or repair costs well over \$100 million in late 1990s (Briaud et al. 1997). In addition to these costs, traffic congestion due to repair works results in 5.7 billion of person-hours of delay (FHWA-HRT-04-053). For each person this delay averages to 36 hours per year. Constant maintenance work, closure of lanes, traffic control and traffic delays have made this a major if not a premier maintenance problem all over the world.

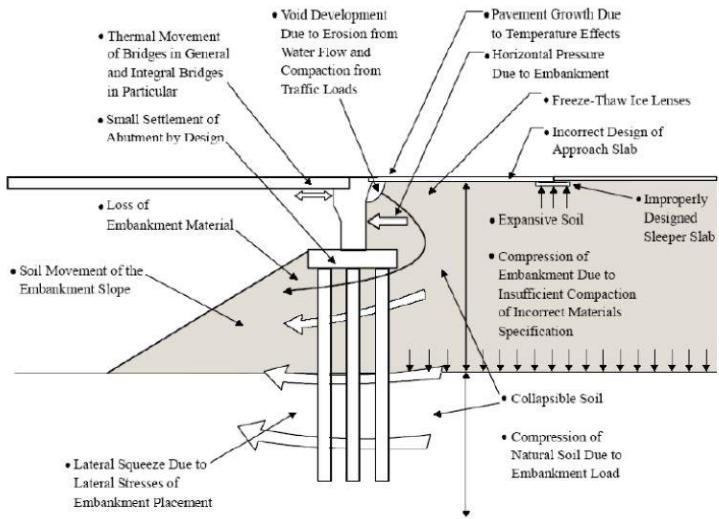


**Figure 1.1: Typical Bridge Approach System (Anwarul Islam, 2010)**

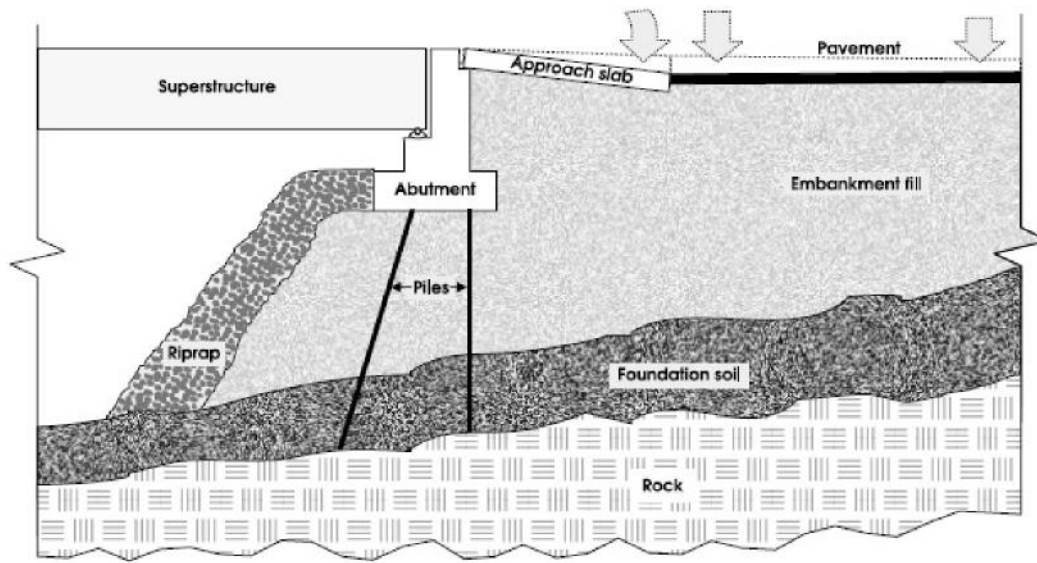


**Figure1.2: Bridge Approach Settlement ('bump' at the end of the bridge) (Hoppe, 1996)**

### **1.1.2 Bump Tolerance**

The point at which the bump needs to be repaired is always dilemma to DOTs. Walkinshaw (1978) suggested that bridges with a differential settlement of 2.5 inch (63 mm) or greater need to be repaired. Bozozuk (1978) stated that settlement bumps could be allowed up to 3.9 inches (100 mm) in the vertical direction and 2.0 inch (50 mm) in the horizontal direction. Several researches define the allowable bumps in terms of gradient as a function of the length of the approach slab. Wahls (1990) and Stark et al. (1995) have suggested an allowable settlement gradient of 1/200 for the approach slab. Das et al. (1990) used the International Roughness Index (IRI) to describe the riding quality. The IRI is defined as the accumulation of undulations of a given segmental length of roadway and is usually reported in m/km or mm/m. The IRI values at the bridge approaches of 10 (mm/m) or greater indicates a very poor riding quality. Albajar et al. (2005) established a vertical settlement on the transition zone of 1.6 inches (4 cm) as a threshold value to initiate maintenance procedures on bridge approach areas. In Australia, a differential settlement or change in grade of 0.3% both in the transverse and the longitudinal direction and a residual settlement of 100 mm for a 40 year design period are considered as limiting values for bridge approach settlement problems (Hsi and Martin, 2005; Hsi, 2007).

### **1.2 Objective of the study**

Objectives of the present study are the following:

- i. To evaluate effectiveness of proposed geogrid granular beds in reducing the differential settlement at



the interface of bridge abutment and approach slab and quantify the improvement with reference to unreinforced granular bed.

- ii. To perform a series of laboratory studies to obtain the load-settlement behavior of geogrid reinforced granular beds for various loading conditions and propose optimal design of reinforcement in terms of length and depth of reinforcement.
- iii. To develop charts depicting the settlement profiles of reinforced granular beds as approach slabs for various loading conditions.

### **1.3 Organization of thesis**

Chapter 2 provides literature review on the studies available to identify the mechanism leading to settlement of approach slabs and leading to differential settlement (bump) at bridge abutment. In this Chapter, along with the causes, the suitable mitigation techniques available to avoid bump problem were provided. A review on the available studies carried out on the reinforced granular fills was discussed.

Chapter 3 deals with the experimental investigations made using the large scale testing. The materials used the testing and tests for finding the properties of materials was explained. The procedure followed during testing for finding various parameters was provided. The discussion on the results obtained for various parameters was provided.

Chapter 4 provides the basic ideas on modelling in FLAC<sup>3D</sup>. The materials used for modelling soil and reinforcement are presented along with the properties. The validation studies have been done, and finally the experimental set up has been modelled and parametric studies were conducted and results were presented.

Chapter 5 covers results from experimental studies and numerical model to study the settlement at bridge abutment along with the optimal design of proposed reinforced granular beds was provided.

# Chapter 2

## Causes and Mitigation techniques for Bump

### 2.1 Mechanisms Causing the Bump

Many studies have been carried out to identify the causes for the settlement of approach slabs. Kramer and Sajer (1991) outlined the factors leading to the bump (Table 2.1). Later, National Cooperative Highway Research Program (NCHRP) report was published identifying the major causes of bridge approach settlement (Briaud et al., 1997). This report presents the following major factors that cause approach slab settlement or bump problems:

- (a) Consolidation settlement of foundation soil
- (b) Poor compaction and consolidation of backfill material
- (c) Poor drainage and soil erosion
- (d) Traffic volume
- (e) Approach slab design, and age of the approach slab
- (f) Skewness of the bridge
- (g) Seasonal temperature variations

**Table. 2.1 Causes for Bridge Approach Settlements (Kramer and Sajer, 1991)**

| <b>1. Differential settlement</b> |  |
|-----------------------------------|--|
| Compression of natural soils      | Primary consolidation, secondary compression, and creep              |
| Compression of embankment soils   | Volume changes and distortional movement's/creep of embankment soils |

|  |  |
|--|--|
| Local compression at bridge pavement interface | Inadequate compaction at bridge/pavement interface, drainage and erosion problems, rutting/distortion of pavement section, traffic loading, and thermal bridge movements |
| <b>2. Movement of abutments</b>                |  |
| Vertical movement                              | Settlement of soil beneath, erosion of soil beneath and around Abutment  |
| Horizontal movement                            | Excessive lateral pressure, thermal movements, swelling pressures from expansive soils, and lateral deformation of embankment and natural soils                          |
| <b>3. Design/construction problems</b>         |  |
| Engineer-related                               | Improper materials, lift thickness, and compaction requirements  |
| Contractor-related                             | Improper equipment, over excavation for abutment construction, and survey/grade errors   |
| Inspector-related/poor quality control         | Lack of inspection personnel and improper inspection personnel training  |
| Design-related                                 | No provision for bridge/contraction spill-through design resulting in the migration of fill material from behind the abutment  |

### 2.1.1 Consolidation settlement of foundation soil

Consolidation of foundation soil under an approach slab embankment was regarded as one of the most important contributing factors to bridge approach settlement (Hopkins, 1969; Wahls, 1990; Dupont and Allen, 2002; Seo, 2003). It usually occurs because of dynamic traffic loads applied at the embankment surface and static load due to the embankment weight itself (Dupont and Allen, 2002). Foundation problems are usually more severe in cohesive soils than in non-cohesive soils. Since consolidation occurs rapidly in non-cohesive soils, they do not normally present a serious problem. On the other hand, cohesive soils, such as soft or high plasticity clay, represent a more critical situation, because of their time dependent behavior.

In addition, cohesive soils are more susceptible to lateral or permanent plastic deformation, which can exacerbate the approach settlement problems. Typically, settlement of soils can be divided into Initial, primary, and secondary consolidation.

#### 2.1.1.1 Initial Consolidation

The initial settlement is the short-term deformation of the foundation when a load was applied. This type of settlement does not contribute to the formation of the bump, because it usually occurs before the construction of the approach structure (Hopkins, 1969). The soil saturation level affects the total contribution of this

settlement and for partially saturated soils; this initial settlement will be generally larger than that of saturated soils.

#### **2.1.1.2 Primary Consolidation**

Primary consolidation settlement is the main factor that contributes to the total settlement of soils. The gradual escape of pore water due to the compression of the loaded soil was believed to be the reason for this type of settlement. This primary consolidation can occur for a period of few months to ten years depending on the type of clay (Hopkins, 1973).

#### **2.1.1.3 Secondary Consolidation**

It occurs as a result of changes in void ratio of the loaded soil after dissipation of excess pore pressure (Hopkins, 1969). In this case, particles and water in the soil mass readjust in a plastic way under a constant applied stress. For the case of very soft, highly plastic or organic clays, secondary consolidation can be as large as the primary consolidation, while in case of granular soils, it was negligible (Hopkins, 1969).

#### **2.1.2 Poor Compaction and Consolidation of Backfill Material**

Approach embankments are usually constructed with the most readily available material at or near the site to minimize construction cost. But when low quality materials (such as locally available soft, cohesive expansive soils and soils sensitive to freeze-thaw) are used, the approach embankment settlement can induce “bumps”. In general, cohesive soils are more difficult to compact to their optimum content and density when compared to coarser or granular fill materials (Hopkins, 1973).

Poor compaction control of the embankment material was found to be a factor, resulting in low density and highly deformable embankment soil mass (Lenke, 2006). Poor compaction can also be attributed to limited access or difficulty in access within the confined working space behind the bridge abutment (Wahls, 1990).

#### **2.1.3 Poor Drainage and Soil Erosion**

Wahls (1990), Jayawickrama et al., (2005), and Abu-Hejleh et al. (2006) identified the drainage system of the abutment and embankment as one of the most important factors that affect approach settlements. The dysfunctional, damaged or blocked drainage system causes erosion in the abutment and slope, increasing soil erosion and void development. The dysfunctional drainage system may be caused by either incorrect construction or improper design. Anand et al (2012) reported that incorrect placement of the drainage pipes such as outlet flow line higher than inlet flow line in a newly constructed bridge can impair the drainage system. Figure 2.1 shows the cross section of wing wall arrangement and drainage system (Briaud et al. 1997).

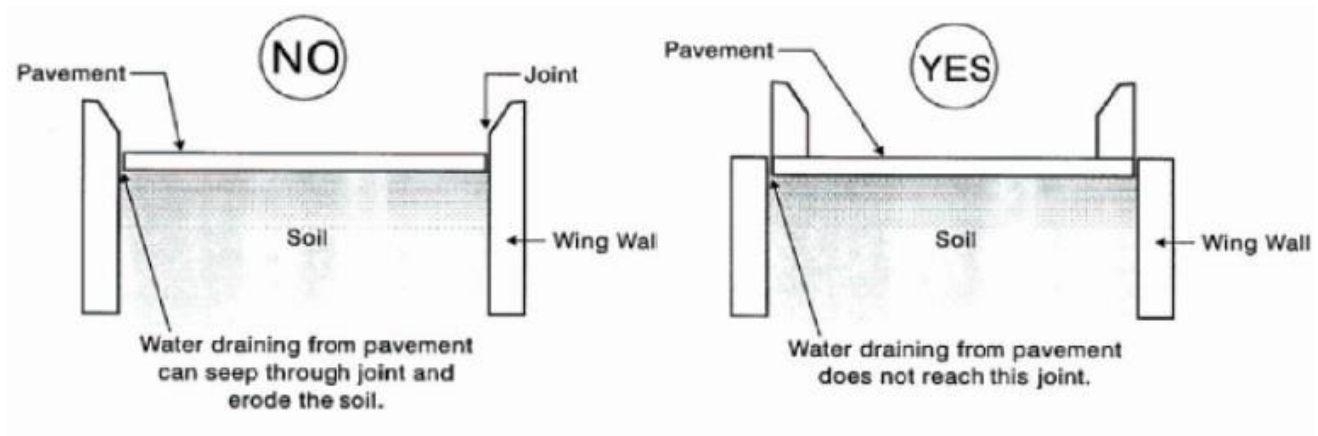


**Figure 2.1: Cross section of a Wing wall and Drainage System (Briaud et al. 1997)**

Jayawickama et al. (2005) noted that the erosion of soil at the abutment face and poor drainage of embankment and abutment backfill material can induce serious approach settlement problems. The intrusion of rain water through weak expansion joints between the approach slab and bridge abutments can erode backfill material and further amplify the problem of approach slab settlements. In addition, the expansion joints should transfer traffic loads, prevent surface water from entering into the abutment and allow pavement expansion without damaging the abutment structure (Wolde-Tinsase et al., 1987). Based on a comprehensive research study performed by White et al. (2005) on many bridges in Iowa, most of the expansion joints of the bridges inspected were not sufficiently filled, allowing water to flow into the underlying fill materials. On the other hand, cracks were often encountered next to closed joint in bridge approaches because of the crushing and cracking of neighboring concrete, allowing for leakage of water as well.

The erodability of soils depends on their grain size distribution. Some soil gradation guidelines proposes that gradation of soil can results in erosion resistant and that prone to erosion. As indicated in Figure 2.2, a gradation band of materials in the sand to silt size was a bad choice for embankment and backfill unless additional preventive measures, such as appropriate drainage design or erosion control systems, are provided (Briaud et al., 1997).

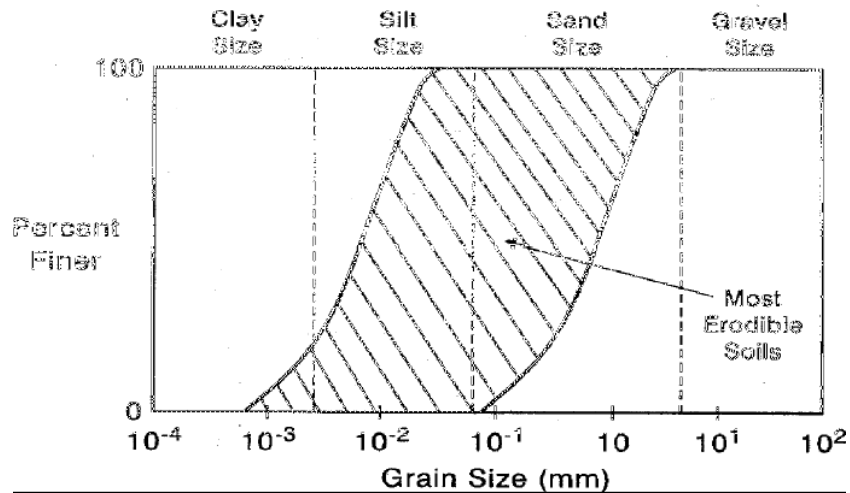


Figure 2.2: Range of Most Erodible Soils (Briaud et al., 1997)

#### 2.1.4 Traffic Volume

Wong and Small (1994) and Lenke (2006) noted that heavy truck traffic has been a major factor contributing to the severity of this bump along with the age of the bridge and approach. High-volume traffic has been found as a compelling reason for including approach slabs in the construction of both conventional and integral bridges. Lenke (2006) noted that “the bump” was found to increase with vehicle velocity, vehicle weight, especially heavy truck traffic, and number of cycles of repetitive loading, in terms of Average Daily Traffic (ADT). On the other hand, Bakeer et al. (2005) have concluded that factors such as speed limit and traffic count have no distinguishable impact on the performance of the approach slab. James et al (1991) indicated that deck cracking under heavily loaded truck traffic was more pronounced on steel I-beam bridges than on pre-stressed concrete girder spans.

#### 2.1.5 Age of the Approach Slab

The age of the approach slab is an important factor in the performance of different elements of bridge structures, especially at the expansion joints next to the approach slab, which could negatively affect the backfill performance in terms of controlling settlement underneath the slab (Laguros et al., 1990; Bakeer et al., 2005). Another factor known as alkali-silica reactivity (ASR) formed under the concrete approach slabs is known to induce expansion stresses. These stresses can potentially lead to slab expansion and distress in the approach slabs, approach joints, and vertical uplift of the slabs and pavement preceding the slabs (Lenke, 2006).

#### 2.1.6 Approach Slab Design

The purpose of the approach slab is to minimize effects of differential settlement between the bridge abutment and the embankment fill, to prevent voids that might occur under the slab and to provide a smooth transition between the pavement and the bridge and a better seal against water percolation and erosion of the backfill

material (Burke, 1987). However, a rough transition can occasionally develop with time in bridge approaches due to differential settlements between the two structure connected by the approach slab. The approach slab and the roadway are typically constructed over an earth embankment or natural soil sub grade, whereas the bridge abutment was usually supported on piles.

Laguros et al. (1990) reported that the flexibility of the approach pavements has a considerable influence as well. They observed greater differential settlement in flexible pavements than rigid pavement during initial stages following construction (short term performance), while both pavement types performed similarly over the long term.

Cia et al. (2005) studied the effect of approach slab settlement on the structural performance of the slab recommended modifications in the approach slab design for settlements greater than 15mm. Finite element modeling was used to predict the internal moments and deflections of the slab.

### **2.1.7 Skewness of the Bridge**

Skew angle also has a significant effect on the formation of approach settlements and the overall bridge performance. Skewed integral bridges tend to rotate under the influence of cyclic changes in earth pressure on the abutment (Hoppe and Gomez, 1996). According to Abendroth et al. (2007), design of skewed integral abutment bridges must account for the transverse horizontal earth pressure applied along the skew. Also, the change in position of the ends of an abutment can be attributed to a combination of two effects: the temperature-dependent volumetric expansion or contraction of concrete in the pile cap and abutment, and the rigid body translation and rotation of the abutment due to the longitudinal expansion or contraction of the superstructure for a skewed integral abutment bridge.

Nassif (2002) conducted a finite element study to understand the influence of skewness of bridge approaches and transition slabs on their behavior. It was found that the skew angle of the approach slab resulted in an uneven distribution of the axial load, so that only one side of the axles actually had contact with the approach slab. Figure 2.3 shows that the tensile axial stress on skewed approach slabs are found to be 20 to 40 percent higher than the same on straight approach slabs for the same loading conditions.

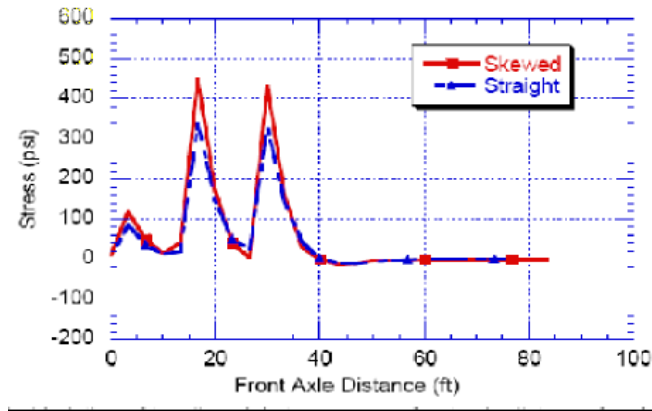


**Figure 2.3: Variation of Tensile Axial stress With Front Axle Distance for Skewed and Straight Approach Slab (Nassif, 2002)**

### 2.1.8 Seasonal Temperature Variations

Temperature change causes cyclical horizontal displacements on the abutment backfill soil, which can create soil displacement behind the abutment, leading to void development under the approach slab (White et al., 2005). As a result, the infiltration of water under the slab and therefore and loss of backfill material may accelerate.

Due to seasonal temperature changes, abutment move inward or outward with respect to the soil that they retain. During winter, the abutment moves away (outward) from the retained earth due to contraction of the bridge structure while in summer they move towards (inner) to the retained soil due to thermal cycle. These movements result in net displacements in abutment inward and outward from the retained soil. This was attributed to the displacement of an active soil wedge, which moves downward and towards the abutment during winter but cannot fully recover due to inelastic behavior of the soil during the summer abutment movements. This phenomenon was noted in all types of embankment materials (Horvath, 2005). Figure 2.4 shows the non-integral type of abutment and the approach slab movement (Brian, 2008).





**Figure 2.4: Elevation of Bump at Approach Slab (Brian, 2008)**

## **2.2 Mitigation Techniques to Alleviate Bump**

From the causes of bump formation we can conclude that compression of fill material, poor drainage and construction procedures are the main causes. Several research studies have been taken up to study the bump problem and to propose suitable mitigation techniques. Use of vertical drains in soft soil foundations, stone columns, deep soil mixing columns and chemical stabilization are proposed for foundation soil improvement. It was also mentioned that a good construction practice should minimize the problem to an extent. The utilization of geosynthetic to reinforce the embankment fill was proposed in recent studies. This aspect was not fully studied. Following sections will give an insight on the mitigation techniques available for bump problems.

### **2.2.1 Improvement of Foundation Soil**

#### **2.2.1.1 Vertical Drains**

Vertical drains in the form of sand drains were successfully used to enhance the consolidation process by shortening the drainage path from the vertical to the radial direction (Nicholson and Jardine, 1982). Recently the usage of sand drains has been replaced by prefabricated vertical drains (PVDs), also known as wick drains, accounting for their ease in installation and economy. Wick drains basically consist of a plastic core with a longitudinal channel wick functioning as a drain and a sleeve of paper or fabric material acting as a filter protecting the core. Configurations of different types of PVDs available in the market are shown in the Figure 2.5. Typically PVDs are 100 mm wide and 6-8 mm thick and are available in rolls.

The main purpose of prefabricated vertical drains was to shorten the drainage path and release the excess pore pressure in the soil and discharge water from deeper depths thereby assisting in a speedy consolidation process of soft soils. Generally vertical drains are installed together with preloading to accelerate the consolidation process. The discharge capacity, spacing, depth of installation and width and thickness of the wick drains are the prime factors controlling the consolidation process. These design factors again depend on the in-situ conditions of the project.

#### **2.2.1.2 Stone Columns**

‘Stone columns’ is one of the ground improvement techniques used in improving the load bearing capacity and to reduce the settlement of the foundation soil. It consists of crushed coarse aggregate of various sizes. The aggregates are then allowed to take the place of the displaced soil which exerts a pressure on the surrounding soil. The primary function of stone columns is to improve the loading carrying capacity of soils

(Madhav and Vitkar, 1978, Barksdale and Bachus, 1983; Michell and Huber, 1985; Copper and Rose, 1999; Serridge and Synac, 2007). The secondary function of the stone columns is to provide the shortest drainage path to the excess pore water to escape from highly impermeable soils (Hausmann, 1990). This technique was best suited for soft to moderately firm cohesive soils and very loose silt sands.

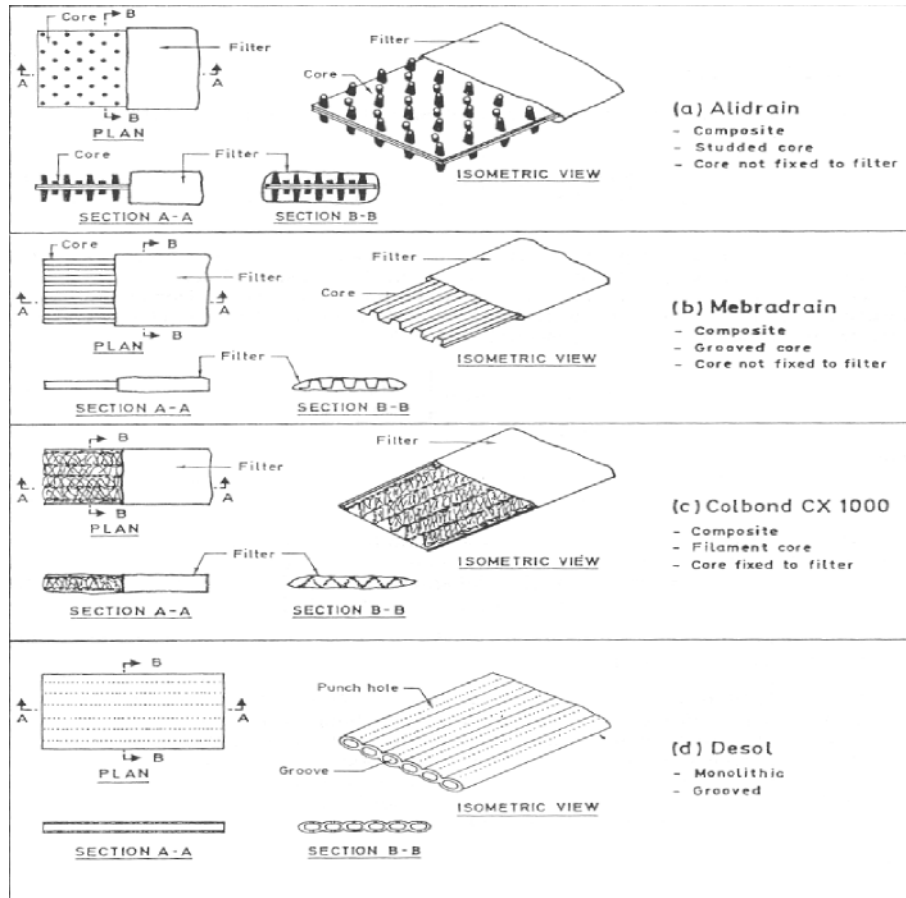


**Figure 2.5: Configurations of Differential Types of Prefabricated Vertical Drains (Bergado et al., 1996)**

Stone column construction involves the partial replacement of native weak unsuitable soil (usually 15-35 percent) with a compacted column of stone that usually penetrates the entire depth of the weak strata (Barksdale and Bachus, 1983). Two methods are generally adopted to construct the stone columns including vibro-replacement, a process in which a high pressure water jet was used by the probe to advance the hole (wet process) and vibro-displacement, a process in which air was used to advance the hole (dry process).

In both the processes, stone was densified using a vibrating probe, also called vibrofloat or poker, which was 12 to 18 inches (300 to 460 mm) in diameter. Once the desired depth was reached, stone was fed from the annular space between the probe and the hole to backfill the hole. The column was created in several lifts with each lift ranging from 1-4 ft. thick. In each lift, the vibrating probe was re-penetrated several times to

densify the stone and push the stone into the surrounding soil. This procedure was repeated till the column reaches the surface of the native soil. Figure 2.6 shows the stages of construction of stone column.

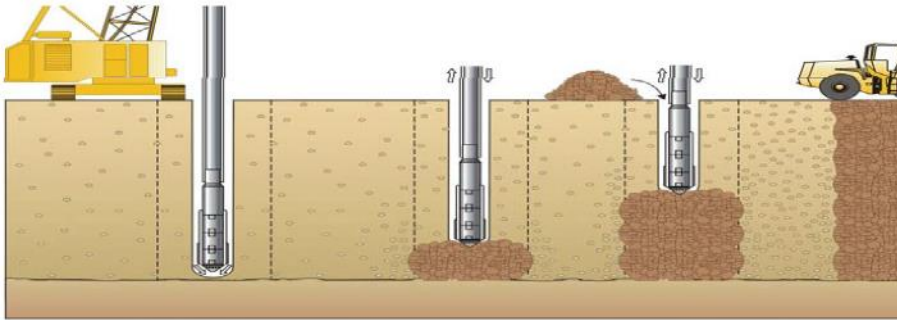


**Figure 2.6: Construction Stages of Stone Column (after Hayward Baker, <http://www.haywardbaker.com>)**

### 2.2.1.3 Deep Soil Mixing Columns

Deep soil Mixing (DSM) technology, was pioneered in Japan in late 1970s, and has gained popularity in other parts of the world over many years in the field of ground improvement. DSM is a process to improve soils by injecting grout through augers that mix in with the soil, forming in-place soil-cement columns (Barron et al., 2006). Recently, the cement binder has been replaced with many other cementitious compounds such as lime, fly ash or exists in combinations. Hence, in a broader sense, the DSM technique is an in-situ mixing of stabilizers such as quicklime, cement, lime-cement or ashes with soft and or expansive soils to form deep columns to modify weak sub grade soils (Porbaha, 1998).

DSM columns have been used on several state highways: to improve the stability of earth structures, to improve bearing capacity of soils, to reduce heave and settlement of embankments and roadways, to provide lateral support during excavation, to improve seismic stability of earthen embankments constructed over soft soils, and to reduce bridge approach settlements. This stabilization technique has been proven effective on soft clays, peats, mixed soil sand loose sandy soils (Rathmayer, 1996; Porbaha, 1998; Lin and Wong, 1999; Burke, 2001).

Lin and Wong (1999) studied the deep cement mixing (DCM) technique to improve the strength of 20m thick soft marine clay with high moisture content to reduce the total and differential settlements at bridge embankments constructed along Fu-Xia expressway in the southeast region of china. The bridge abutments rest on deep pile foundations with little to no allowable settlement. The maximum settlement of the embankment fill on the soft marine clays was predicted as 300 mm. To alleviate these differential settlements between pile-supported abutment and embankment fills, soil-cement deep soil mixing columns were selected to reinforce the embankment foundation soil.

Use of the DCM columns of uniform and varying length having longer columns towards the pile supported abutments allowed the construction of the embankment to their full design height with acceptable post construction total differential settlement at the bridge approaches (Puppala et al. 2009). Typical DSM operation was shown in Figure 2.7.

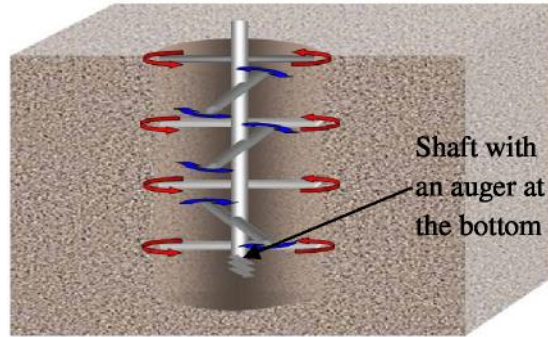


**Figure 2.7: Deep Soil Mixing (DSM) Operation (Puppala et al. 2009)**

**2.2.1.4 Compaction Piles**

A series of compaction piles are used to improve the foundation soils, only when the deep deposits of loose granular soils such as sand or gravel are present and they can be densified by vibro-compaction or vibro-replacement methods (Hausmann, 1990). In this technique a probe was inserted into the soil until it reaches the desired treatment depth. Then, the loosely deposited sands are vibrated in combination with air or water-jet at a design frequency. Some amount of granular backfill materials are added to compensate for the void spaces resulting from the compaction. Finally, the probe was removed and the compacted granular backfill column was left in-situ. Figure 2.8 gives the sequential operations involved in the construction in the construction of compaction piles. Normally, the spacing of compaction piles was in between 3 and 10 ft. and the depth of improvement can be achieved up to 50 ft. (15 m) (Wahls, 1990). However, the vibro compaction has its own limitation upon the grain size distribution of the granular fill material, which must contain fine material less than 20 percent.

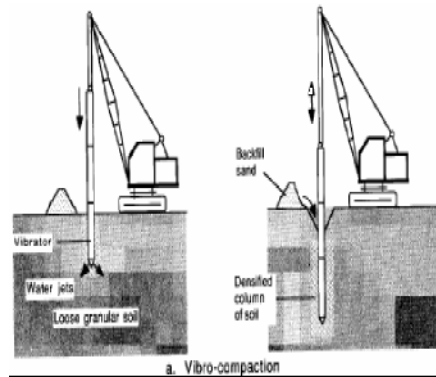


**Figure 2.8: Sequential Operations Involved in the Construction of Compaction Piles  
(Hausmann, 1990)**

### **2.2.2 Improvement of approach embankment/backfill material**

The bridge approach embankment has two functions; first to support the highway pavement system, and second to connect the main road with the bridge deck. Most of the approach embankments are normally constructed by conventional compaction procedures using materials from nearby roadway excavations or a convenient borrow pit close to the bridge site. In addition, since the embankment must provide a good transition between the roadway and the bridge, the standards for design and construction considerations both in materials quality requirements and compaction specifications must be specified in order to limit the settlement magnitude within a small acceptable degree (Wahls, 1990).

Generally, the materials for embankment construction should have these following properties (White, 2005):

- Easy of compaction,
- Time independent,
- Not sensitive to moisture,
- Providing good drainage,
- Erosion resistance and
- Shear resistance.

Dupont and Allen (2002) cited that the most successful method to construct the approach embankments was to select high quality fill material, with the majority of them being a coarse granular material with high internal frictional characteristics. Several research methods have been attempted to define methods to minimize potential of settlement and lateral movement development in the approach embankments and these studies are discussed in the following paragraphs.

#### **2.2.2.1 Use of Geosynthetic Reinforcement in backfill/foundation soil**

The acceptance of geosynthetics has increased in the last 2 to 3 decades owing to the poor quality of construction materials available and the advantages of using geosynthetics in civil infrastructure. Geosynthetics have gained popularity due to their many functions including, reinforcement, separation, membrane, filter etc. (Koerner 2006). Of these, the geosynthetics reinforcement function was most important for increased performance in terms of bearing pressure and settlement reduction. These functions are clearly described in the following sections:

##### **Effect of Shear Reduction**

A geosynthetic layer reduces the outward shear stress transmitted from the overlying soil layer to the top of the underlying foundation soil. This action was known as shear stress reduction effect (Shukla, 2003; Figure 2.9).

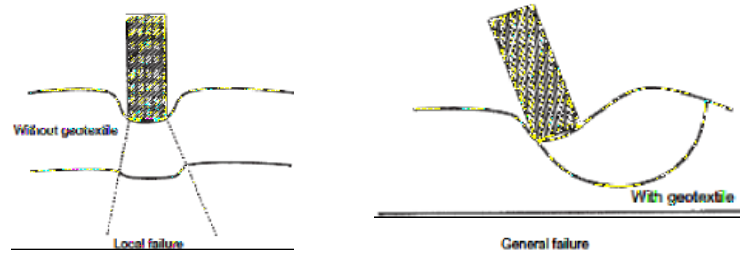


**Figure 2.9: Change of Failure Pattern (Shukla, 2003)**

From Figure 2.9, it can be seen that it will result in a general shear failure rather than local shear failure, thereby causing an increase in load bearing capacity. The reduction in shear stress and the change in the failure are the primary benefits of the geogrid layer at small deformation.

### **Confinement Effect**

A geogrid layer redistributes the applied surface load by providing restraint of the granular fill if embedded in it or by friction between the soil and the geogrid. Figure 2.10 depicts the redistribution of loads in geosynthetic reinforced bed.

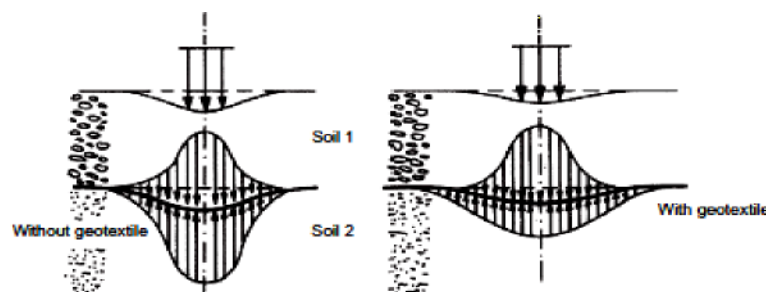


**Figure 2.10: Redistribution of surface Loads (Pinto, 2003)**

### Membrane Effect

The deformed geogrid, sustaining normal and shear stress, has a membrane force with a vertical component that resist applied load: that was the deformed geosynthetic provides a vertical support to the overlying soil mass subjected to loading. This action of geogrid was popularly known as soil membrane effect (Pinto, 2003). Figure 2.11 shows the membrane effect of a geogrid.

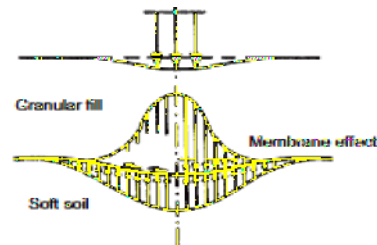


Figure 2.11: Membrane Effect (Pinto, 2003)

### Anchorage Effect

In the aperture of the geogrid, the soil particle will interlock and exert a passive pressure, causes the soil layer to increase its load carrying capacity and decrease in its settlement nature to the applied load. Figure 2.12 refers the interlocking effect of geogrids. Abdi et al., (2011) have shown that the pullout resistance of geogrid was more in sands when compared to clays. The pullout resistance depends on the particle size and the aperture opening size (Brown et al., 2007).

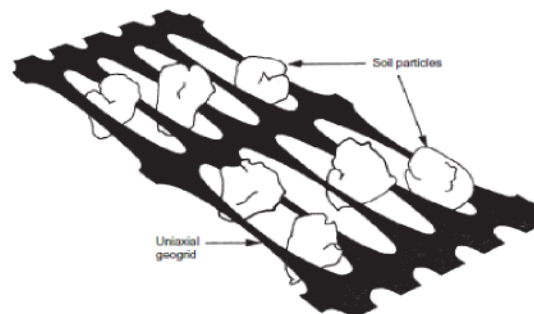


Figure 2.12: Interlocking Effect (Pinto, 2003)

Several researchers have studied the reinforcement and membrane effects of geogrids in sand and clay foundations under different loading conditions (Sireesh and Sitharam, 2004; Madhavi Latha, 2009) and concluded that the reinforcement and membrane effects are more predominant in sandy soils than clays. The studies show that the bearing pressure on the reinforced beds has increased by at least four folds when compared to unreinforced beds and the settlements were reduced by 80%. The effective depth of the zone of reinforcement below a square/circular footing was twice the width of the footing, beyond which the inclusion of reinforcing layers will not result in significant improvement in the bearing capacity of the footing (Sireesh and Sitharam, 2004; Madhavi Latha, 2009).

### **2.2.2.2 Mechanically Stabilized Earth (MSE) Wall**

Mechanically Stabilized Earth (MSE) wall has rapidly developed since the 1970's and this technology was widely used throughout the world. The MSE method was a mitigation technique that involves the mechanical stabilization of soil with the assistance of tied-back walls. As shown in Figure 2.13, a footing of the bridge was directly supported by backfill; therefore, a reinforcement system in the upper layer of the embankment where the backfill was most affected by the transferred load from the superstructure must be carefully designed (Wahls, 1990). On the contrary, the facing element of the wall does not have to be designed for the loading, since the transferred load from the bridge in the MSE scheme does not act on the MSE wall (Wahls, 1990).

Based on a study conducted by Lenke (2006), the results of research shows that the MSE walls tend to have lesser approach slab settlements than other types of bridge abutment systems due to these following reasons; first, the MSE walls will have excellent lateral constraints provided by the vertical wall system, second, the tie back straps in the MSE system can provide additional stability to the embankment. These two reasons can minimize lateral loads in the embankment beneath the abutment. Consequently, the potentials of lateral settlements are reduced (Dupont and Allen, 2002).

Other advantages of the use of MSE walls are that it reduces the time-dependent post construction foundation settlements of very soft clay as noted by White et al. (2005). Also, the MSE wall with the use of geosynthetic reinforced backfill and a compressible material between the abutment and the backfill can tolerate a larger recoverable cyclic movement as noted by Wahls (1990) and Horvath (1991).

Regarding construction aspects, the MSE walls have recently become a preferred practice in many state agencies (Wahls, 1990). First, the MSE was considerably an economical alternative to deep foundation or treatment of soft soil foundation. Second, the MSE can be constructed economically and quickly when compared to conventional slopes and reinforced concrete retaining walls. Third, a compacted density in the MSE construction can be achieved easily by increasing lateral constraint. Finally, the MSE is also practical to build in urban areas, where the right of way and work area are restricted (Wahls, 1990). Abu-Hejleh et al. (2006) cited that the use of an MSE wall for an abutment system should be considered as a viable alternative for all future bridges and it was reported as one of the practical embankment treatment systems to alleviate the bridge bump problem.



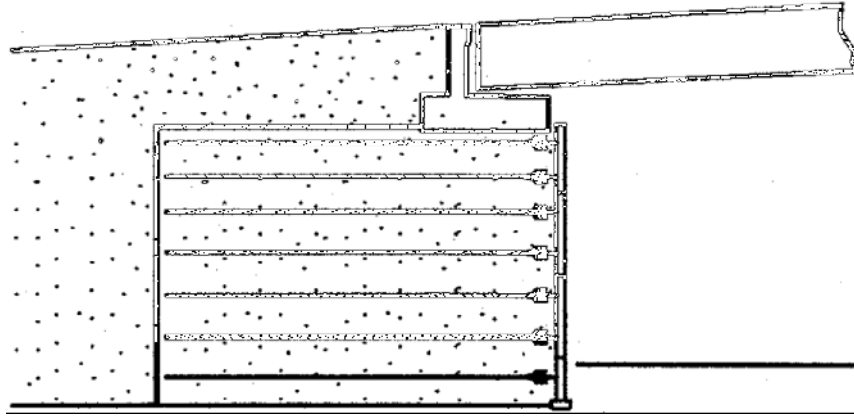


**Figure 2.13: Typical Mechanically Stabilized Abutment (Wahl's, 1990)**

### 2.2.2.3 Geosynthetic Reinforced Soils (GRS)

Geosynthetic Reinforced Soil (GRS) was recommended as a method to achieve a backfill compaction at the optimal moisture content, especially for a coarse-grained backfill material (Abu-Hejleh et al., 2006). The GRS was a geosynthetic-reinforced soil structure constructed either vertically or horizontally in order to minimize the uneven settlements between the bridge and its approach. Figure 2.14 shows a schematic diagram of a GRS wall structure and a complete typical GRS system after construction. Based on the studies performed by Abu-Hejleh et al. (2006), it was discovered that with the use of GRS, the monitored movements of the bridge structure were smaller than those anticipated in the design or allowed by performance requirements. In addition, they also stated that with the use of GRS systems, post construction movements can be reduced substantially, thus the bump problem at the bridge transition was minimized. Another advantage of geosynthetic-reinforced soil is that, it increases backfill load carrying capacity and reduces erosion of the backfill material; both can help in the mitigation of approach bumps. Some states have also used layers of geosynthetic reinforcement soil in combination with shallow foundations to support the bridge abutment (Abu-Hejleh et al., 2000).

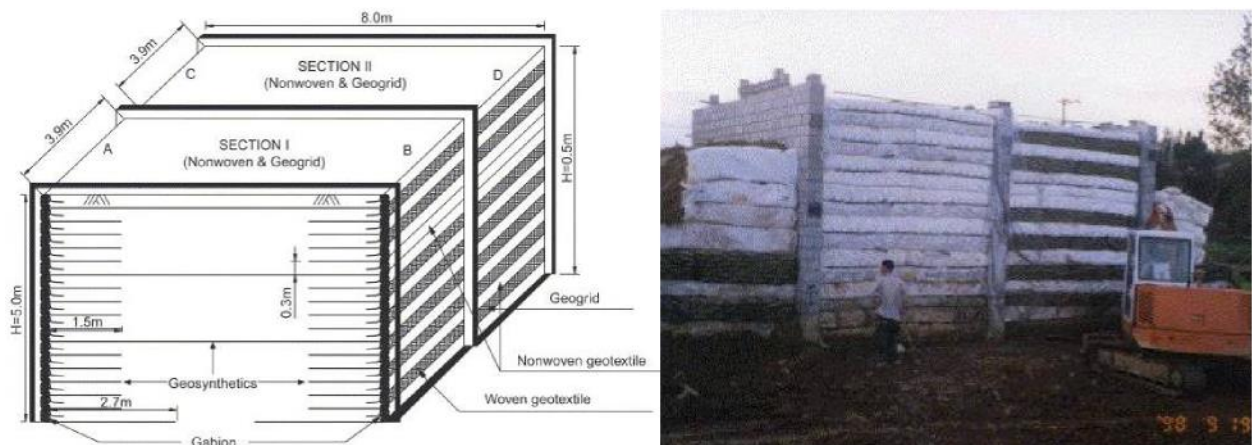


**Figure 2.14: Schematic Diagram of a GRS Wall and GRS System after Construction (Won and Kim, 2007)**

According to Wu et al. (2003), the GRS system becomes a more viable alternative than other conventional bridge abutments. It provides many advantages, such as being more ductile, more flexible (hence more tolerant to differential settlement), more adaptable to the use of low quality backfill, easier to construct, more economical, and less over-excavation required. Wu et al. also presented a case study where the GRS was used in a condition in which each footing bears several preloading cycles greater than their design load and sustained for several minutes. It was found that after the first few cycles of preloads, the observed settlement reduced to negligible amounts and subsequent service settlements were less than 0.5 inch. The Wyoming Highway Department has used multiple layers of geosynthetic reinforcement within compacted granular material since the 1980s (Monley and Wu, 1993).

Edgar et al. (1989) stated that of the ninety approach slabs placed on geosynthetic reinforced embankments, it either was zero required maintenance or requires repair only after 5 years of service. Excellent performance of these systems was also reported by Abu-Hejleh et al. (2006) for both short- and long-term performance of the GRS approaches.

Wu et al. (2006) summarized the advantages of the GRS bridge abutments with flexible or rigid facing over conventional reinforced concrete abutments as follows:

- GRS abutment increases tolerance of foundation settlement to seismic loading
- GRS abutments are remarkably more stable and have higher ductility
- With a proper design and construction, “bumps” can be alleviated
- GRS abutments are constructed more rapidly and less expensive
- GRS abutments do not require embedment into the foundation soil for stability
- The lateral earth pressure behind a GRS abutment wall was much smaller
- GRS performs satisfactorily longer under in-service conditions
- The load-carrying capacity by GRS was significantly greater

The GRS bridge-supporting structures can be grouped into two types: “rigid” facing and “flexible” facing structures (Wu et al., 2006). Flexibility or rigidity of GRS walls was explained in relation to its deformation capability and its responses to temperature changes in different seasons (Wu et al. 2006). If the construction was done in cold dry seasons (fall/winter), the GRS walls present a rigid response whereas constructions of GRS walls during warm, wet, and thawing seasons result in GRS walls with a flexible response, capable of undergoing relatively large deformations.

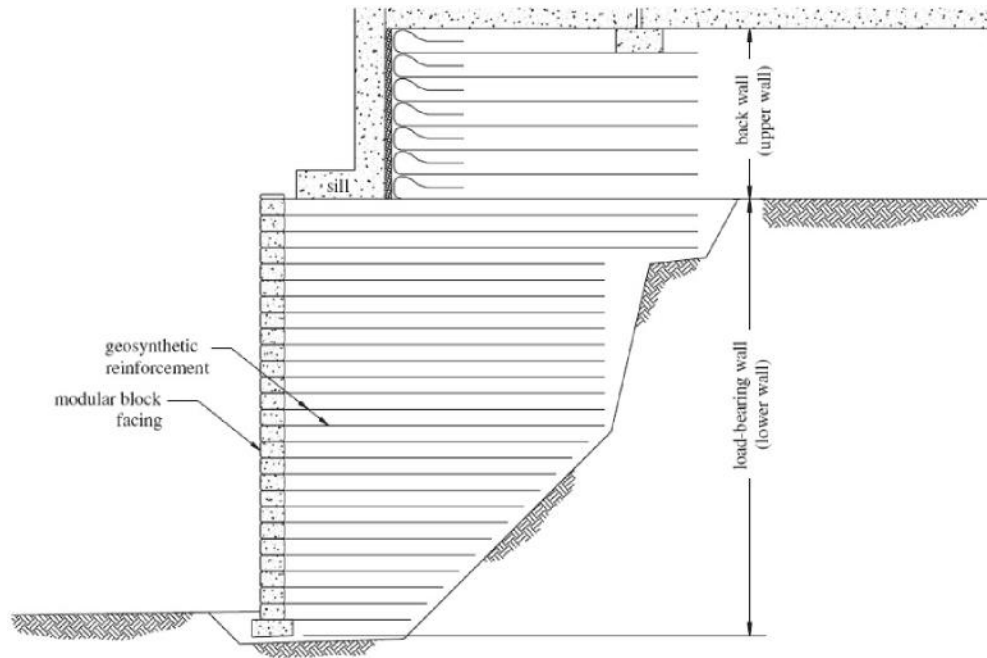


**Figure 2.15: Typical GRS Bridge Abutment with a Segmental Concrete Block Facing**

A typical cross section of a GRS system with rigid facing was shown in Figure 2.15. Rigid facing was typically a continuous reinforced concrete panel, either precast or cast in-place. Rigid facings offers a significant degree of “global” bending resistance along the entire height of the facing panel, thus offering greater resistance to global flexural deformation caused by lateral earth pressure exerted on the facing.

Flexible facing was typically a form of wrapped geosynthetic sheets, dry-stacked concrete modular blocks, timbers, natural rocks, or gabions. These wall structures have shown great promise in terms of ductility, flexibility, constructability, and costs. The main advantages of this system over the rigid facing are summarized as (Abu-Hejleh et al., 2003, Wu et al., 2006):

- Larger mobilization of the shear resistance of the backfill, thus taking more of the lateral earth pressure off the facing and connections
- More flexible structure, hence more tolerant to differential settlement
- More adaptable to low-quality backfill

Guidelines of GRS walls are provided by the Colorado DOT for designing and constructing GRS bridge abutments (Abu-Hejleh et al., 2000) and a few of the assumptions used in this guidelines are presented here:

- The foundation soil should be firm enough to limit post construction settlement
- The desired settlement of the bridge abutment should be less than 1 inch (25 mm)
- The maximum tension line needed in the internal stability analysis should be assumed nonlinear
- Ideally construction should be done in the warm and dry season

- The backfill behind the abutment wall should be placed before the girders.

Overall, the GRS system walls have been used with mixed results to alleviate approach settlement problems. However, very few state DOTs have implemented this in practice, probably due to the limited familiarity of this method.

In this research, a detailed study was undertaken to understand the behavior of geogrid reinforced granular beds to mitigate the issues related to the bump at the end of the bridge. The literature available on reinforced granular beds was detailed next.

## **2.3 Geosynthetic Reinforced Granular Fills**

The technique of reinforcing granular fill material with extensible or inextensible-type reinforcement was one of the fastest growing techniques in the field of geotechnical engineering. Reinforcing the fill material offers an economic solution in improving the load-settlement and the load carrying characteristics of granular fill. Since Binquet and Lee (1975a, b) published the experimental test results on granular soil bed reinforced with horizontal strips of reinforcement and proposed an analytical solution to model the behavior of reinforced granular soil beds. Extensive research has been done on the problem of reinforced granular soil beds. Some of literature on reinforced granular fills are presented here. Research publications on this topic can broadly be classified into two categories: (a) Numerical studies on reinforced granular fills, and (b) experimental or prototype studies on reinforced granular fills.

### **2.3.1 Numerical studies on Reinforced Granular Fills**

Madhav and Poorooshab (1988) had a parametric study on the load-settlement response of a granular fill-reinforced-soft soil system due to a strip load. Three different material were modeled: Granular fill, reinforced with geofabric, overlies a soft soil deposit (Figure 2.16). Granular fill was modeled as a shear layer, geofabric as a rough membrane, and soft soil by Winkler springs. This model considers four different parameters - shear modulus  $G$  and thickness  $H$  of the granular fill, coefficient of friction ( $\mu$ ) between fill/soil and fabric, and modulus of subgrade reaction ( $k$ ) of soil. A more generalized model was later developed by Ghosh and Madhav (1994a) by incorporating the nonlinear load-settlement responses for granular fill and soft soil deposit under plane strain loading conditions. It was concluded that membrane effect becomes significant at low values of shear stiffness of the granular fill and that the membrane effect improves the load-settlement of the system with increases in the soil-reinforcement interface friction coefficient.

Madhav and Poorooshab (1988) modeled the response of a granular-fill-geosynthetic-soft soil system due to a uniform strip load by accounting for the increase in the confining stress in the granular fill with the mobilization of tension in the reinforcement (Figure 2.17). Pasternak type foundation model was modified to study the effect of reinforcement (modeled as a rough membrane) in increasing the confining stress in

the granular fill with a consequent increase in the shear modulus. The shear parameter was assumed to decrease exponentially with the distance measured from the center of the footing (Figure 2.17 b). Ghosh and Madhav (1994b) later extended this model and developed a generalized model. This model account for nonlinear load-settlement behavior of soft soil and granular fill with variable shear moduli by using empirical relation proposed by Hardin and Drnevich (1972). The effect of confinement was found to be pronounced at large shear stiffness values of granular fill material.

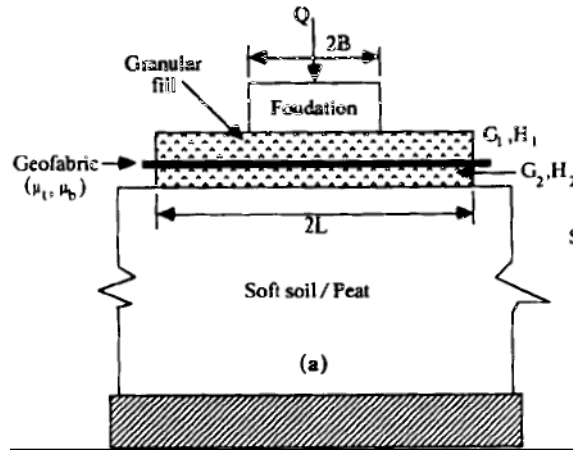


Figure 2.16: Granular-Fill-Geofabric-soft soil system (Madhav and Poorooshab, 1988)

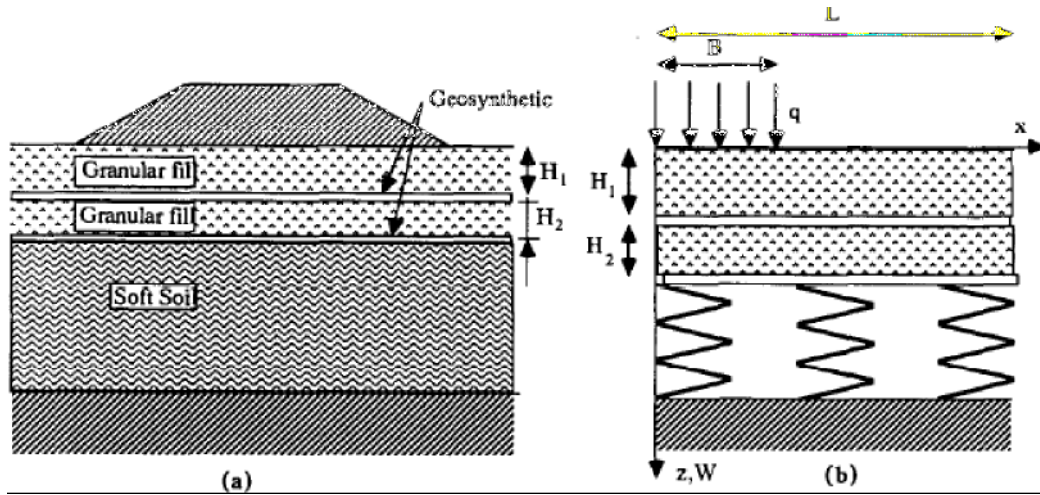


Figure 2.17: (a) Granular-Fill-Geofabric-soft soil system, and (b) model representation (Madhav and Poorooshab, 1988)

Raghavendra (2004) used a Finite element (FE) formulation to model the soil-reinforcement interaction and studied the effects of reinforcement properties and the length of reinforcement on the load carrying capacity of the footing. FE results were compared with the model tests performed on a sand bed reinforced with aluminum strips. The optimum length of reinforcement to mobilize full reinforcement-soil interaction was found to be two to three times the size of footing. The load carrying capacity of reinforced sand beds

increases up to three layers of reinforcement, there after increase in the number of reinforcement layers did not contribute to the improvement in load carrying capacity of the footing. Optimum embedment depth of reinforcement and spacing of reinforcement layers were also proposed in this study.

Deb et al. (2007) performed numerical analysis to study the behavior of granular bed, reinforced with multi layers of geosynthetic reinforcement, and overlying a soft soil deposit. Fast Lagrangian Analysis of Continua (FLAC) program was used for the analysis. In this study, granular fill, soft soil and geosynthetic reinforcement were modeled as linear elastic and the geosynthetic reinforcements was modeled as cable elements fully bonded with the surrounding granular fill material. Results indicated that reinforcement with tensile stiffness higher than 5000 kN/m does not affect the settlement response of the reinforced granular beds.

### **2.3.2 Experimental or Prototype Studies on Reinforced Granular Fills**

Adams and Collin (1996) performed large-scale tests at Federal Highway Administration's Turner-Fairbank Highway research center (TFHRC) in a test chamber with dimensions 6.9m x 5.4m x 6m (length x width x depth). Four different sizes of footings were modeled – 0.3m x 0.3m, 0.46m x 0.46m, 0.61m x 0.61m and 0.91m x 0.91m. Two types of reinforcement were tested: geogrid with aperture size 25 x 30mm and ultimate strength in machine direction = 25 kN/m, and geocell with cell dimensions 200x 244mm and minimum welded seam strength = 2kN. Fine concrete mortar sand was used to prepare the sand bed and studies were conducted on reinforced beds to evaluate the performance with respect to the bearing capacity and settlement. The improvement in the bearing capacity ratio (BCR) was significant for three layers of geogrid (BCR>2.6) compared to one or two layers of grid. At small strains, maximum improvement in bearing capacity was found when the depth of top layer of reinforcement was placed at a depth within 0.25 times the width of footing.

Kumar and Saran (2003, 2004) conducted small-scale model studies and proposed a model to study the interference effects on bearing capacity and settlements of closely spaced footings on the geogrid-reinforced granular beds. It was observed that a significant improvement in bearing capacity, settlement and tilt of adjacent footings occurs. This was due to provision of continuous reinforcement layers beneath closely spaced footings.

Sireesh and Sitharam (2004) performed model studies on circular footings embedded in sand beds reinforced with layers of geogrid reinforcement. Sand beds were prepared (at a relative density DR=70%) in a test tank of 900mm x 900mm x 600mm size. The model footing was 150mm in diameter and 30mm in

thickness. Number of layers of reinforcement  $N$  was varied from 1-6 and the embedment depth of footing from 0-0.6 times the diameter of the footing. Model studies showed that the initial stiffness (obtained from bearing pressure vs. footing settlement curves) for the reinforced case was about 1.5-2.0 times that of unreinforced case as the number of layers of reinforcement increased from 1-to-6.

Perkins and Cortez (2005) performed prototype tests to evaluate the performance of pavement reinforced with three geosynthetic products. Four test sections were constructed in an indoor facility located at US Army Corps of Engineers Research and Development Center Cold Regions Research and Engineering Laboratory (CRREL). Traffic load was applied on the four test sections (Figure 2.18) using a Heavy Vehicle Simulator (HVS), stresses and strains in the pavement were monitored. CRREL3 was reinforced with woven geotextile (type: Amoco Propex 2006) with tensile modulus at 2% strain = 213 kN/m (machine direction), CRREL2 with biaxial geogrid (type: Tensar BX 1100) with tensile modulus at 2% strain = 248 kN/m (machine direction) and CRREL4 with biaxial geogrid (type: Tensar BX 1200) with tensile modulus at 2% strain = 321 kN/m (machine direction). Section reinforced with BX 1200 (CRREL4) showed the best performance in terms of rutting.

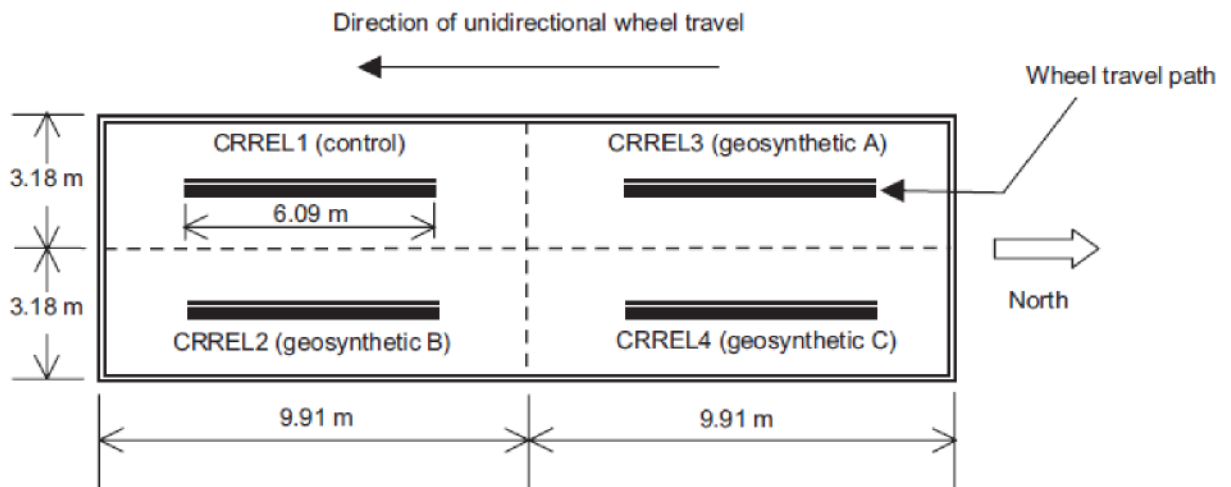


**Figure 2.18: Control Sections (Perkins and Cortez, 2005)**

Kumar and Walia (2006) performed model tests on a square footing resting on a two-layer system with the top layer reinforced with geogrid (type: Tensor geogrid SS 40 with tensile strength of 40 kN/m in both longitudinal and transverse directions). Thickness of the top layer and bottom layer was varied from 0.5-to-2.0m and 2.0-to-3.5m respectively. Model tank with inside dimensions 1.8m x 1.2m x 1.2 m was used for testing. Based on the model test results, an equation was proposed to predict the ultimate bearing capacity of square and rectangular footings resting on reinforced layered soils.

Brown et al. (2007) conducted full-scale experiments on geogrid reinforced railway ballast to study the permanent deformation under repeated loading conditions. Geogrid with a square aperture size of 65 mm with different nominal tensile strengths of 15 kN/m, 20 kN/m, 30 kN/m and 45 kN/m were used in the testing. A cyclic load of 20 kN was applied using a hydraulic actuator at a frequency of 2 Hz. The effectiveness of the reinforcement increased by the use of a stiffer geogrid. Ballast reinforced with geogrid of tensile strength equal to 45 kN/m showed 50% increase in the strength compared to that of ballast reinforced with geogrid of tensile strength equal to 30 kN/m.

Chung and Cascante (2007) performed experimental and numerical studies and recommended use of 2-4 layers of reinforcement for design of reinforced granular beds. Based on two types of reinforcements- fiberglass meshes and aluminum meshes used in the study, authors reported that the critical zone for placement of reinforcement was 0.3- 0.5 times the width of square footing for maximizing the benefits of reinforcement. The reinforcement placed beyond a depth equal to width of footing will be ineffective when placed in silica sand.

Basudhar et al. (2007) studied the behavior of circular footings resting on sand beds reinforced with geotextiles. Both experimental and numerical studies were performed with number of layers of reinforcement varying from 0 to 3 and relative density of sand bed varying from 45% -to-84%. Model studies were performed in a square tank of 0.44m x 0.44m x 0.21m using three model circular footings with diameter equal to 30mm, 45mm and 60mm. For sand bed reinforced with three-layers of reinforcement, bearing capacity ratio improvement of about 4.5 times that of unreinforced case using for 30mm diameter model footing was obtained.

Mosallanezhad et al. (2008) performed tests on sand beds reinforced with a new reinforcing system named as 'grid-anchor'. It was a 3-dimensional reinforcement system made by adding anchors at an angle of  $45^{\circ}$  with the geogrid; the anchors form 1x 1x 1 cm cubic elements and are made from high density polyethylene (HDPE). Authors investigated the bearing capacity of square footings resting on reinforced sand bed for various vertical spacing between the layers, number of reinforcement layers, embedment depth and the length of reinforcement. Later, Boushehrian et al. (2011) conducted experimental and numerical studies to study the behavior of granular fill reinforced with the proposed 'grid-anchor' type reinforcement due to cyclic load. Numerical modeling was done with the aid of FE software (PLAXIS 3D).

Phanikumar et al. (2009) performed plate load tests on geogrid (type: Netlon CE 121 with tensile strength 7.68 kN/m) reinforced sand beds. Sand beds were prepared with three sizes of sand – fine, medium and



coarse ( $D_{10}=0.25, 0.59$  and  $1.3$  mm) at  $DR=50\%$  were used for the model tests. Test chamber consisted of a cylindrical tank of diameter equal to  $600$ mm and height equal to  $300$ mm. Effects of increasing the number of reinforcement layers from 1-3 and the spacing between geogrids on load-settlement response were studied. Load improvement ratio (LIR) for reinforced coarse sand bed was higher than that of reinforced fine and medium sand beds. LIR of about 3.2 was obtained for coarse sand bed reinforced with three layers of reinforcement corresponding to footing settlement equal to  $0.5$ mm.

Madhavi Latha and Somwanshi (2009) performed model tests on square footings resting on sand beds and reinforced with various reinforcement types – weak biaxial geogrid (ultimate tensile strength=  $20$  kN/m), strong biaxial geogrid (ultimate tensile strength=  $40$  kN/m), uniaxial geogrid (ultimate tensile strength=  $40$  kN/m) and geonet (ultimate tensile strength=  $7.6$  kN/m). Model test were performed in a test tank of dimensions  $900$ mm x  $900$ mm x  $600$ mm using a model footing of  $150$ mm x  $150$ mm in plan dimensions and  $25$ mm in thickness. The effects of reinforcement length and spacing between the reinforcement layers for 1-4 layers of reinforcement were studied. It was found that the placement of reinforcement at a depth beyond two times the width of the footing did not contribute to the improvement in bearing capacity of the footing. Optimum width of reinforcement was about four times the width of the footing and the optimum spacing was found to be  $0.4$  times the width of the footing.

# Chapter 3

## Experimental Investigation

In this chapter, the complex interactions that take place between the structural components of the integral bridge and the soil was investigated through experimental studies. The experimental studies include study of various parameters affecting the differential settlement between bridge abutment and granular beds (which are used to replace the approach slab). The experimental investigation discusses about the materials and its properties used in the model tests, test setup and procedure adopted for the model tests.

### 3.1 Laboratory Testing Setup

#### 3.1.1 Reaction frame

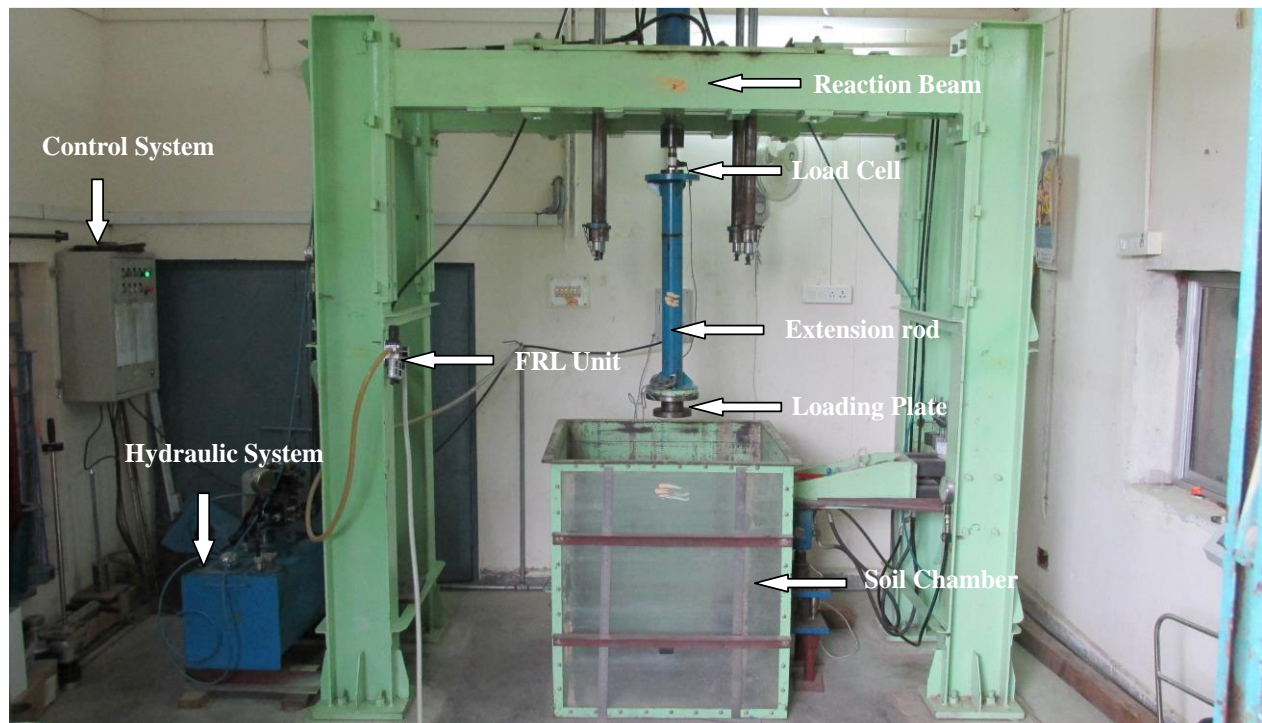


### **Figure 3.1: Reaction frame with loading system and soil chamber**

In order to perform large scale testing, a reaction frame with capacity of upto 12 tonnes was fabricated to sustain the reaction from the sand. Lots of reviews and discussions have been done in favor of fabricating the reaction frame according to current practices and to also be suitable for further usage. An overhead plate was fixed at middle of the two I-sectioned beams of length 2.2m each which was supported by four I-sectioned columns of height 2.3m that supports the hydraulic loading system. The Figure 3.1 shows the reaction frame designed for the present study to conduct full scale load tests.

#### **3.1.2 Loading system**

A hydraulic system was used for applying the load on soil sample. It was fixed to the reaction frame by an overhead plate supported on two I-sectioned beams. It has a capacity of up to 8 tonnes with the hydraulic stroke of 650 mm. A rigid circular plate was designed, in order to simulate wheel load on the reinforced granular bed. The dimension of wheel load was decided using based on Class 'B' Train of Vehicles from IRC: 6-2010 which was having ground contact area of (125\*175). A circular plate with radius of 167 mm with equivalent area of wheel load was used in this study. The thickness of loading plate was large enough that it can be considered as rigid plate with negligible bending while applying the load.

#### **3.1.3 Soil chamber**

In order to perform the large scale testing, a soil chamber of (900\*900\*1000) mm is fabricated by using 6 mm steel sheets (Figure 3.2). One side of the chamber is provided with Perspex sheet to view the deformation of the soil sample while testing. A sand outlet is provided on one side of the chamber to collect the sand from the box after completing the experiment.



**Figure 3.2: Soil chamber (900\*900\*1000) mm**

### 3.1.4 Compactor

It is not an easy task to acquire an undisturbed sand sample with cost effectiveness, so reconstituted samples made by using disturbed material are widely used for laboratory testing. The aim of preparing reconstituted specimens is to exactly simulate the field properties such as relative density and soil fabric in the laboratory. The density of soil packing is one of the key factor that determines the ability of the sand bed to carry out all Geotechnical problems.

The knowledge of soil density and its likely variability are the needful factors to an experimentalist to simulate systematic laboratory studies on large non cohesive soil samples. In order to carry out plate load testing, foundation and retaining wall modelling the soil properties should be close to in situ condition. A pneumatically-operated piston vibrator was used to compact the samples inside the test chamber. This is a piston-type vibratory compactor (Model: BH-2 IGO, manufactured by NAVCO) with recommended FRL (filter-regulator-lubricator) unit. A steel plate of dimensions equal to 300mm x 300mm x 10 mm is bolted at the bottom of the compactor (**Error! Reference source not found.**). Total weight of vibrator with steel plate was about 18 kg. Based on the calibration studies, it was observed that the relative density of the backfill increases with increase in the compaction time and pressure in the vibratory compactor.

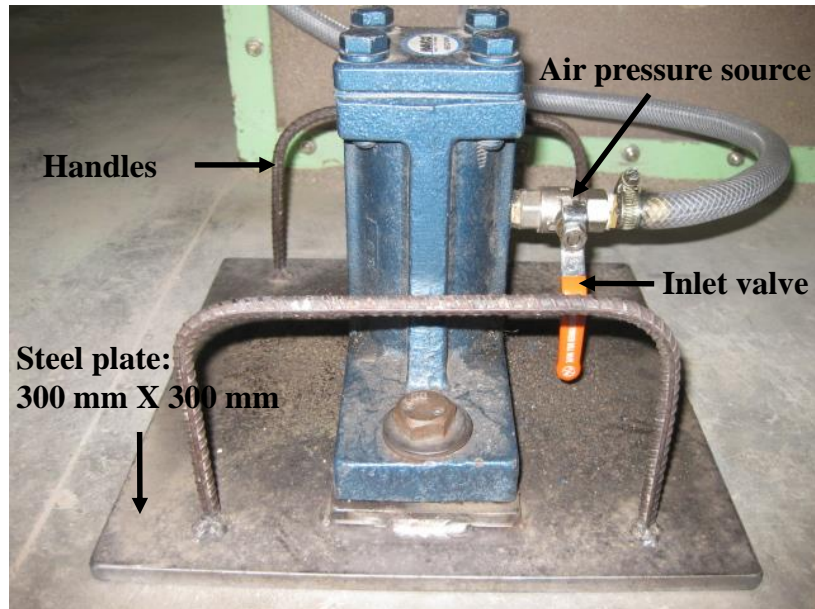


**Figure 3.3: Piston-type Vibrator connected to a steel plate (Model: BH-2 IGO, Manufactured by NAVCO)**

### **3.2 Instrumentation**

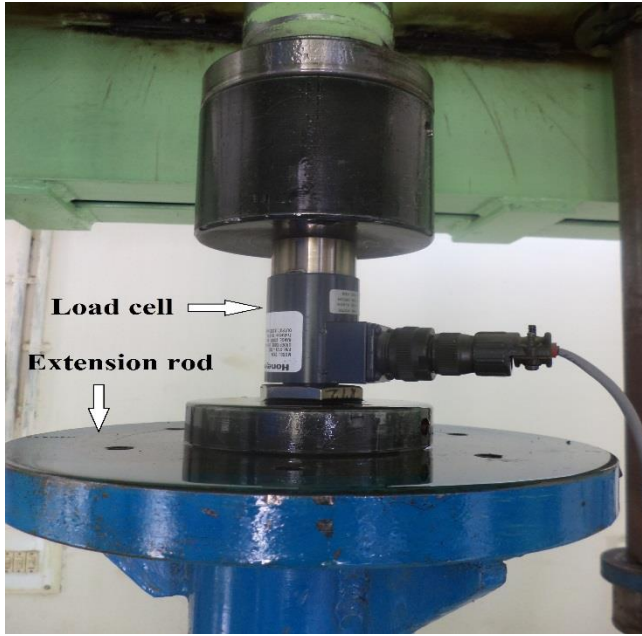
In order to control the accuracy of measurement due to distortions in material, there must be a control system with sequential measurement process which is continuous and gives precise values of actual tension in the material. HBM Data Acquisition System (DAQ) is used to collect the real-time data from the following sensors:

- Load cell
- Potentiometers or LVDT

Electronic load cells are transducers, in which the most sensitive component of measurement system is present. It measures very accurately, when mounted on a sensing or measuring roll in continuous contact with the material. A tension & compression in-line model load cell (Honeywell (Model: 3124)) is used in testing.

A captive guided JEC-C DLE model LVDT (make of Honeywell) as shown in Figure 3.4 (a) and potentiometers as shown in Figure 3.4 (b) are used to measure the settlements in the soil. This LVDT or potentiometers are placed at various distances on horizontal plane to measure the settlement profile.





(a)



(b)

**Figure 3.4: (a) Load cell, (b) Potentiometer**

### 3.3 Sample preparation

A locally available dry river sand was placed and compacted in lifts in the soil chamber. The thickness of each layer is taken as 200 mm. The thickness of each lift is determined from number of trial tests. This trials are done for getting targeted relative density in a calibration box with (600\*600\*600) mm dimensions with variation of pressure intensity in pneumatic vibrator and time taken for compaction of each lift.

In order to achieve the targeted relative density, the vibrating pressure varied from 100 kPa to 300 kPa in pneumatic vibrator and time of vibration is varied as 30 sec, 60 sec and 90 seconds per unit area. Unit area is considered as the area of plate which is connected to pneumatic vibrator. Different targeted relative densities are achieved from several trials with variation of pressure and time of vibration, (ex. For 92% relative density, the pressure required is 100 kPa and the time of vibration is 90 seconds per unit area). Each lift is compacted by traversing the pneumatic vibrator uniformly with time. The pattern of traversing is initially along the walls of soil chamber and then the inner portion of the soil chamber. The same procedure is followed for all lifts in the preparation of the sample in the soil chamber for all model tests. The testing bed is compacted to a relative density of 92% for the present study.

### 3.4 Materials Properties

The experiments are conducted in such a way that it simulates the site conditions such as interactions that take place between the structural components of the integral bridge and the soil and the preparation of subgrade and granular sub-base layers.

#### 3.4.1 Sand

##### 3.4.1.1 Gradation analysis

A locally available dry river sand is used in this study as backfill material with coefficient of uniformity,  $C_u$ , equal to 2.42, and the coefficient of curvature,  $C_c$ , equal to 0.99, and the effective particle size,  $D_{10}$ , equal to 0.34 mm. The specific gravity of the soil was obtained as 2.64. The maximum and minimum dry unit weights of the sand were obtained as  $17.8 \text{ kN/m}^3$  and  $15.1 \text{ kN/m}^3$ , respectively. According to Indian Standard Soil Classification System, the soil is classified as poorly-graded sand (SP). **Error! Reference source not found.**3.5 shows the gradation curve for the dry river sand.

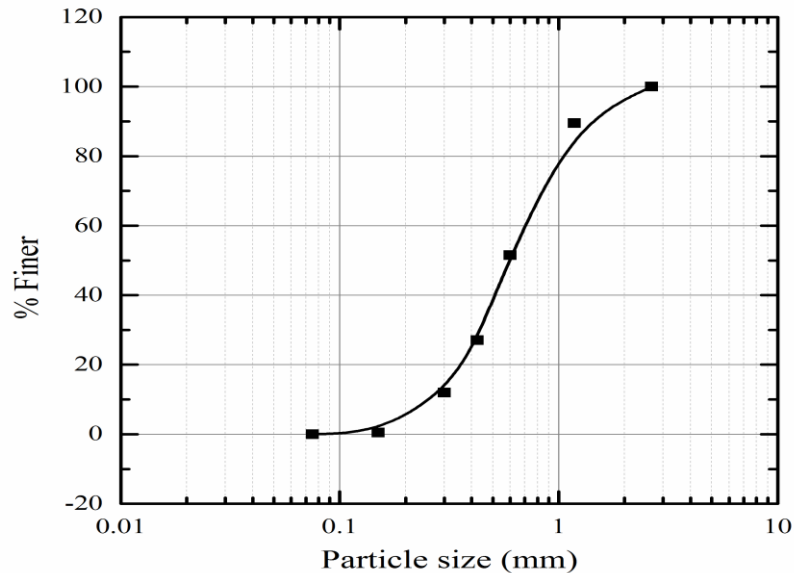


Figure 3.5: The gradation curve for River sand

##### 3.4.1.2 Shear parameters of sand

The shear strength of the soil is the most important aspect of geotechnical engineering. The shear strength of soil is the resistance to deformation by continuous shear displacement of soil particle or on masses upon the action of shear stress. The method used to determine the shear characteristics, i.e., angle of shear resistance and cohesion intercept, in the laboratory must be understood in detail in order to permit an

intelligent application of laboratory results to field application. The measurement of shear parameters of soil involves certain test observations at failure with the help of which the failure envelope or strength envelope can be plotted to a given drainage conditions. Laboratory testing can be used for determining the peak friction angle  $\Phi'_p$  of the fill material, which are placed under specified conditions. In the present study, shear parameters was determined in the laboratory using direct shear test.

Direct shear test is a simple and commonly used test and was performed in a shear box apparatus. The size of the specimens used in the present study was equal to 300 mm x 300 mm and about 200 mm high.

### ***Preparation of specimens***

The relative density is used to define the state of the soil sample prepared. It is based on the maximum unit weight, minimum unit weight, and natural unit weight. The correct prediction of relative density is not possible since it is difficult to obtain the maximum and the minimum unit weight values within a definite accurate range. Reconstitution of soil samples to a target relative density is the fundamental in analysis of geotechnical problems. In the present study, the sample was prepared using pluviation method to obtain the targeted relative density. Pluviation of sand particles through air is the most preferred method as it produces reasonably homogenous specimens and replicates the soil fabric similar to the process of natural deposition of sands (Oda et al. 1978).

Calibration was done to obtain target relative density by dry pluviation method. Relative density obtained from pluviation method depends on the opening size of the mesh and height of drop of sand particle. Figure 3.6 shows the preparation of sand specimen in the large-size direct shear box using pluviation method.



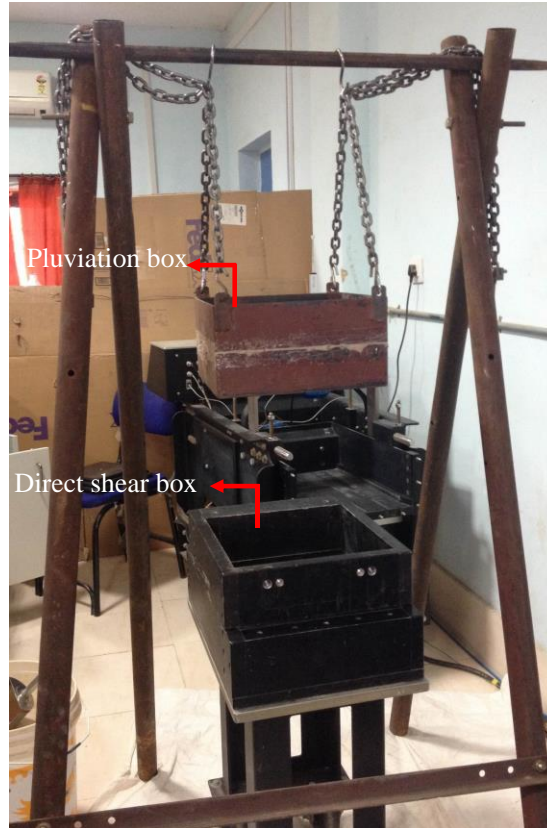


**Figure 3.6: Sample preparation by pluviation method**

In the present study, a drop height equal to 50 cm and two sieves with opening sizes equal to 6mm and 4mm, respectively, were adopted to achieve a target relative density of 88%. Direct shear tests were repeated on three similar specimens at various normal stresses. Figure 3.7 shows the plot of shear stress against horizontal displacement for dry dense sands. These observations were obtained from a strain-controlled test.

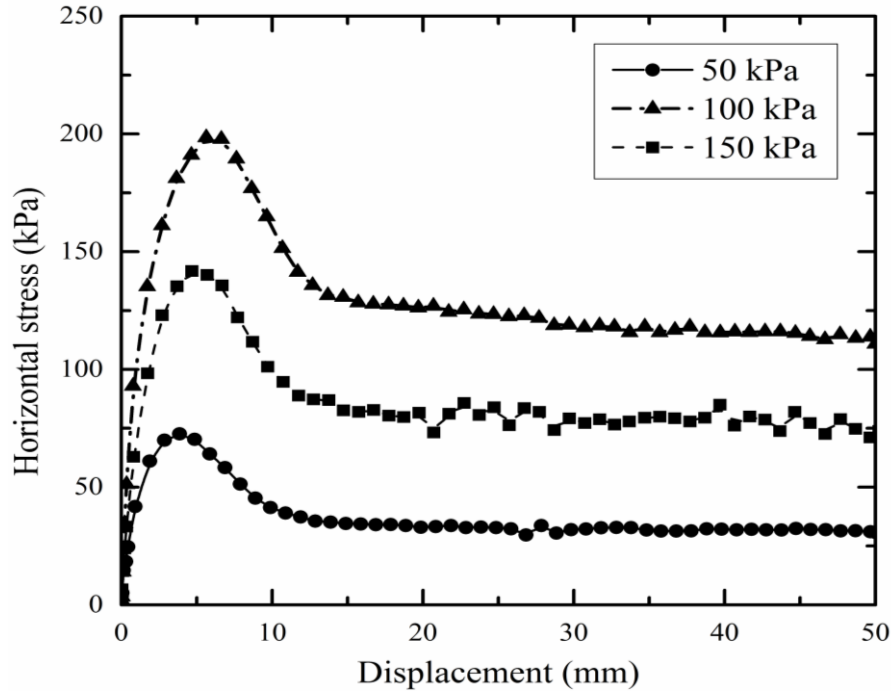


**Figure 3.7: Plot of shear stress against shear displacement for dry sand from direct shear tests.**

The normal stresses and the corresponding values of shear strength,  $\tau_f$ , obtained from a number of tests are plotted on a graph from which the shear strength parameters were determined. The peak values of shear stress were considered and were referred to as the peak shear strength. **Error! Reference source not found.** 3.7 shows the variation of shear stress with horizontal displacement of the lower box. Figure 3.8 shows the plot of shear stress at peak state with the normal stress applied on the samples. It is important to note that, in dry sands

$$\sigma = \sigma'$$

$$c' = 0$$

It is important to note that in situ cemented sands may show  $c'$  intercept, which is apparent cohesion intercept.

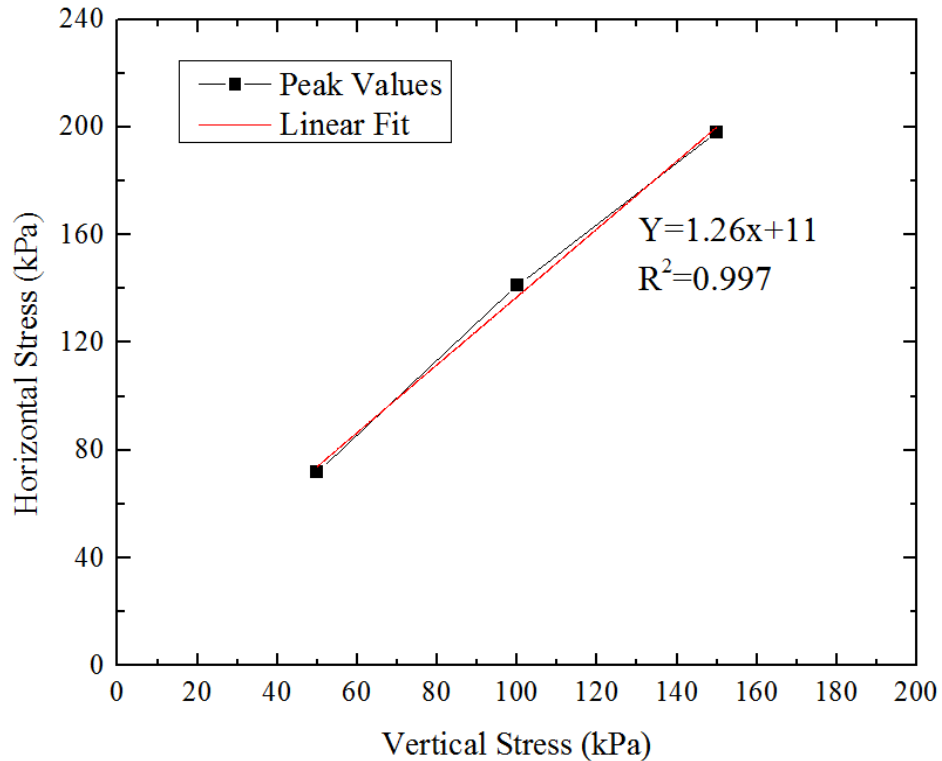


**Figure 3.8: Failure envelope for dry sand from direct shear tests**

The equation for average line obtained from above plot is

$$\tau_f = c' + \sigma' \tan \Phi' \quad \dots\dots\dots (1)$$

i.e.

$$y = 11 + 1.26x$$

So, friction angle can be determined as follows,

$$\Phi' = \tan^{-1} \left( \frac{\tau_f}{\sigma'} \right)$$

$$\Phi' = \tan^{-1}(1.26)$$

$$\Phi' = 51^\circ$$

From the above observations of fitted regression line it is concluded that the sand specimen used in the present study has cohesion intercept of  $c'$  as 11 kPa and the peak angle of internal friction ( $\Phi'_p$ ) of  $51^\circ$ .

### 3.4.1.3 Elastic modulus of sand

The modulus of elasticity of soil is an important soil parameter used in estimation of settlement under static or dynamic loads. This represents the ratio of stress and strain, when the material is within elastic limit. Elasticity assumes that the strains experienced by the soil and are linearly related to the stresses applied. Briaud (1997) proposed that the modulus of elasticity of a material depends on various factors such as the

loading process, soil particle organization, and water content, etc., though for a single specimen at different penetration involves different modulus values of that material.

### ***Methodology***

For determining the modulus of elasticity of sand, a large scale tests were done in testing tank with circular load. Dimensions of the testing tank is 900x900x1000 mm. A circular plate of 167 mm diameter and 20 mm thickness was used for applying uniform load. As the tank dimensions are much higher when compared to loading plate dimension, it was assumed as semi-infinite testing condition. In this study, the sand was compacted to a relative density of 92% with pneumatic vibrator. Figure 3.9 shows the full scale testing setup.

According to Briaud (2000), the modulus of elasticity is not the slope of stress strain curve. Hence in this study, finite element analytical software PLAXIS 2D (PLAXIS 2D Version 9.0 (PLAXIS 2008)) is used to obtain the modulus of elasticity. It is done by back calculating using the data points, i.e., the amount of load at specific settlement. The experimental model was simulated in PLAXIS 2D. Several simulations were done in PLAXIS and appropriate value of elastic modulus was calculated.

### ***Experimental load test***

The aim of this full scale load test is to obtain the data points. Though loading was applied using hydraulic system, the amount of load applied on the plate was determined with the load cell which was mounted in between extension rod and hydraulic cylinder. Settlement of circular plate was determined using LVDT which was placed on the plate. It was supported by a stand which connected from testing box as shown in Figure 3.9. Loading is applied in a step wise manner to simulate the static load. The load was kept constant for 3 minutes to stabilize the load distribution. A data acquisition system was used to collect the data points at 10Hz frequency.



**Figure 3.9: Determining the Modulus of elasticity of sand bed experimentally**

### *Numerical analysis*

A finite element (FE) analysis of the load settlement behavior of a circular footing resting on semi-infinite sand beds was carried out using commercially available finite element software package PLAXIS 2D(Version 12). PLAXIS is a user friendly software popular for geotechnical engineering applications.

The FE analyses were carried out using an axisymmetric model. The mesh boundaries were fixed based on the testing tank dimensions. Preliminary analyses were done to fix the boundary distances such that the boundary distance should not affect the results. The boundary conditions in PLAXIS was defined as full fixity ( $\Delta x=0$ ,  $\Delta y=0$ ) at the base of the geometry and smooth conditions ( $\Delta x=0$ ) at vertical sides. The settlement of a rigid footing was simulated using non-zero prescribed displacement.

In order to simulate the behavior of the soil, a suitable soil model and appropriate material parameters must be assigned to the model. PLAXIS provides different constitutive models. As the sand used in the laboratory testing behaved non-linearly, Mohr-Coulomb model was used in PLAXIS. The basic soil parameters based on non-linear behavior can be obtained from direct-shear tests; internal frictional angle and cohesion intercept. The modulus of elasticity also required for Mohr-Coulomb model. Even though more advanced soil models are available, the Mohr-Coulomb model was considered for the purpose of investigating the modulus of elasticity of soil model. The sand medium was modeled using 15-noded triangular elements.

Figure 3.10 (a) shows the model in PLAXIS 2D. The material properties for sand medium used in PLAXIS was given in Table 3.1.

Table 3.1 Material properties of sand used in PLAXIS

| Material Properties             |                 |
|---------------------------------|-----------------|
| Unit weight(kN/m <sup>3</sup> ) | 17.5            |
| Cohesion (kPa)                  | 1               |
| Angle of shearing resistance    | 51 <sup>0</sup> |
| Poisson's ratio                 | 0.3             |
| Dilatancy angle                 | 21 <sup>0</sup> |
| Prescribed displacement (mm)    | 5               |

PLAXIS provides an automated mesh generation system, in which the model is discretized into standard elements. A mesh sensitivity analysis was conducted to determine a suitable mesh density and in this study a medium size mesh was adopted for the further analyses. An example of FE mesh comprising of soil and foundation is illustrated in Figure 3.10 (b).

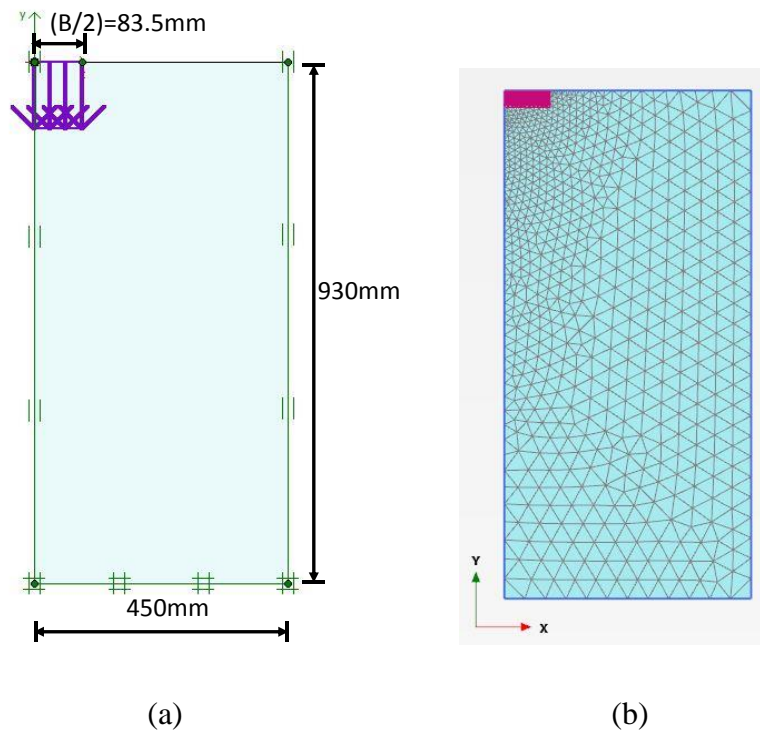
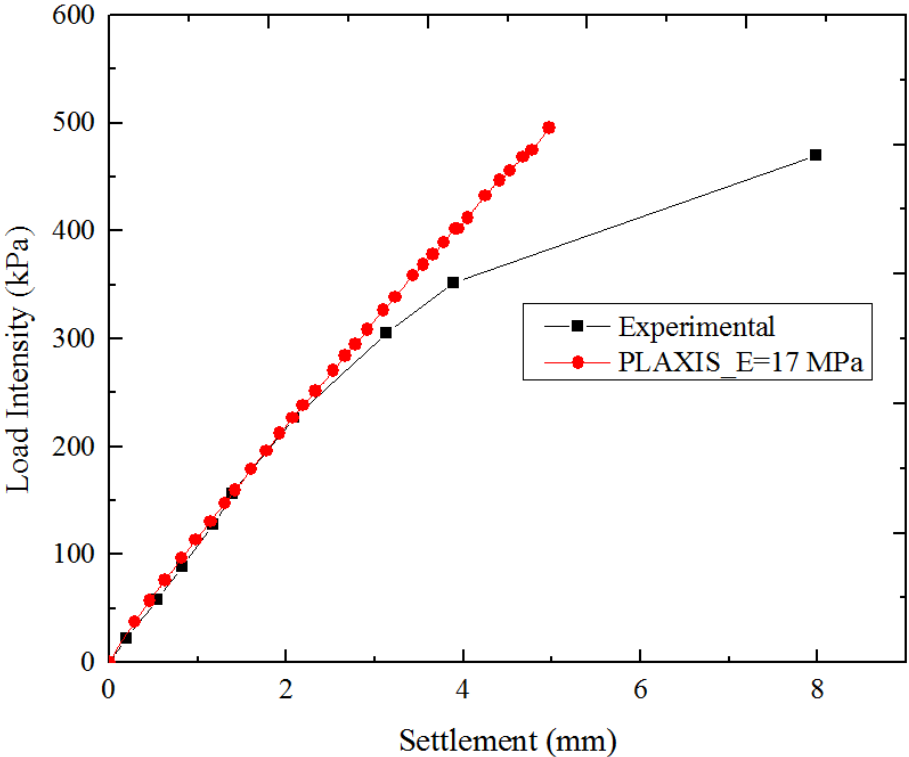


Figure 3.10: (a) Geometric model showing boundary conditions, (b) FE mesh for model

Small-strain FE analyses were carried out in PLAXIS and therefore, a comparison between numerical and experimental results was considered only for settlements up to 2mm, beyond which the numerical results severely deviate from experimental results. Figure 3.11 shows the comparison of load settlement behavior between experimental data and numerical modelling (PLAXIS) with  $E_s$  of soil equals to 17 MPa.



**Figure 3.11: Comparison of load settlement behavior for experimental and from PLAXIS**

**Analytical**

It is necessary to describe the stress strain behavior of the soil in quantitative terms, to perform the non-linear stress analysis and to develop techniques for incorporate this behavior in analyses. Duncan and Chang (1970), described a simplified, practical nonlinear stress-strain relation for soils which is convenient for use with the finite element method of analyses. The two parameters involved in this relation are  $c$  and  $\Phi$ , the Mohr-Coulomb strength parameters. There are different factors which influences the nonlinear stress-strain behavior of any type of soil such as density, water content, drainage conditions, duration of loading, stress history, confining pressure and shear stress. It may be possible to take account of this factors in many cases and to simulate corresponding field conditions, by taking care in selection of soil samples and maintaining proper testing conditions. When this can be done accurately, it would be expected that the results from the laboratory would be representative of the same field stress conditions.

Kondner (1963) reported the nonlinear stress-strain curves for sands may be approximated by hyperbola with a high degree accuracy. The hyperbolic equation proposed by Kondner was

$$(\sigma_1 - \sigma_3) = \frac{\epsilon}{(a+b\epsilon)} \quad \dots\dots\dots (2)$$

In which  $\sigma_1$  and  $\sigma_3$  = the major and minor principal stresses,  $\epsilon$  = the axial strain, a and b = constants whose values may be determined experimentally. Both of these constants a and b have readily visualized physical meanings. As shown in Figure 3.12 (a), a is the reciprocal of initial tangent modulus, E, and b is the reciprocal of the asymptotic value of stress difference which the stress-strain curve approaches at infinite strain  $(\sigma_1 - \sigma_3)_{ult}$ .

Kondner stated that the values of coefficient of a and b may be determined most readily if the stress-strain data potted are on transformed axes as shown in Figure 3.12 (b). Then the above equation is rewritten in the following form

$$(a + b\epsilon) = \frac{\epsilon}{(\sigma_1 - \sigma_3)} \quad \dots\dots\dots (3)$$

It may be noted that a and b are the intercept and the slope of resulting straight line respectively. By plotting the stress-strain data as shown in Figure 3.12 (b), it is easy to determine the values of the parameters a and b corresponding to best fit between hyperbola and test data.

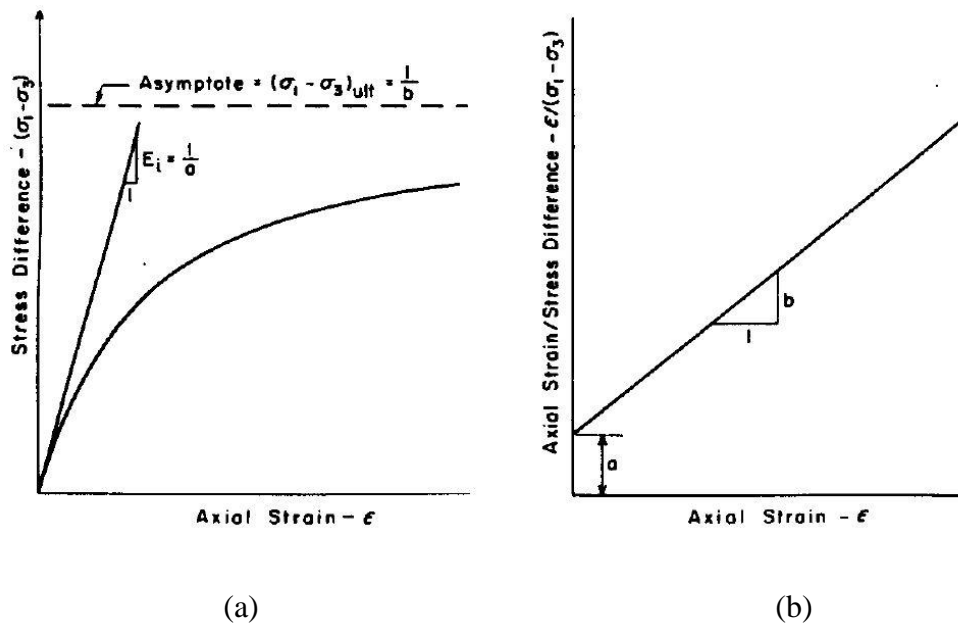


Figure 3.12: (a) Hyperbolic stress-strain curve, (b) Transformed hyperbolic stress-strain curve (Duncan & Cheng, 1970)



In order to fit a hyperbola to the test data, MATLAB software was used in the present study. MATLAB is a high-level language and interactive environment for numerical computation, visualization, and programming. An inbuilt tool named curve fitting tool is available in MATLAB software with which it is very easy to perform functions for fitting linear and nonlinear curves and surfaces to test data. It is possible to fit the curve for any type of model by giving the model equation and it gives the intercept and slope of that model curve directly. Figure 3.13 shows the best fit of hyperbola to the test data for finding the intercept and initial slope of the curve.

From the Figure 3.13 the intercept and slope of the curve were determined. The reciprocal of the initial tangent modulus which can also called as the modulus of subgrade reaction ( $k_s$ ) was found to be  $144\text{MN/m}^3$ .

The modulus of subgrade reaction is a conceptual relation between the soil pressure and the deflection that takes place in the foundation members. Vesic (1961) proposed that the modulus of subgrade reaction can be computed using the stress-strain modulus  $E_s$  as

$$k_s = \frac{E_s}{B(1-\mu^2)} \dots\dots\dots (4)$$

Where  $E_s$  = modulus of the soil,  $B$  = width of the footing, and  $\mu$  = Poisson's ratio. By using Vesic equation, the modulus of elasticity of the sand is found to be  $E_s = 17 \text{ MPa}$ .

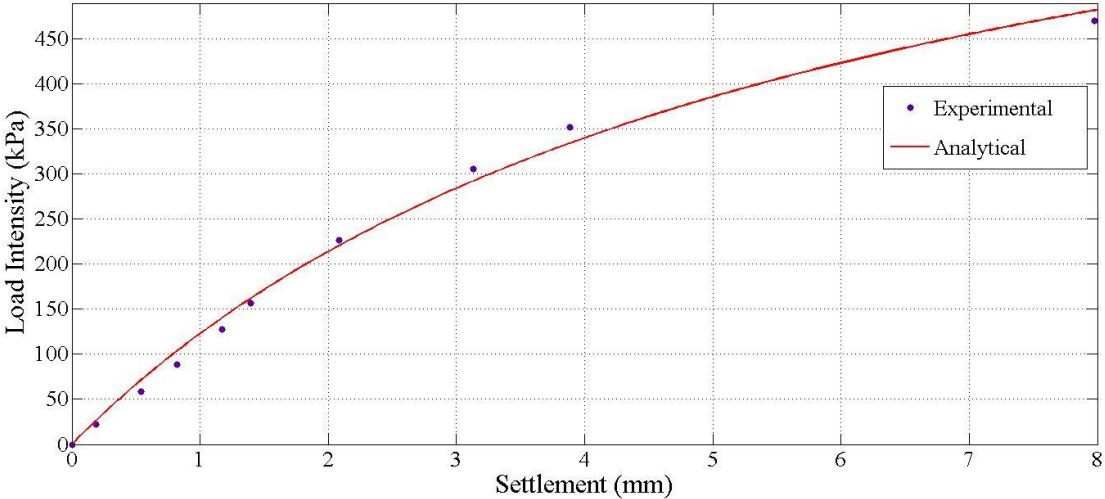


**Figure 3.13: Hyperbola curve fitting to the test data**

From the above studies experimental test data has been verified using PLAXIS 2D modelling and fitting nonlinear curve using MATLAB to the test data. With these results it was concluded that for the soil samples prepared for full scale load tests, the modulus of elasticity ( $E_s$ ) is  $17 \text{ MPa}$ .

### 3.4.2 Granular Sub Base (GSB)

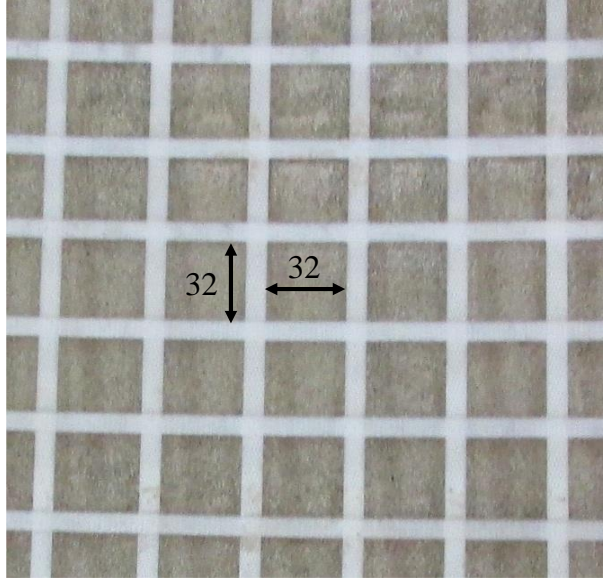
For modelling granular sub-base, a uniform mixture of sand and aggregates was prepared according to the proportions of MORTH (Fourth revision) specifications. This granular sub-base material is graded as coarse graded Granular Sub-Base material according to MORTH specifications for Road & Bridge works, Fourth revision. The grading of the GSB material is given in Table below.

Table 3.2 Grading for Granular Sub-Base material

| IS Sieve Designation | % weight passing through IS Sieve |
|----------------------|-----------------------------------|
| 75 mm                | -----                             |
| 53.0 mm              | 100                               |
| 26.5 mm              | 50-80                             |
| 9.5 mm               |                                   |
| 4.75 mm              | 15-35                             |
| 2.36 mm              |                                   |
| 0.425 mm             |                                   |
| 0.075 mm             | <10                               |

### 3.4.3 Reinforcement (Geogrid)

The reinforcement used for model tests in this study was Secugrid® 40/40 Q1 biaxial geogrids. It is a biaxial geogrid with an aperture size of 32mm and the ultimate tensile strength of geogrid is 40 kN/m. The tensile modulus of the geogrid at 1% and 2 % strain is 800 kN/m and 600 kN/m respectively. Figure 3.14 shows the geogrid used in the present study



**Figure 3.14: Geogrid (Secugrid® 40/40 Q1 biaxial geogrid)**

### **3.5 Results and Discussions**

The objective of the experimental investigation is to reduce the differential settlement by replacing the traditional approach slab with proposed geogrid reinforced granular beds. It is very difficult to simulate the exact field condition of interaction between the approach slab and abutment, as it has the abutment step over which the approach slab will rests. This condition is simulated by placing concrete blocks on one side of the soil chamber. The experimental investigation includes studying the various parameters which reduces the differential settlement effectively with reinforced granular beds instead of traditional concrete approach slabs. The parameters such as thickness of top granular sub-base layer, length of reinforcement, initial depth of reinforcement from top and the effect of edge distance of wheel load from edge of an abutment were studied thoroughly and optimum values are found.

#### **3.5.1 Optimum thickness of Granular Sub-base layer ( $H_1$ )**

The best program consists primarily of load tests with circular wheel model placed on embankment fill material with varying the thickness of top layer ( $H_1$ ) i.e. thickness of Granular Sub Base material without reinforcement. Figure 3.15 shows the schematic diagram of full scale model.

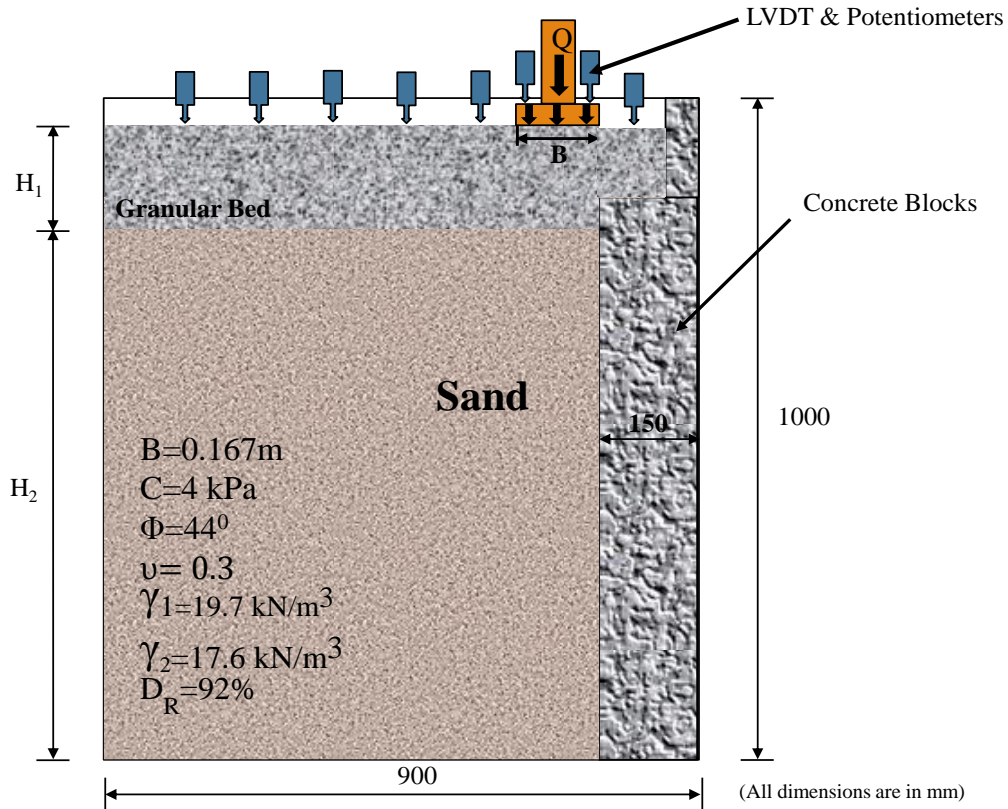


**Figure 3.15: Schematic diagram of full scale loading setup**

Initially the soil chamber was filled with sand in 4 layers and compaction is done with pneumatic vibrator uniformly to get a relative density up to 92 %. The thickness of fill material layer ( $H_2$ ) i.e. sand layer was assumed to be constant to avoid the effect of bottom layer. The thickness of sand layer was considered as 81 cm thick throughout the study. The thickness of each layer was selected based on experimental trials for achieving the targeted relative density for entire sand bed. A layer of compacted granular sub-base was laid over the sand layer and thickness was varied from  $0.48B$ ,  $0.72B$ ,  $0.96B$  and without any granular sub-base layer. Figure 3.16 compares the load-settlement response of circular wheel load on sand bed with different thickness of granular sub-base layer over it.

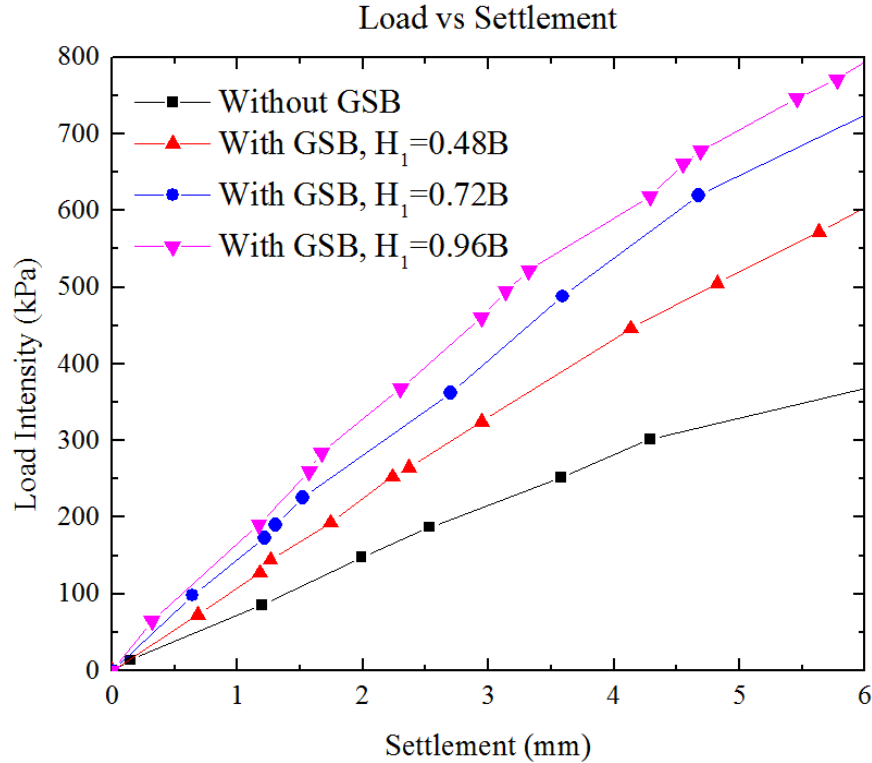


**Figure 3.16: Load settlement behavior for various  $H_1$**

Addition of granular layer over the sand bed improving the load intensity for a particular settlement significantly. With respect to the case without granular bed, the improvement in average load intensity for a particular settlement was 67%, 100% and 122% as the thickness of granular sub-base layer was increased to 0.48B, 0.72B and 0.96B respectively. The rate of improvement in the average load intensity was observed as 50% when the thickness of granular layer increased from 0.48B to 0.72B. But thereafter the rate improvement in load intensity was decreased to 22 % as thickness was increased from 0.72B to 1B. It was observed that the improvement in load-settlement response was minimum when  $H_1/B$  was increased from 0.72B to 1B. It was clearly understood that increase in the thickness of granular sub-base layer beyond 0.72 times the diameter of the wheel load would not contribute to the improvement of load intensity greatly. So, the optimum thickness of the granular bed is considered as 0.72 times the diameter of the wheel load. And this thickness is maintained in the further parametric studies.

The surface settlement are calculated using potentiometers placing at various distances from the wheel as shown in Figure 3.15. The surface settlement profiles for various thickness of GSB layer including without GSB layer is shown in Figure 3.17. From the plot it infer that the GSB layer plays a key role in reducing the settlement below wheel load and less heave formation around the wheel load was found when compared to the case without granular bed. The formation of heave in the case of absence of GSB clearly indicates

that the punching failure occurs in fill material. It can be concluded that the addition of granular bed will increase the bearing capacity of embankment fill and significantly reduce the settlements below wheel.

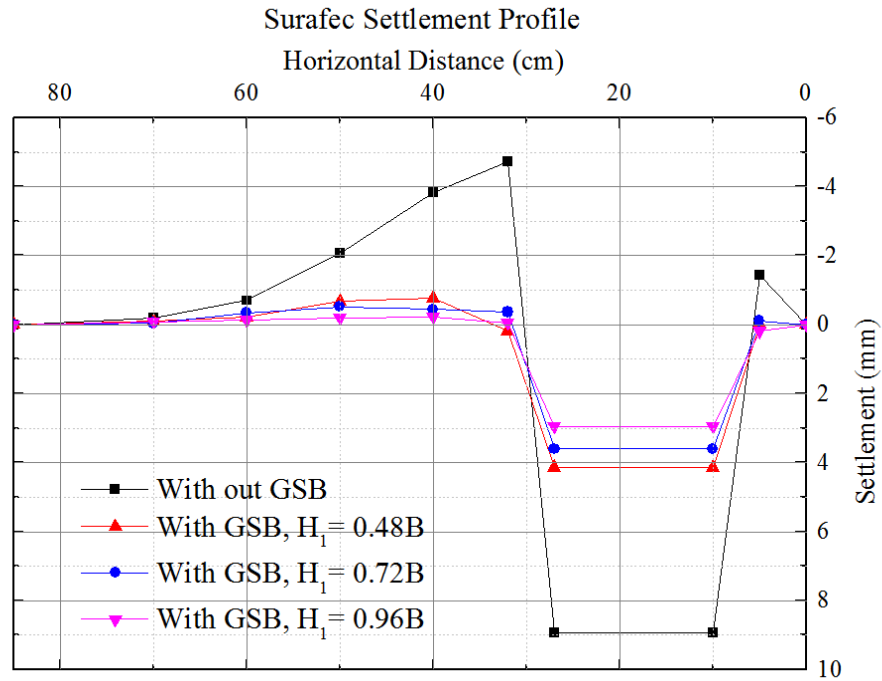
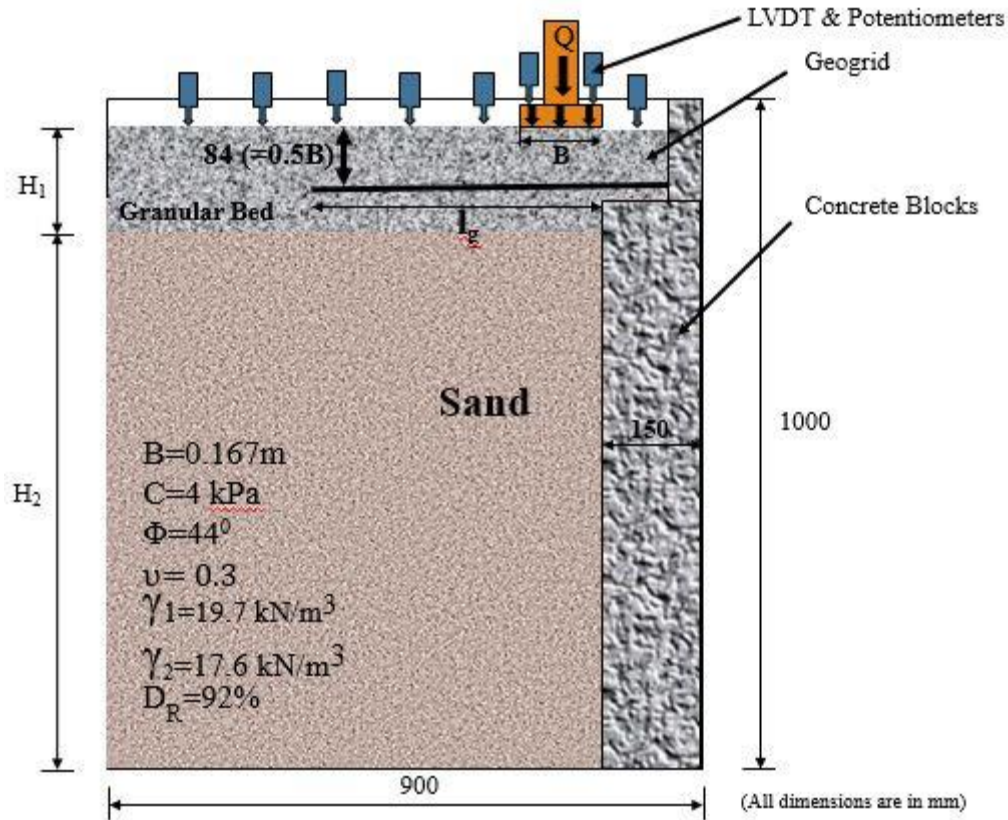


Figure 3.17: surface settlement profile for various  $H_1$

### 3.5.2 Optimum length of reinforcement ( $l_g$ )

In this series of tests, tests were conducted to investigate the optimum length of geogrid ( $l_g$ ) in improving the load-settlement response and decreasing the settlement near the abutments. Other parameters such as thickness of granular sub-base layer ( $H_1$ ) and the initial depth of reinforcement was kept constant as  $0.72B$  and  $0.5B$  respectively, to study the effect of length of reinforcement ( $l_g$ ). The length of geogrid ( $l_g$ ) is varied as  $3B$ ,  $3.5B$ ,  $4B$  and  $4.5B$  which were used to reinforce the granular sub-base layer. The length of reinforcement starts from the edge of an abutment. The Figure 3.18 shows the schematic view of model testing with geogrid reinforcement in granular bed.



**Figure 3.18: Model testing with Geogrid reinforcement**

The load-settlement response and the surface settlement profiles are compared in Figure 3.19 (a) and (b) for unreinforced and reinforced cases for various reinforcement lengths respectively. For the reinforcement length of  $3B$ , increase in the load intensity for a particular settlement was 31%, while the increase was 60% for the length of reinforcement as  $4B$ . The increase in the load intensity was attributed to the wide width effect. The reinforcement intersects the slip line and extends through the failure zone which results in increasing the load intensity with increase in the length of reinforcement. Figure 3.19 (a) shows the load intensity for lengths of reinforcement  $4B$  and  $4.5B$  are almost equal. It can be concluded that the increase in the length of reinforcement of more than four times the diameter of the wheel load does not result in significant improvement in load intensity for the wheel load.

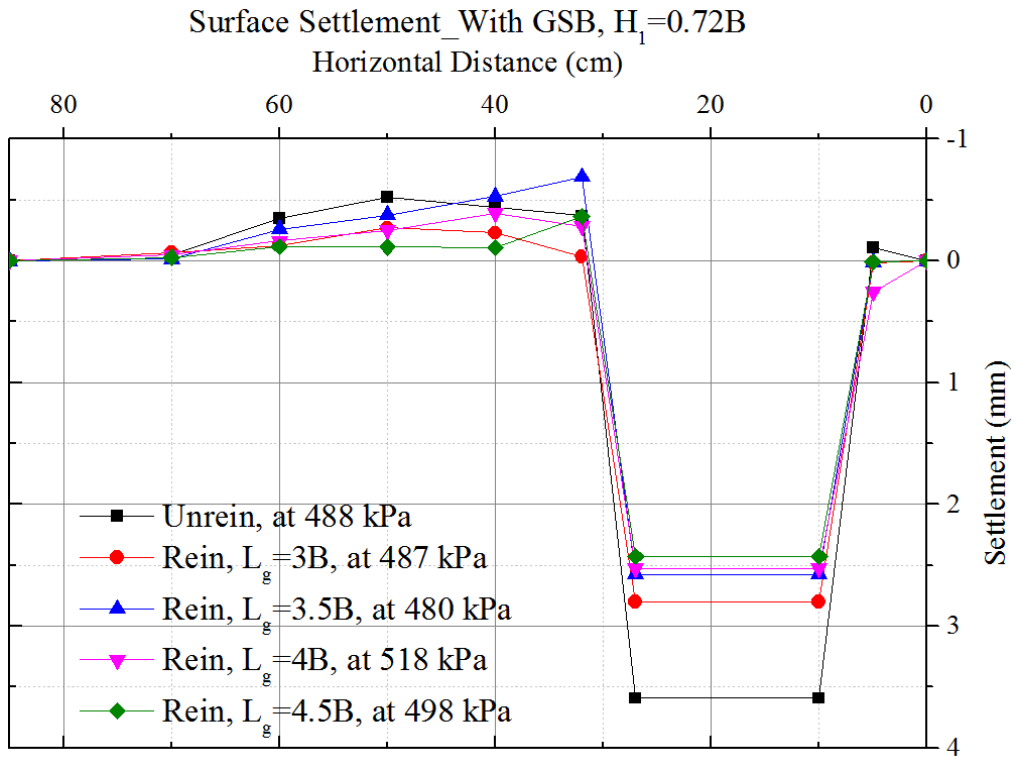
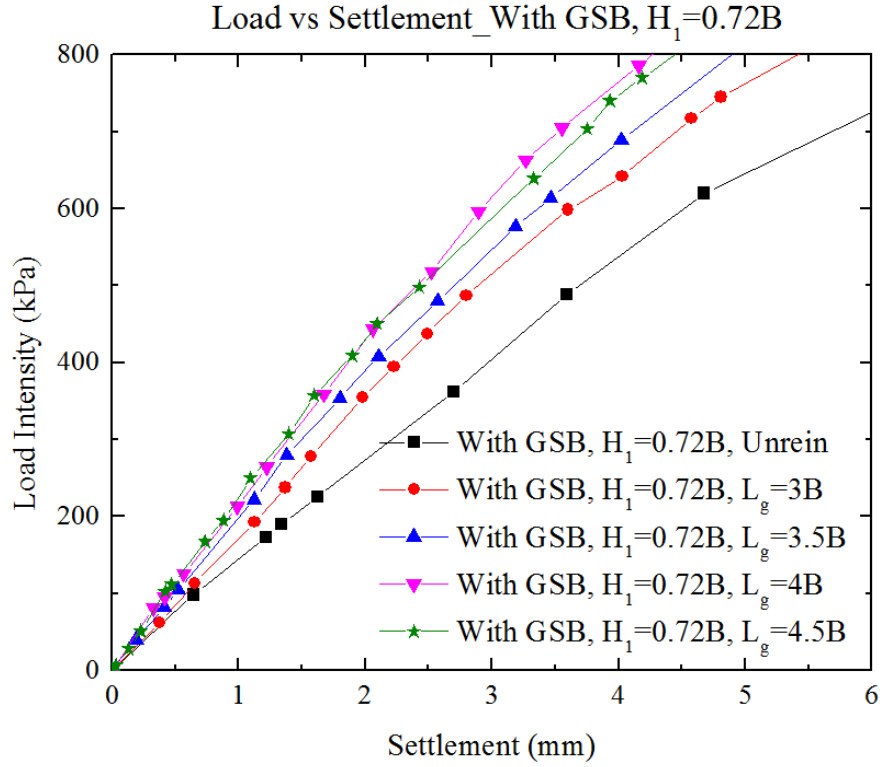


Figure 3.19 (a) Load settlement behavior, (b) Surface settlement profile, for the various  $l_g$



Figure 3.19 (b) shows the surface settlement profile along the horizontal distance of the model testing chamber. It was clear that reinforcing the granular sub-base layer decreases the settlement just after abutment i.e. heave formation or the differential settlement between abutment and reinforced granular sub-base layer. Bump formation was significantly reduced when the reinforcement length is  $4B$  when compared to other cases. It can be concluded that the optimum length of reinforcement is obtained as four times the diameter of wheel.

### 3.5.3 Optimum depth of reinforcement ( $d_i$ )

In this series of tests, the thickness of granular sub-base layer and the length of reinforcement was kept constant as  $0.72B$  and  $4B$  respectively to study the effect of initial depth of reinforcement from surface. The initial depth of reinforcement ( $d_i$ ) was varied as  $d_i = 0.3B, 0.4B, 0.5B$  and  $0.7B$ , where  $d_i$  is the depth of reinforcement from the surface of wheel load and  $B$  was the diameter of the wheel load. Figure 3.20 shows the schematic diagram of model test for finding the optimum initial depth of geogrid.

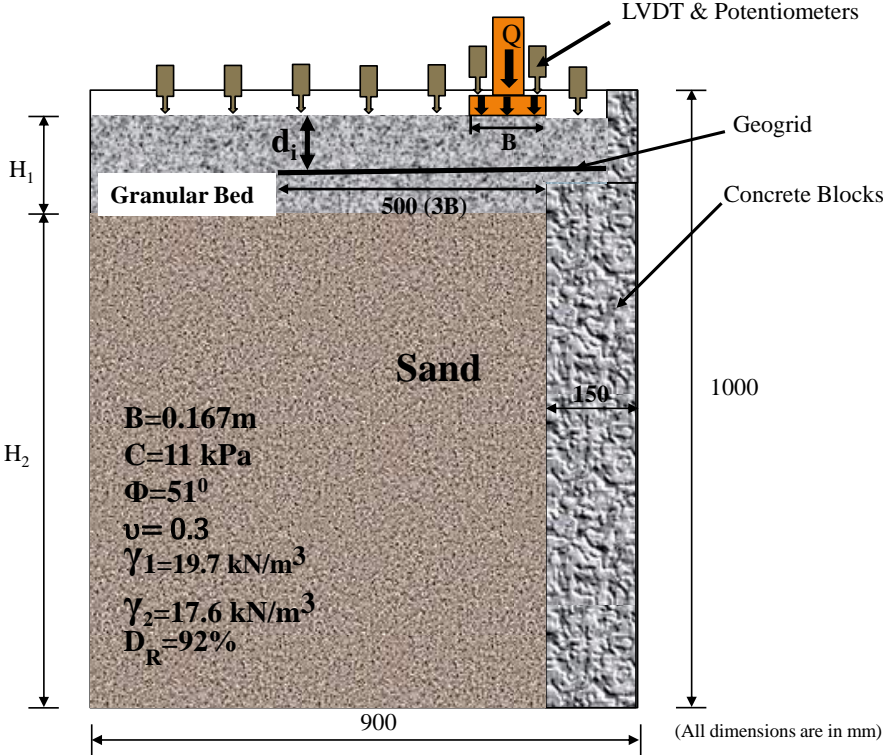
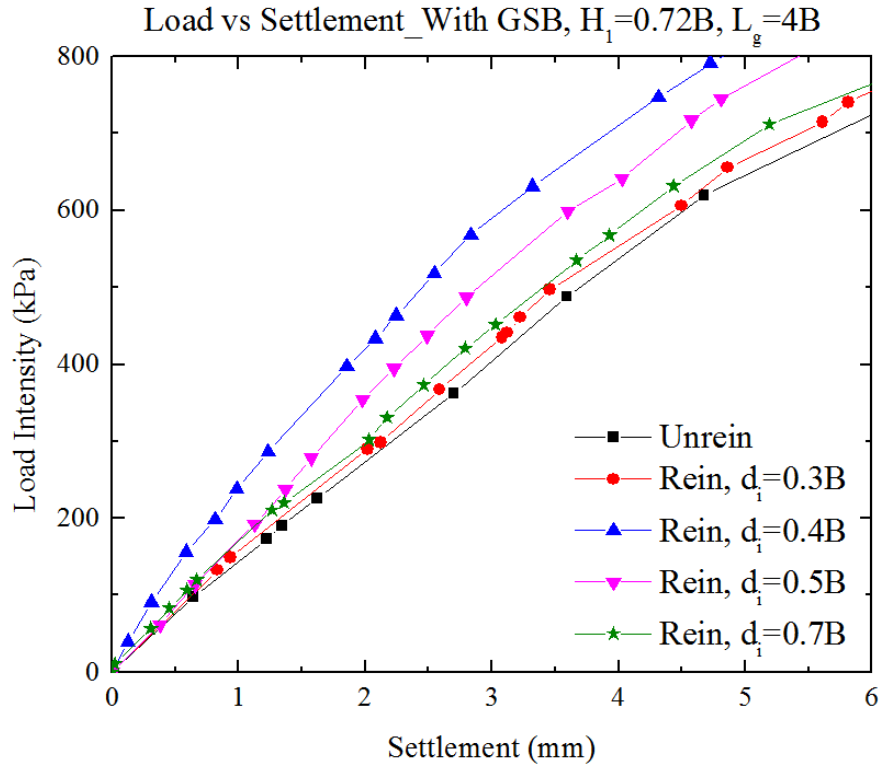
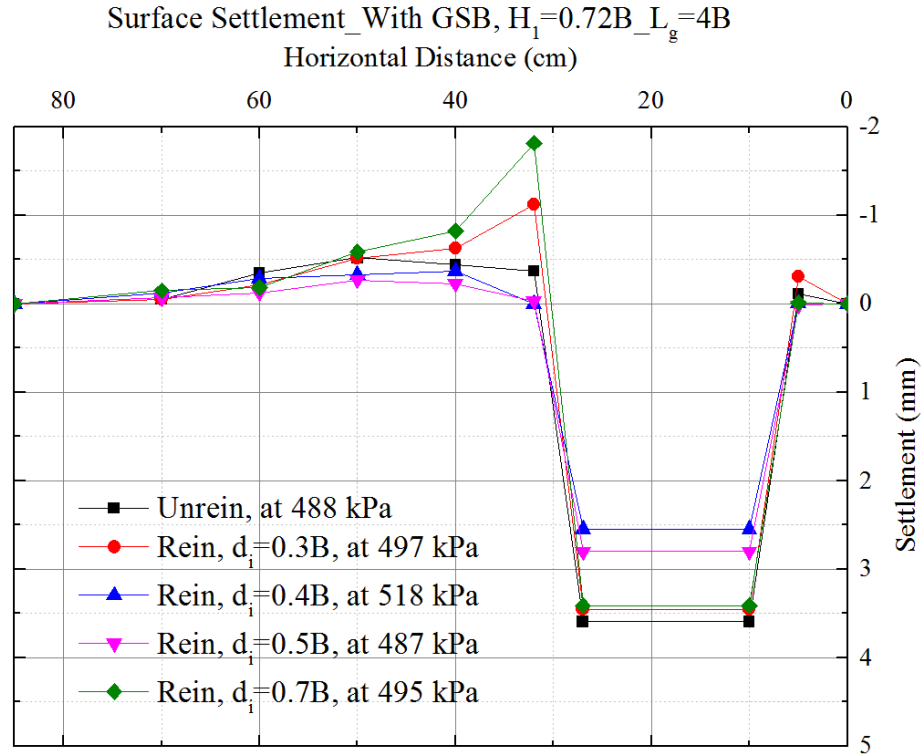


Figure 3.20: Model testing for finding initial depth of reinforcement ( $d_i$ )



**Figure 3.21: Load settlement plot for optimizing the initial depth ( $d_i$ ) of geogrid**

Figure 3.21 compares the load-settlement response curve for wheel loading on unreinforced and reinforced granular sub-base with varying initial depth of reinforcement ( $d_i$ ). The improvement in load intensity was about 33% for a particular settlement, when the depth increases from 0.3B to 0.4B, but thereafter the load intensity decreased with increase in the initial depth of reinforcement ( $d_i$ ). It was observed that the load intensity decreased when the depth of reinforcement ( $d_i$ ) was increased from 0.4B to 0.5B. So, it was clearly understood that the increase in the depth of placement of reinforcement beyond 0.4 times the diameter of wheel load would not contribute for the improvement of load intensity.



**Figure 3.22: Surface settlement profile for various initial depths ( $d_i$ ) of geogrid**

Figure 3.22 compares the surface settlement profile for wheel load resting on unreinforced and reinforced granular sub-base with varying depth of reinforcement ( $d_i$ ). It was observed that there was a significant decrease in the bump i.e. differential settlement between abutment and reinforced granular sub-base layer with the depth of reinforcement of  $0.4B$ , but thereafter the bump was increased with increase in the depth of reinforcement where reinforcement does not help in significantly decreasing the settlements. So, the depth of reinforcement of  $0.4B$  was considered as the optimum initial depth of placement of reinforcement ( $d_i$ ) from the surface as it decreases the heave formation and increases the load intensity at a particular settlement.

### 3.5.4 Effect of edge distance of wheel load from edge of an abutment ( $d_e$ )

This series of tests were conducted to investigate the effect of edge distance of wheel load from the edge of an abutment ( $d_e$ ). This study results in finding the distance effected by the wheel load with respect to occurrence of bump at interface of abutment and the reinforced granular sub-base layer. This also helps in finding the length of reinforcement required from the edge of abutment.. The thickness of granular sub-base layer was assigned as  $0.72B$ , length of reinforcement as  $4B$  and the depth of reinforcement as  $0.4B$  from surface of wheel load were kept constant where the edge distance between wheel load and abutment

was varied as  $d_e = 0$  to  $1.2B$  from the edge of the abutment. Figure 3.23 shows the schematic of model test used for the study of effect of edge distance of wheel from edge of an abutment.

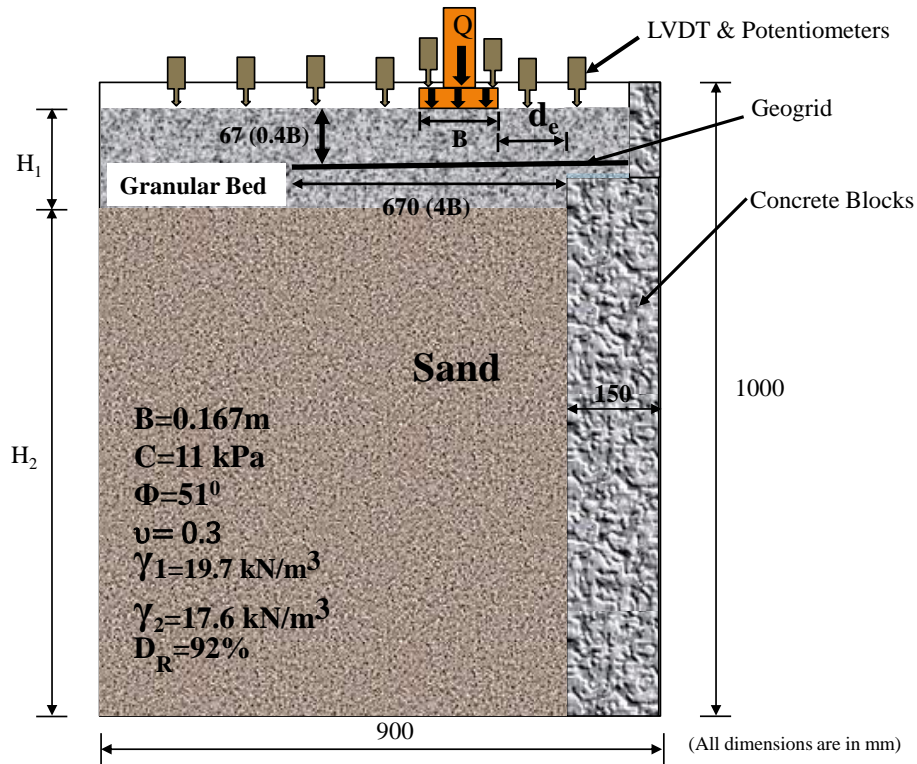
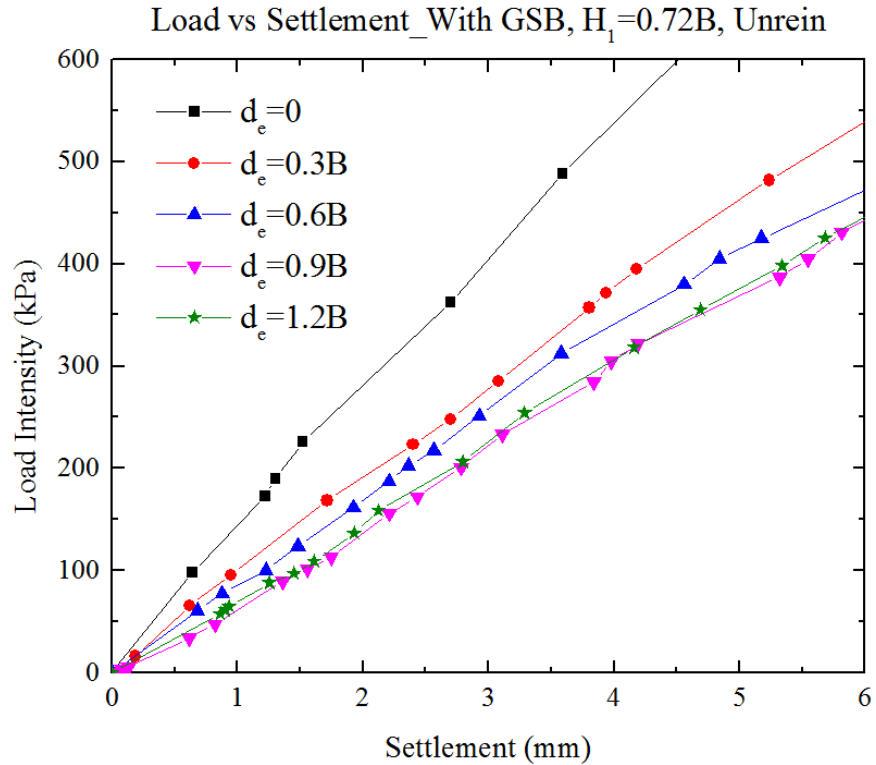


Figure 3.23: Model testing for studying the effect of edge distance of wheel from edge of an abutment ( $d_e$ )

This study aided in understanding the behavior of granular sub base layer in unreinforced and reinforced case which was subjected to wheel load. Figure 3.24 shows the load settlement behavior of GSB layer in unreinforced case. Results indicates that as the wheel moves towards the abutment, the GSB layer becomes stiffer and as the wheel approaches the abutment, most of the load might be taken by the structure element of bridge i.e. abutment.



**Figure 3.24: Load settlement behavior for unreinforced condition with variation of  $d_e$**

Where as in reinforced case, the GSB layer was gives more settlements as the wheel approaches nearer (i.e. till  $d_e=0.3B$  away from abutment) to the abutment. But from  $d_e=0.3B$  to  $d_e=0$ , the settlements reduced drastically. The reinforcement was playing a key role here in reducing the settlements just after the abutment. Figure 3.25 shows the load settlement behavior of GSB layer for reinforced case.

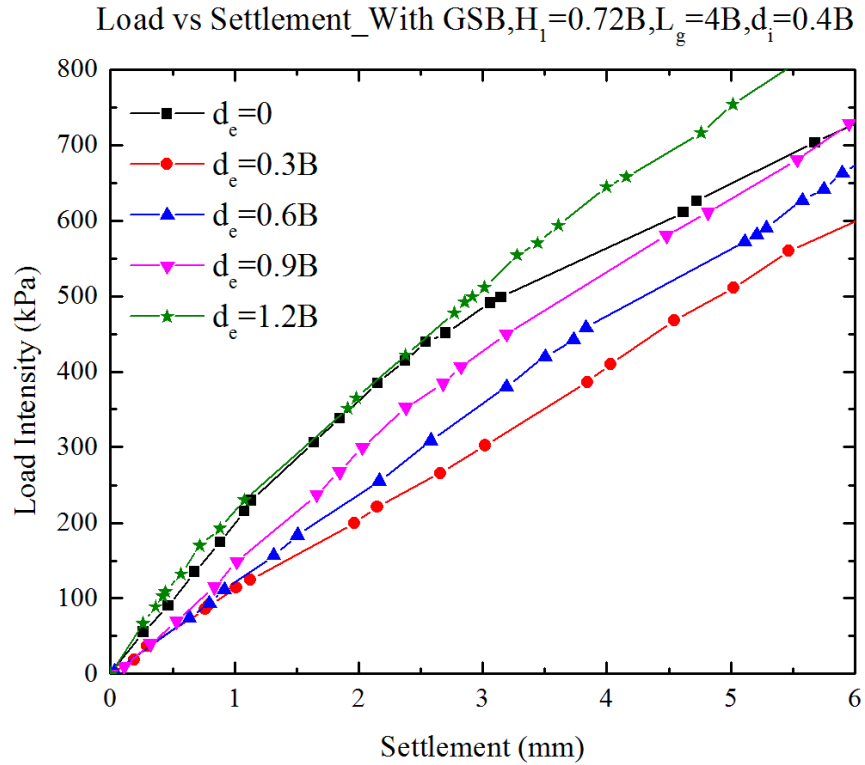


**Figure 3.25: Load settlement behavior for reinforced condition with variation of  $d_e$**

The behavior of GSB layer in reinforced case was completely different from unreinforced case. The reason might be the effect of reinforcement. As the wheel moves away from the abutment, the effective length of reinforcement for anchorage or interlocking with the granular sub-base material on abutment side will increase and therefore reduce the sagging of reinforcement which leading to the reduction in settlements. Figure 3.26 shows the surface settlement profile for the reinforced case. The formation of heave is negligible in the reinforced case.

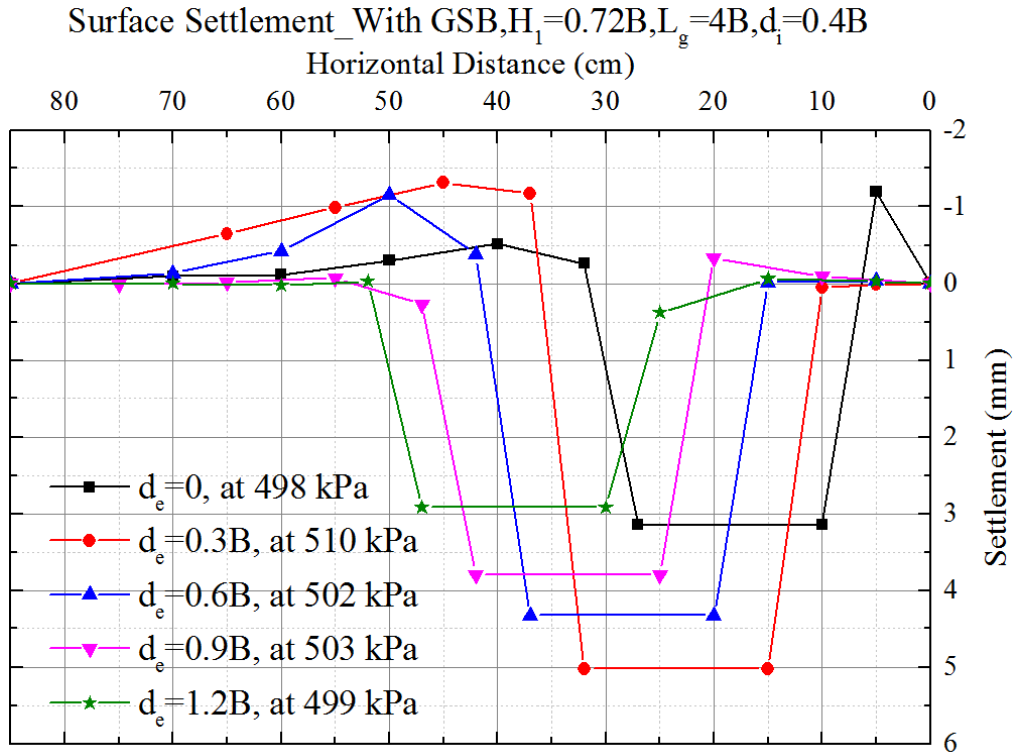


**Figure 3.26: Surface settlement profile for reinforced condition with variation of  $d_e$**

Introduction of reinforcement significantly improve the mechanical behavior of GSB layer. The comparison of results of load settlement response between unreinforced and reinforced GSB layer for  $d_e=0.6B$  is shown in Figure 3.27 (a). The reinforced GSB layer can reduce the settlements by 40% than unreinforced GSB layer at the load of 700 kPa. Figure 3.27 (b) shows the comparison of surface settlement profiles between unreinforced and reinforced cases for  $d_e=0.6B$ . The surface settlement plot indicates that the heave formation is negligible in the reinforced case. It can conclude that the introduction of reinforcement will significantly reduce the settlements and improve the mechanical behavior of granular layer.

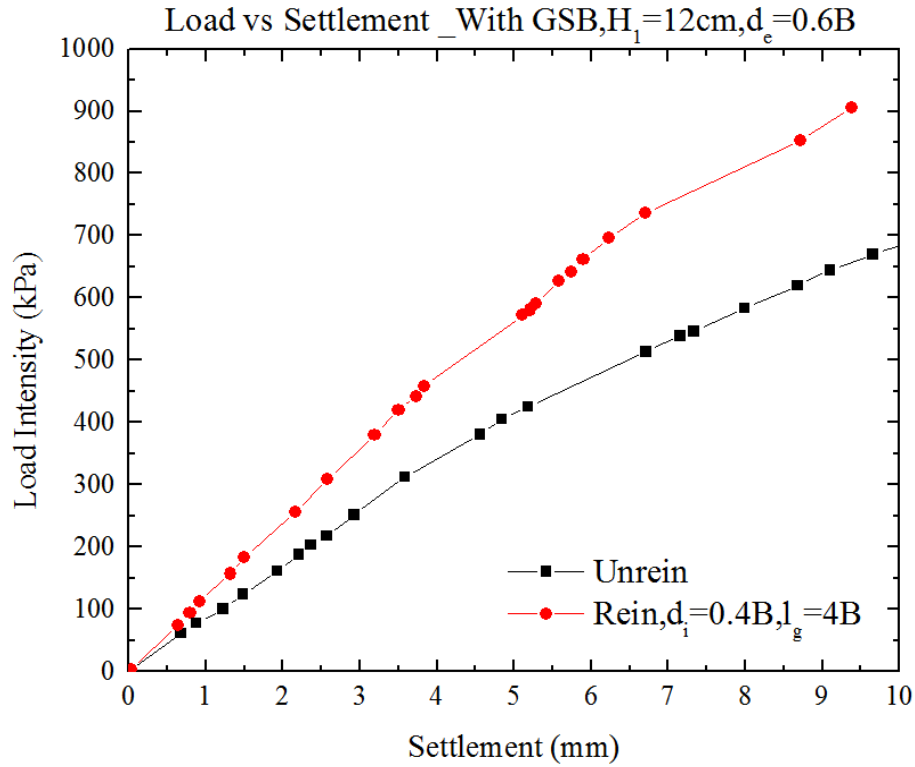


Figure 3.27: (a) Comparison of load settlement response at  $d_e=0.6B$

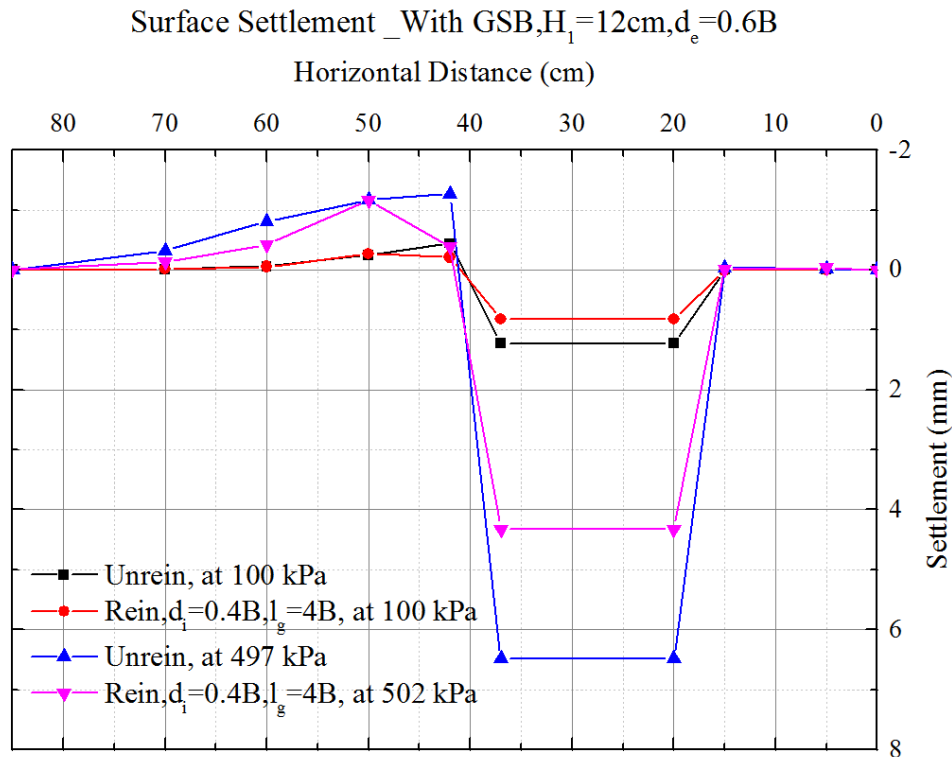


Figure 3.27: (b) Comparison of Surface settlement profile at  $d_e=0.6B$



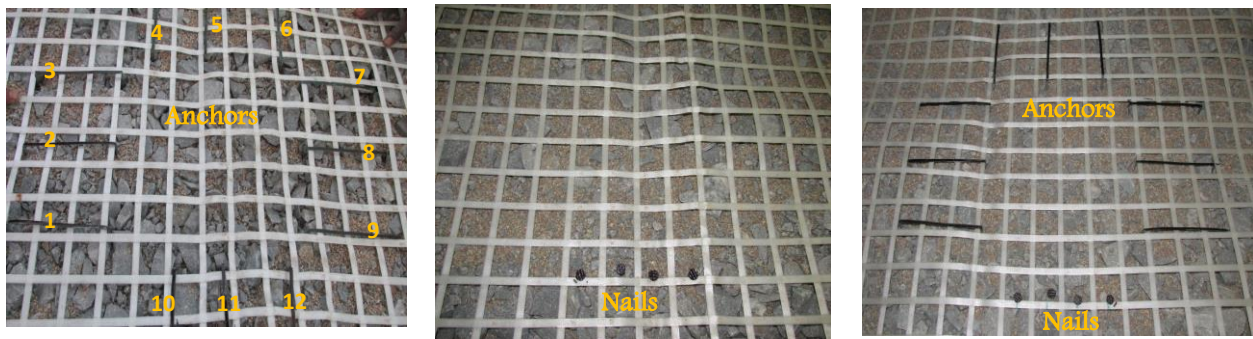
From the above graphs it can be inferred that the settlement for a particular load is more pronounced in the unreinforced case than that of the reinforced case. It can also be inferred that the difference in settlement between the reinforced and the unreinforced case increases with the magnitude of load.

From the surface settlement graphs it can be observed that the surface settlement reduced in the reinforced case than that of the unreinforced case. Heave formation was more pronounced in the unreinforced case while in the reinforced case it is minimized as expected.

### 3.6 Special Recommendations

Load carrying capacity of the geogrid reinforcement can be improved by increasing the anchorage effect in the geogrid. Though the geogrid itself possesses some amount of anchorage effect, external anchors and nails are used to further increase the anchorage effect in the geogrid externally. Three cases were considered: (i) with only anchors, (ii) With only nails, (iii) with anchors and nails together. The critical distance of wheel from the abutment i.e. an edge distance of wheel from abutment ( $d_e$ ) was taken as  $0.3B$  to study the improvement in load carrying capacity with provision of anchors and nails to the geogrid.

In the first case, three anchors of length 100 mm length and depth 40mm were used on each side of loading plate as shown in Figure 3.28(a). In the second case, four nails were used with an equal distance of 30 mm in between as in Figure 3.28(b). The nails were driven into the abutment through the granular material after placing the geogrid. Care should be taken while inserting the nails into the abutment in minimizing the lateral movement of geogrid in the direction of loading plate. In the third case, the anchors and nails are used together as shown in Figure 3.28(c).



(a)

(b)

(c)

**Figure 3.28: (a) with only anchors, (b) With only nails, (c) with anchors and nails together**

The anchors and nails that are fixed to the geogrid, increases its anchorage effect by restricting its lateral movement and mobilizing the tensile strength to the higher values. Figure 3.29 shows the load settlement

profiles for various recommending conditions and compared with the unreinforced and reinforced condition without nails and anchors. It can be inferred that providing nails alone is not improving the load carrying capacity, while the providing anchors alone is improving the load carrying capacity by about 20% over reinforced condition without anchors at 2% of settlement to the diameter of loading plate. But the improvement in load carrying capacity if anchors and nails are provided together is significant about 42% and 18% at same settlement over the reinforced condition without anchors and nails, and reinforced condition with only anchors respectively.

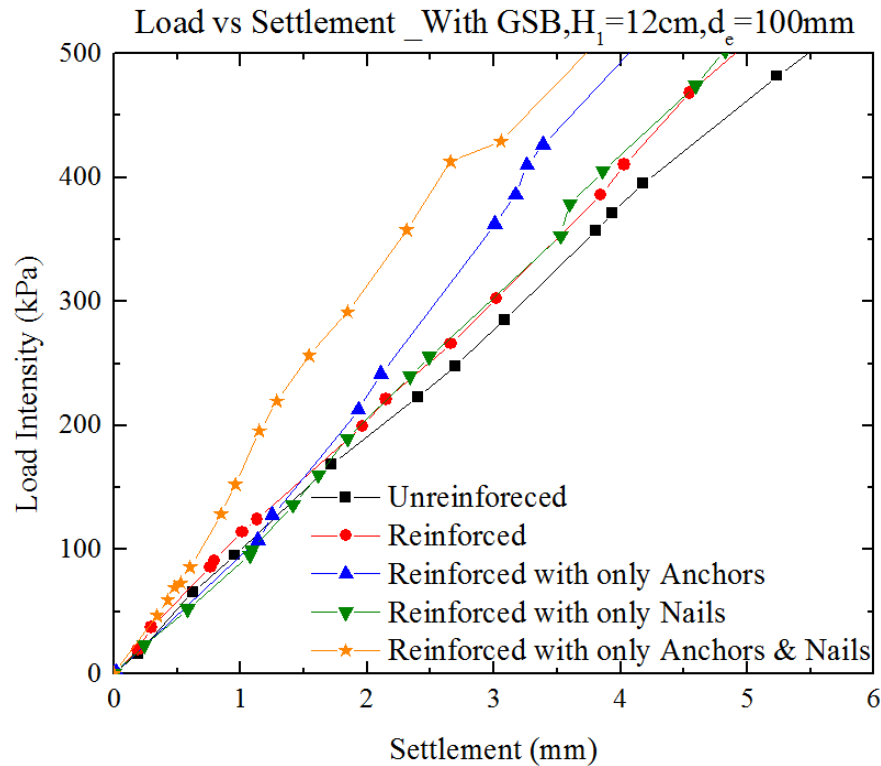


**Figure 3.29: Comparison of load settlement response at  $d_e=0.3B$  with various special recommending conditions**

From this study, it can be proposed to provide both anchors and nails to the reinforcement in order to improve the load carrying capacity and to reduce the settlements effectively.

# Chapter 4

## Modeling in FLAC 2D

### 4.1 Problem definition

The differential settlement at bridge approaches occurs mainly due to the two different support systems on which the reinforced concrete approach slab will rest. This two different supporting systems, one is bridge abutment i.e. very stiff material compared to the embankment backfill material whose stiffness will be very less. The embankment experiences large settlements due to compression and consolidation of the ground, whereas the settlement of the bridge abutment will be negligible. In order to avoid this differential settlements, the embankment backfill material has to be strengthened by increasing its stiffness. In the present study, a geogrid reinforced granular beds are used to replace the traditional concrete approach slabs, to increase the stiffness of embankment material.

Experimental results suggest that by replacing the geogrid reinforced granular beds with traditional approach slabs, load carrying capacity and stiffness can be improved significantly. However, the mechanism render this improvement are not well understood. The objective of this numerical study is to examine the findings from the laboratory study and understand the behavior of reinforced granular bed in distributing the load and settlements below wheel load. A three-dimensional explicit finite difference program (FLAC<sup>3D</sup>) was used to simulate the problem and estimate the settlement between geogrid reinforced granular bed and bridge abutment. Fast Lagrangian Analysis of Continua (FLAC<sup>3D</sup>) was used in this study as it is a very effective software in simulating various complex three dimensional problems in geotechnical engineering.

### 4.2 FLAC – an overview

Fast Lagrangian Analysis of Continua (FLAC) is a three-dimensional explicit finite difference program which is very effective in simulating large deformation in structures built of soil, rock, or other materials that may undergo the plastic flow at yield condition. Materials are represented by zones which form a grid

that is adjusted by the user to fit the shape of the object to be modeled. Each zone behaves according to a prescribed linear or non-linear stress/strain law in response to the applied forces or boundary restraints. The material can yield and flow and the grid can deform (large-strain mode) and move with the material that is represented. FLAC is an effective tool to solve complex problems in mechanics due to its formulation based on dynamic equations of motions that uses an explicit Lagrangian calculation scheme and mixed discretization techniques. In geotechnical and mining engineering, FLAC is a useful tool because of its ability to analyze plastic collapse and flow of highly nonlinear materials very accurately. The great advantage of FLAC<sup>3D</sup> is, it comprises of various built-in material models; different structural element models such as reinforcements in soils, tunnel liners, piles, and rock bolts; suitable interface elements and a built-in programming language FISH.

### **4.3 Finite difference program**

Finite difference Method divides the problem into small time steps and predicts the stresses and strains of the next time step based on the present time step using finite difference formulation such as forward, backward and central differences. In the finite difference method, all the differential equations are replaced directly with the algebraic expressions in terms of the field variables (e.g., stress or displacement) at the discrete points in the space called as grid points in this software. These variables are undefined within elements. Detailed formulation of the material and structural elements can be found in the FLAC manuals (Itasca 1995). In FLAC, the incremental displacements are added to the coordinates so that grid deforms with the material. This is termed as Lagrangian formulation. The constitutive formulation at each step is a small-strain formulation; but is equivalent to large strain formulation over many steps. The isotropic stress and strain components are taken to be constant over the whole quadrilateral element, while the deviatoric components are treated separately for each triangular sub-element. This procedure, referred to as mixed discretization, is described by Marti and Cundall (1982). In FLAC, central differences formulation are considered in calculating the stresses and strains of the next time step based on the present time.

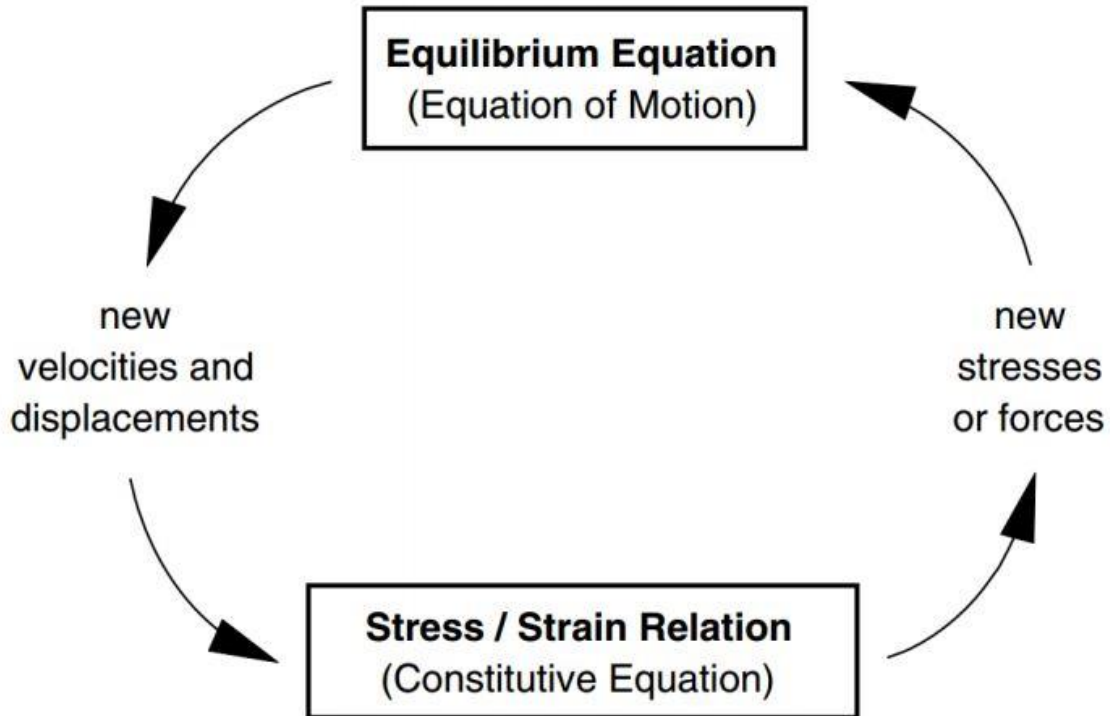


**Figure 4.1: General explicit calculation procedure in FLAC**

The method first involves the equations of motion to derive new velocities and displacements from stresses and forces. The strain rates are then derived from velocities, and new stresses are obtained from strain rates. It takes one time step for every cycle around the loop.

#### **4.4 Material Models**

The material models which are available in the FLAC and used to simulate soil-reinforcement interaction in the present study were elaborated below.

##### **4.4.1 Mohr-Coulomb Model**

Mohr-Coulomb model is an elasto-plastic model. The Mohr-Coulomb model is the conventional model used to represent shear failure in soils and rocks. Vermeer and deBorst (1984) conducted laboratory tests and reported the results for sand and concrete that match well with the Mohr-Coulomb criterion.

The failure envelope for this model corresponds to a Mohr-Coulomb criterion (shear yield function) with tension cutoff (tension yield function). The position of a stress point on this envelope is controlled by a non-associated flow rule for shear failure, and an associated rule for tension failure.

The Mohr-Coulomb criterion in FLAC<sup>3D</sup> is expressed in terms of the principal stresses  $\sigma_1$ ,  $\sigma_2$  and  $\sigma_3$ , which are the three components of the generalized stress vector for this model ( $n = 3$ ). The components of the corresponding generalized strain vector are the principal strains  $\epsilon_1$ ,  $\epsilon_2$  and  $\epsilon_3$ .

The incremental expression of Hooke's law in terms of the generalized stress and stress increments has the form

$$\Delta\sigma_1 = \alpha_1\Delta\epsilon_1^e + \alpha_2(\Delta\epsilon_2^e + \Delta\epsilon_3^e)$$

$$\Delta\sigma_2 = \alpha_1\Delta\epsilon_2^e + \alpha_2(\Delta\epsilon_1^e + \Delta\epsilon_3^e)$$

$$\Delta\sigma_3 = \alpha_1\Delta\epsilon_3^e + \alpha_2(\Delta\epsilon_1^e + \Delta\epsilon_2^e)$$

Where  $\alpha_1$  and  $\alpha_2$  are the material constants defined in terms of the shear modulus,  $G$ , and bulk modulus,  $K$ , as

$$\alpha_1 = K + \frac{4}{3} G$$

$$\alpha_2 = K - \frac{2}{3} G$$

Embankment backfill soil in present study was modelled as Mohr-coulomb materials. The shear strength parameters of soil i.e. cohesion, friction angle, and dilation angle should be mentioned in the model along with the elastic properties of soil. The shear strength parameters (cohesion and Friction angle) values can be obtained by performing different tests like direct shear test, triaxial test, etc. The dilatancy angle values are calculated from the correlations available in literature for corresponding frictional angle and used in the model.

#### 4.4.2 Reinforcement model

The use of structural support to stabilize a rock or soil mass is an important aspect in geomechanical analysis and design. Structures of arbitrary geometry and properties, and their interaction with a rock or soil mass, can be modeled with FLAC<sup>3D</sup>. Six different types of structural-support members (beams, cables, piles, shells, geogrids and liners), or structural elements, available in FLAC<sup>3D</sup>. The structural elements can either be independent of, or coupled to, the grid representing the solid continuum. The structural-element logic is implemented with the same explicit, Lagrangian solution procedure. The full dynamic equations of motion are solved, even for modeling processes that are essentially static. Large displacements, including geometric nonlinearity, can be accommodated by specifying a large-strain solution mode.

**Geogrid Structural Elements** – Geogrid structural elements (geogridSEs) are three-noded, flat, finite elements that are assigned a finite-element type that resists membrane but does not resist bending loading.

A physical membrane can be modeled as a collection of geogridSELs. The geogridSEL behaves as an isotropic or orthotropic, linearly elastic material with no failure limit. A shear-directed (in the tangent plane to the geogrid surface) frictional interaction occurs between the geogrid and the FLAC<sup>3D</sup> grid, and the geogrid is restricted to the grid motion in the normal direction. A geogrid can be anchored at a specific point in the FLAC<sup>3D</sup> grid, or attached so that stress develops along its surface in response to relative motion between the geogrid and the FLAC<sup>3D</sup> grid. GeogridSELs are used to model flexible membranes whose shear interaction with the soil are important, such as geotextiles and geogrids.

The behavior at the geogrid-soil interface with the stresses acting on the geogrid and the membrane stresses that develop within the geogrid are shown in Figure 4.2. The orientation of the interface spring-slider changes in response to relative shear displacement, between the geogrid and the soil medium, as shown in Figure 4.3.

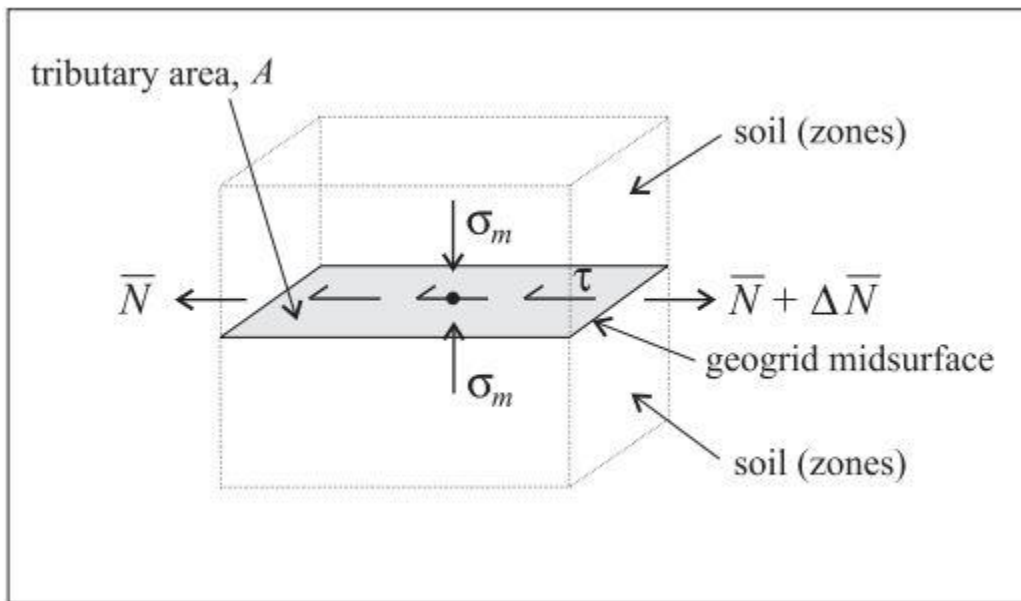
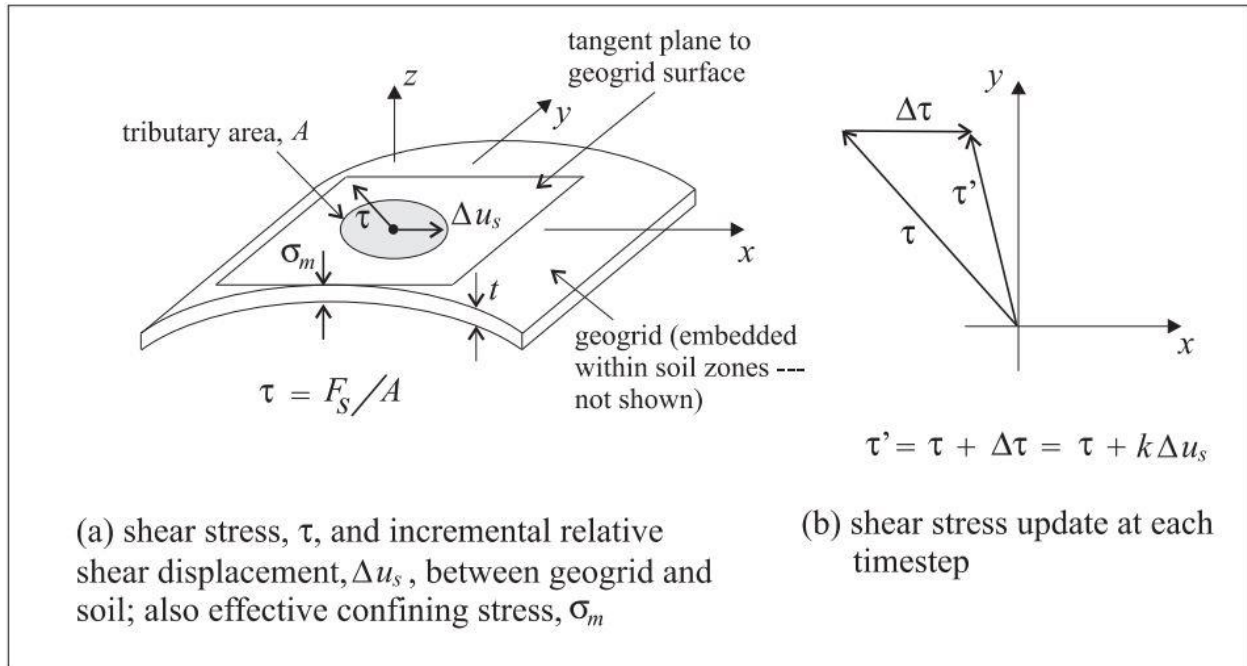


Figure 4.2: Stress acting on geogridSELs surrounding a node



**Figure 4.3: Idealization of interface behavior at a geogrid node**

The effective confining stress,  $\sigma_m$ , acts perpendicular to the geogrid surface, and is computed at each geogrid node, based on the stress acting in the single zone to which the node is linked. The value of  $\sigma_m$  is taken as

$$\sigma_m = \sigma_{zz} + p$$

Where  $p$  = pore pressure

Geogrids support large-strain sliding (by setting the **slide** property to **on**), whereby the interpolation locations (used by the geogrid nodes to transfer forces and velocities to and from the zones) will migrate through the grid when running in large-strain mode. This allows one to calculate the large-strain, post-failure behavior of a geogrid, whereby substantial sliding between the geogrid nodes and the zones occurs.

#### 4.5 Validation study using FLAC<sup>3D</sup>

Numerical studies were attempted using a circular footing on semi-infinite medium to validate the model. The model was developed using command driven procedure. In this section, the study was conducted using a circular footing of diameter 0.1m, on homogeneous and two layered soil system. Improvement in the load carrying capacity was studied by providing the stiff layer on top of weak layer. Later, the effect of reinforcement in both the case was studied with varying various parameters such as length of reinforcement,



initial depth of reinforcement and number of reinforcement layers. This entire study was conducted in various stages as listed below:

- i. Homogeneous soil system - Unreinforced condition
- ii. Homogeneous soil system – Single layer of reinforcement condition
- iii. Homogeneous soil system – Two layers of reinforcement condition
- iv. Two layered soil system - Unreinforced condition
- v. Two layered soil system – Single layer of reinforcement condition
- vi. Two layered soil system – Two layers of reinforcement condition

#### 4.5.1 Homogeneous soil system - Unreinforced condition

A circular footing of diameter (B) 0.1m on semi-infinite soil medium was used in this study. The elastic-perfectly plastic Mohr-Coulomb model was used for modelling the soil. As the soil-footing-reinforcement system is symmetry, to reduce the computational time for analysis, quarter symmetrical model was simulated. Dimensions of model of  $10B \times 10B \times 20B$  was used to construct the one fourth of the 3D media. Boundary distances are considered in respect to neglect the influence of boundary condition on the results. Figure 4.4 shows the schematic model constructed in FLAC<sup>3D</sup>.

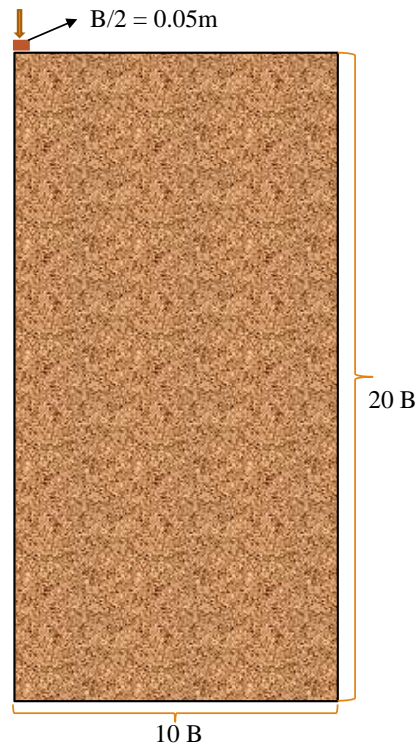


Figure 4.4: Schematic of the model on homogeneous medium with unreinforced condition

#### Soil Properties

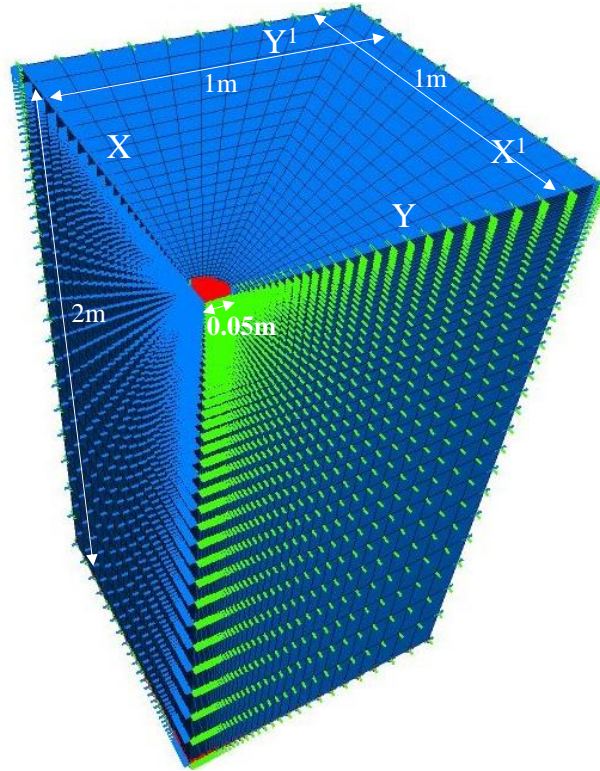
A sandy soil was assumed to be model in FLAC<sup>3D</sup>. The nonlinear behavior of soil was modelled using Mohr-Coulomb criterion. The Mohr-Coulomb model presents a first-order approximation of soil behavior. This model involves the properties namely unit weight ( $\gamma$ ), bulk modulus (K), shear modulus (G), Poisson's ratio ( $\nu$ ), shear strength parameters cohesion (c) and angle of internal friction ( $\phi$ ) and dilatancy angle ( $\psi$ ). The values of parameters used in this study were given in Table.4.1.

Table 4.1: Mechanical properties of soil

| Parameter                        | Value           |
|----------------------------------|-----------------|
| Unit weight (kN/m <sup>3</sup> ) | 20              |
| Poisson's ratio                  | 0.3             |
| Bulk Modulus (MPa)               | 4.2             |
| Shear Modulus (MPa)              | 1.9             |
| Cohesion (kPa)                   | 1               |
| Angle of Internal friction       | 35 <sup>0</sup> |

Semi-infinite boundary conditions are implemented in the model, as the displacement of the bottom boundary is restricted in all the directions, while the outer boundaries  $X_1$  and  $Y_1$  are restricted only in horizontal directions and free to move in vertical direction (Figure 4.5). For the inner boundaries i.e. X and Y, the displacement in the direction perpendicular to the direction of axis is restricted while displacements along the directions of axis and in vertical direction are allowed. Figure 4.5 shows, the generated mesh for the quarter model of circular footing on semi-infinite soil medium.

In all analysis conducted in the present study, it was assumed that the footing was located on the ground surface. As a rigid surface footing was simulated, a uniform settlement over the footing area was applied. In FLAC displacement can be applied by giving the velocity (displacement per step) in that direction. Frydman and Burd (1997) used FLAC and showed that the change in velocity applied on footing nodes and zone dimension has significant effect on bearing capacity. Some studies investigated the variation of bearing capacity with applied velocity vector. According to the present study on variation of applied velocity, an applied displacement of  $1 \times 10^{-6}$  m was sufficient in each step of the analysis. The above mentioned velocity was chosen for the further studies as the numerical error (represented as unbalance force ratio in FLAC) is in permissible limits. This velocity for the application of velocity has been chosen from the analysis with this velocity was found to be within the range as mentioned in the FLAC manual.



**Figure 4.5: Mesh generation for the model.**

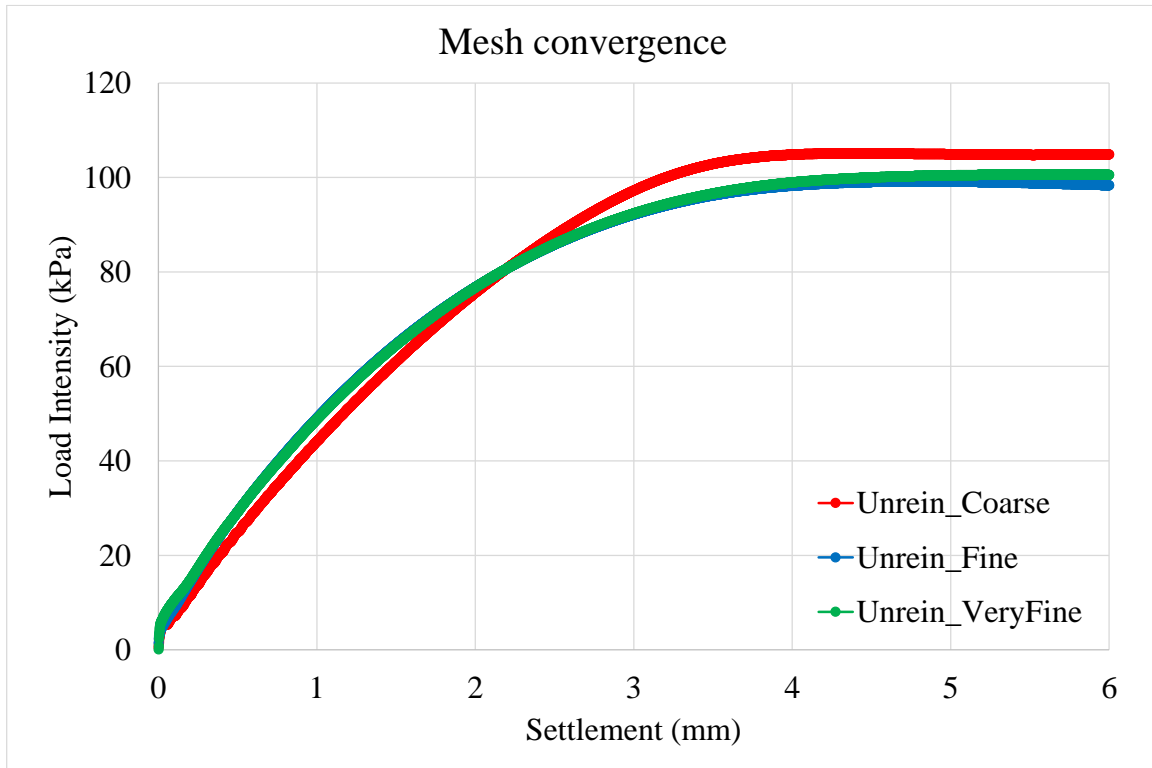
The domain was discretized using radial cylindrical zones below footing and a rectangular zones outside the footing. Mesh convergence studies were conducted on the model using three different mesh configurations coarse, fine and very fine, in which the number of zones are increased as 24750, 32500 and 82500 respectively. It was found that the mesh density should be more refined at the edges of the footing than in the center, as the stress concentration at this corners will be high. As the number of zones increased from coarse mesh to very fine mesh, the size of zone decreased, that leads to increase in the computational time for analysis. Table 4.2 shows the various mesh configurations with number of zones and computational time required for the analysis.

Table 4.2 Mesh configurations with computational time

| Mesh Type      | Number of zones | Computational time (hours) |
|----------------|-----------------|----------------------------|
| Coarse mesh    | 24750           | 2-3                        |
| Fine mesh      | 32500           | 5-6                        |
| Very fine mesh | 82500           | 10-12                      |

Figure 4.6 shows the Load-Settlement curves for different mesh configurations. It can be inferred from the figure that the fine and very fine mesh configurations are giving similar load carrying capacity which is matching with the theoretical bearing capacity value with only 1% of error. So, the mesh has converged

with these two configurations. But as the computational times required for the analysis in the case of fine mesh is reduced to half the computational time compared to the very fine mesh configuration, fine mesh was opted as the optimum mesh configuration in this study.



**Figure 4.6: Load-Settlement curves for Mesh convergence**

In Mohr-Coulomb failure criterion, the angle of shearing resistance of soil  $\phi$  is assumed to be constant along the slip plane. However, over the second half of the last century, it is well recognized that the dilatancy angle ( $\psi$ ) influences the shear strength of sand. Many researchers have proposed correlations between the angle of shearing resistance at peak state in terms of intrinsic soil variables and soil state variables. DeBorst and Vermeer (1984), Frydman and Burd (1997), Yin et al. (2001), Erickson and Drescher (2002), and found that the effect of dilatancy angle is significant in the numerical estimation of bearing capacity. This significance is more for higher values of  $\phi$ . For a rough footing on a soil with  $\phi = 45^\circ$  and  $\psi = 45^\circ$ , with decrease in  $\psi$  leads to an increase in the non-associativity, the bearing capacity factors reduced about 40%. Non-Associative plastic rule occurs when there is difference between  $\phi$  and  $\psi$ , which means that the plastic potential surface is not identical to the yield surface. Erickson and Drescher (2002) showed that the numerical analysis with FLAC, that the best results are obtained by considering a dilation angle corresponds to  $\psi = 2/3\phi$ . In this study, numerical simulations were performed to find the dilation angle giving the best results compatible with theoretical bearing capacity.

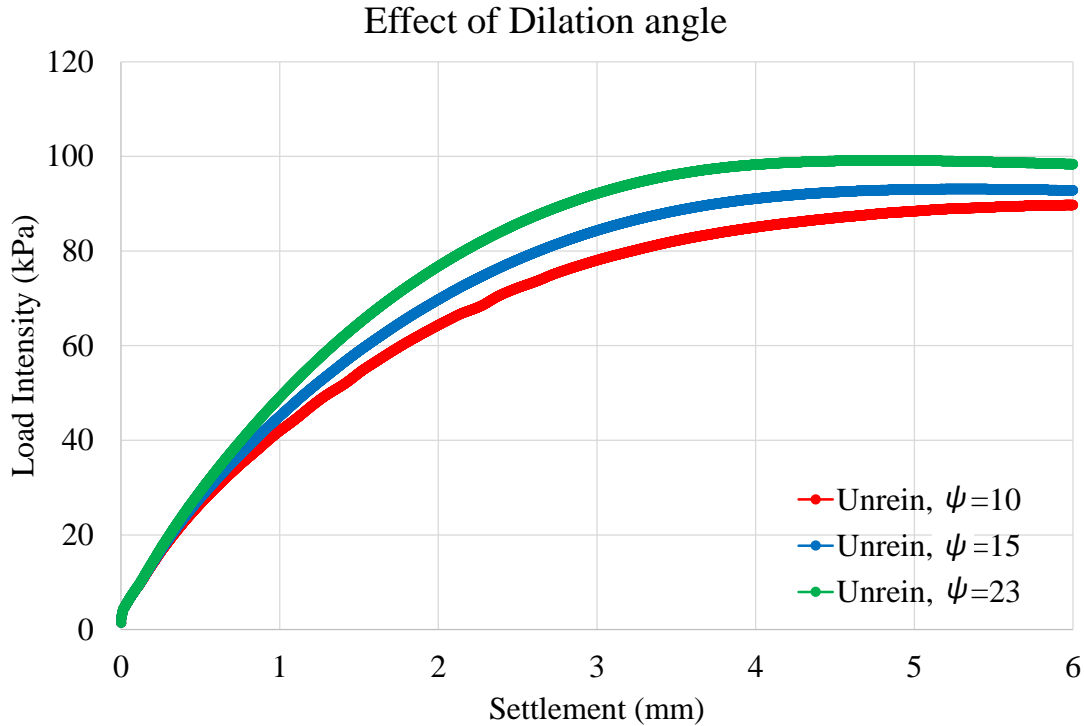


**Figure 4.7: Load-Settlement curves for studying effect of dilation angle**

The load-Settlement profiles for three different dilation angles ( $10^{\circ}$ ,  $15^{\circ}$  and  $23^{\circ}$ ) are shown in Figure 4.7. It can be concluded that the dilation angle corresponding to the 2/3rd of angle of internal friction is giving better estimation of load carrying capacity of footing, as it is also matching with the theoretical calculation of bearing capacity of footing with only 1% error. So the dilation angle of  $23^{\circ}$  was used for this soil in this study, corresponds to the angle of internal friction of  $35^{\circ}$ .

From this study it can be concluded that the model from FLAC<sup>3D</sup> has been validated using theoretical estimation of bearing capacity with optimum fine mesh configuration and the material properties as stated.

#### **4.5.2 Homogeneous soil system – Single layer of reinforcement condition**

In this section, reinforcement has been introduced into the homogeneous soil medium to study the improvement in load carrying capacity. The effect of reinforcement and effect of stiffness of reinforcement was studied using circular footing of diameter 0.1m on semi-infinite soil medium. The material properties for sand medium was considered similar to the earlier study. The reinforcement parameters that influencing the improvement have been studied in this section. The parameters such as initial depth of reinforcement, length and the stiffness of reinforcement have been studied with various simulations. Figure 4.8 shows the typical layout of model with the reinforcement at effective initial depth of  $0.3 \times B$  and the length of reinforcement  $4 \times B$ . Details regarding selection of this parameters have given in later studies.



**Figure 4.8: Schematic of the model on homogeneous medium with single layer of reinforcement**

In this section, reinforcement has been introduced into the homogeneous soil medium with the properties shown on Table 4.3.

Table 4.3: Reinforcement properties for the case homogeneous case with single layer of reinforcement

| <b>Reinforcement properties</b> |                 |
|---------------------------------|-----------------|
| Thickness (mm)                  | 2               |
| Spring Friction angle (degree)  | 24 <sup>0</sup> |
| Spring Stiffness (MPa/m)        | 2.5             |
| Spring Cohesion (kPa)           | 1               |
| Youngs Modulus (GPa)            | 25              |
| Poissons ratio                  | 0.3             |
| Axial Stiffness (kN/m)          | 50000           |

The load settlement profiles with reinforcement has shown in Figure 4.9 which compares with the unreinforced condition. It can be inferred that reinforcement (with axial stiffness 50000 kN/m) increases the load carrying capacity of footing about 58% at the settlement, 6% of diameter of the footing.

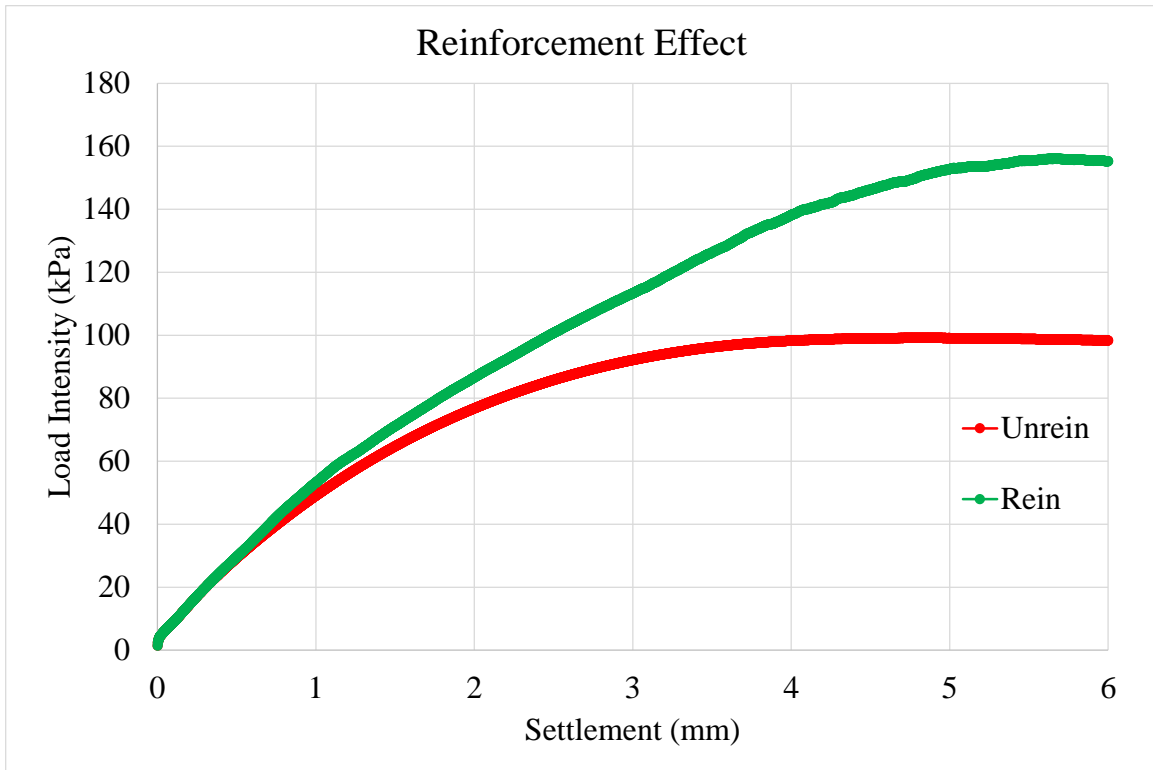


**Figure 4.9: Load-Settlement curves for studying effect of reinforcement in homogeneous soil system.**

In this section, another study on the effect of stiffness of reinforcement was conducted by varying the stiffness parameter. Different stiffness values of reinforcement from 5000 kN/m to 50000 kN/m was considered in this study. Figure 4.10 shows the load settlement profiles for various stiffness values for reinforcement. This profiles are compared with the unreinforced condition to estimate the percentage improvement in load carrying capacity.

Figure 4.10 states that there was significant improvement in the load carrying capacity with high stiffness values for reinforcement. By reducing the stiffness of reinforcement, the load carrying capacity of footing was reducing. But by increasing the stiffness value of reinforcement more than 5000 kN/m, the rate of increment in load carrying capacity was found to be marginal.

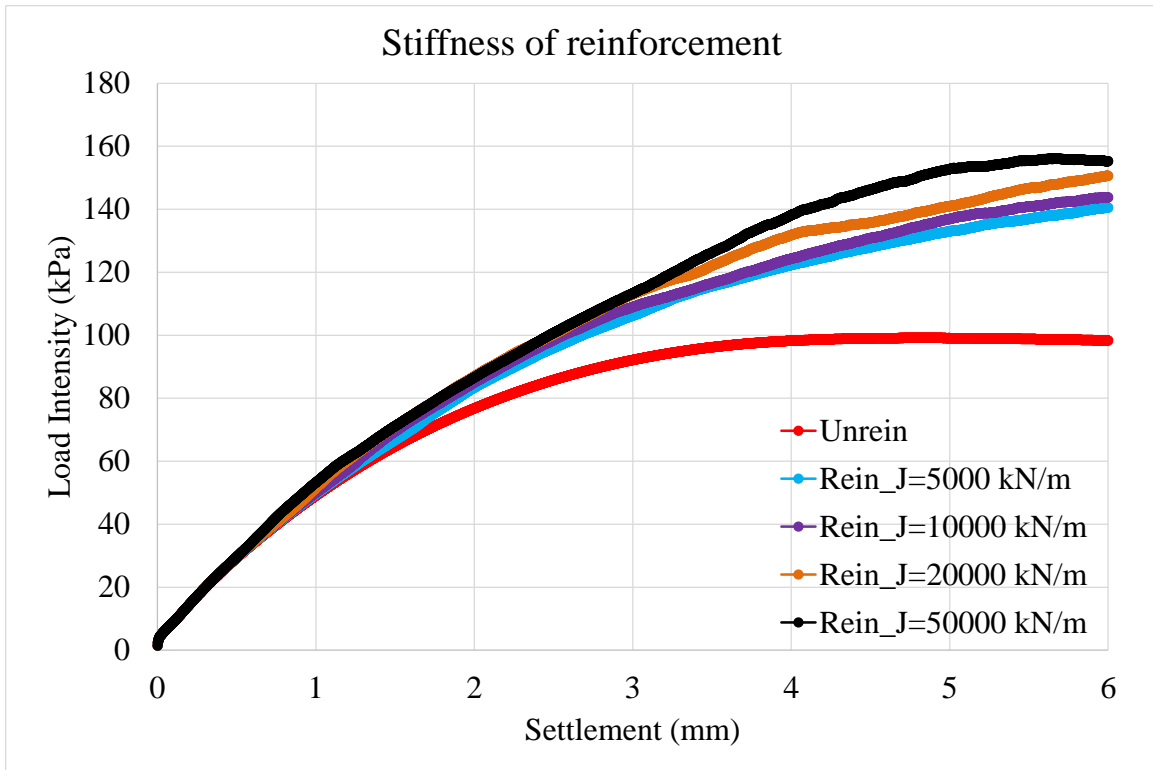


**Figure 4.10: Load-Settlement curves for studying effect of stiffness of reinforcement in homogeneous soil system.**

Table 4.4 states the percentage improvement in load carrying capacity with various reinforcement stiffness values for various settlements below footing.

Table 4.4: Improvement in load carrying capacity with reinforcement in homogeneous condition

| Settlement (w/B) (%) | Improvement in load carrying capacity (%) |              |              |
|----------------------|---|--------------|--------------|
|                      | J=10000 kN/m                              | J=20000 kN/m | J=50000 kN/m |
| 2                    | 10  | 13           | 13           |
| 3                    | 18  | 23           | 23           |
| 4                    | 26  | 35           | 41           |
| 5                    | 38  | 40           | 55           |
| 6                    | 43  | 52           | 58           |

The results conclude that the improvement in load carrying capacity was about 40% with stiffness value of 5000 kN/m, while increasing the stiffness to 10000 kN/m, the increase in the load carrying capacity was up to 43% only. This shows the rate of improvement in load carrying capacity with respect to unreinforced condition was less, if we increase the stiffness of reinforcement more than 5000 kN/m. With this study, it



can be concluded that 5000 kN/m was the optimum stiffness for the reinforcement, and used in the later studies.

#### 4.5.3 Homogeneous soil system – Two layers of reinforcement condition

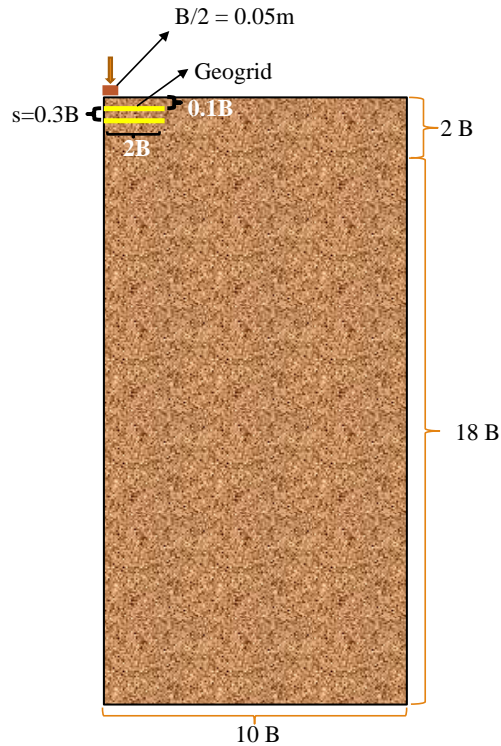
In this section, the effect of number of reinforcement layers and the vertical spacing between two reinforcement layers was studied using circular surface footing on the semi-infinite soil medium. The material properties for sand medium was used similar as in the earlier studies and for the reinforcement, optimal stiffness values which were concluded from earlier study are used in this study. The reinforcement properties which were used in the present study are given in Table 4.5.

Table 4.5: Reinforcement properties for the case homogeneous case with two layers of reinforcement

| <b>Reinforcement properties</b> |                 |
|---------------------------------|-----------------|
| Thickness (mm)                  | 2               |
| Length (m)                      | 0.4             |
| Width (m)                       | 0.4             |
| Spring Friction angle (degree)  | 24 <sup>0</sup> |
| Spring Stiffness (MPa/m)        | 2.5             |
| Spring Cohesion (kPa)           | 1               |
| Youngs Modulus (GPa)            | 2.5             |
| Poissons ratio                  | 0.3             |
| Axial Stiffness (kN/m)          | 5000            |

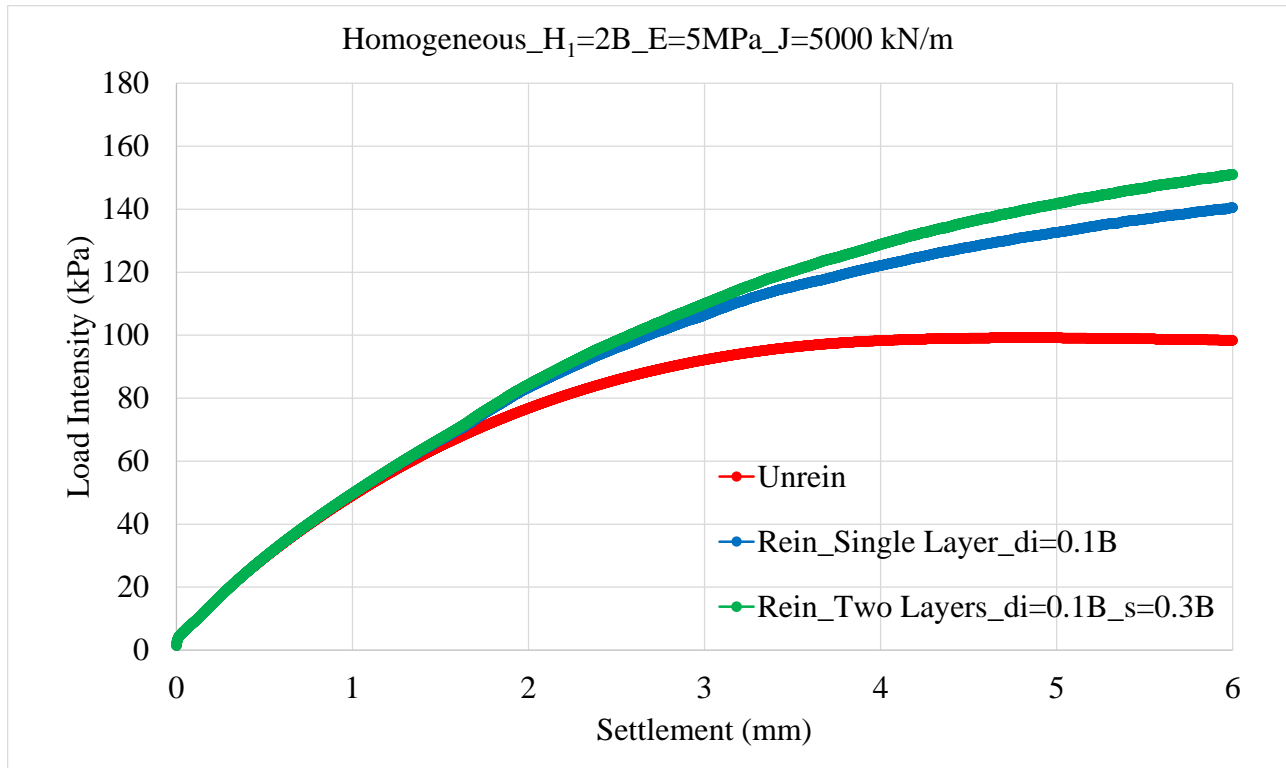
The objective in this section is to find the improvement in load carrying capacity by using two layers of reinforcement at effective spacing between reinforcement layers. The effective spacing value between two reinforcement layers was chosen from the results shown in later studies. In this section the spacing between two reinforcement layers was considered as 0.3 times the diameter of the footing.

Figure 4.11 shows the schematic diagram of the model for circular footing on semi-infinite sand medium with two layers of reinforcement with initial depth of reinforcement as  $0.1 \times B$  and spacing as  $0.3 \times B$ .



**Figure 4.11: Schematic of the model on homogeneous medium with two layers of reinforcement**

The improvement in load carrying capacity with two layers of reinforcement was given using load settlement curves in Figure 4.12. The load settlement profile are compared with the unreinforced condition and single layer of reinforcement condition. From Figure 4.12, it can be observe that the improvement in load carrying capacity with two layers of reinforcement was about 52% over unreinforced condition, while the improvement was about only 7% over single layer reinforcement condition. It can be inferred that the provision of two layers of reinforcement doesn't improve the load carrying capacity significantly.



**Figure 4.12: Load-Settlement curves for studying the effect of number of reinforcement layers in homogeneous soil system.**

#### 4.5.4 Two layered soil system – Unreinforced condition

In the previous section the model was simulated in three conditions namely unreinforced, single layer and two layers reinforced conditions for homogeneous soil system. The improvement in the load carrying capacity was studied with reinforcement and the effect of the parameters such as reinforcement stiffness, number of reinforcement layers and spacing between layers was studied. In the present section, a stiff granular layer was introduced over the weak soil. The effect of stiff layer was studied by modelling a two layered soil system with unreinforced condition as shown in Figure 4.13 (a). The top layer thickness was considered as 2 times the diameter of the footing in this study. The stiffness of top layer was considered as ten times the stiffness of bottom layer. The material properties for the two layers was listed in Table 4.6. Boundary distances and boundary conditions are used same as that of the homogeneous soil system. The mesh generation plot for the two layered soil system has shown in Figure 4.13 (b).

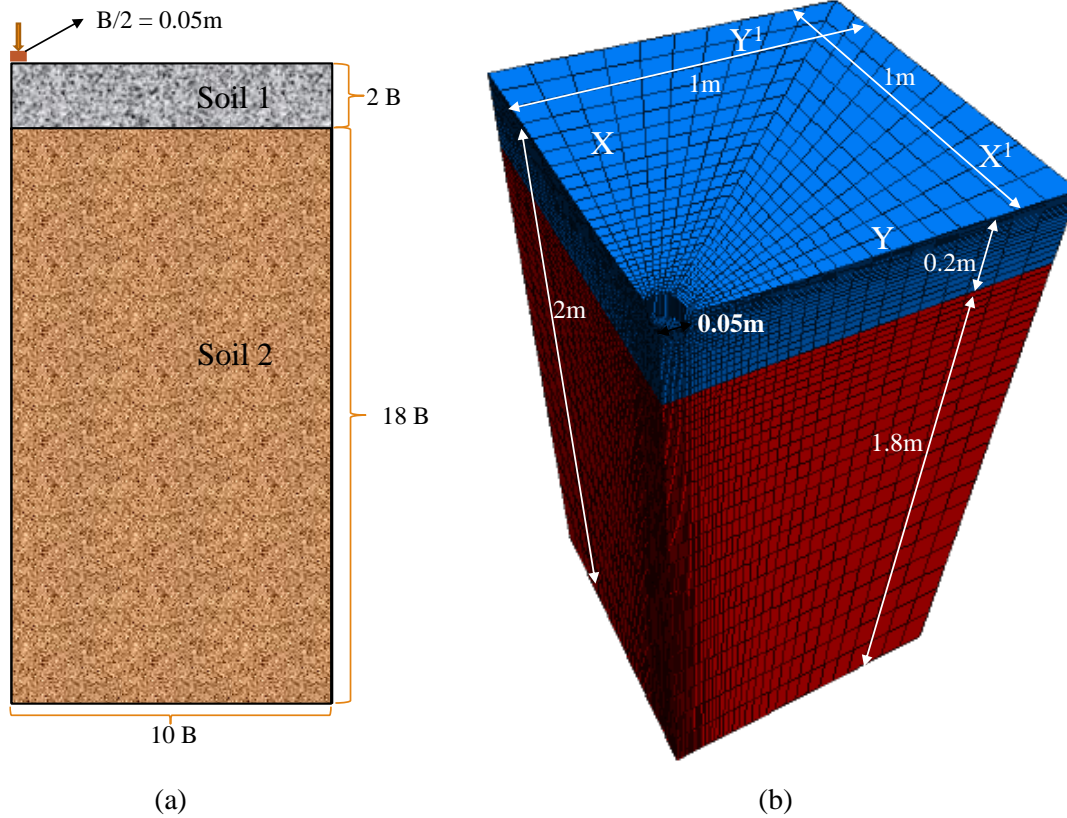


**Figure 4.13: (a) Schematic model of two layers soil system with unreinforced condition, (b) Mesh generation of the model**

Table 4.6: Material properties of two soils for the case of two layered soil system

| Parameter                        | Soil1 (Top Layer) | Soil2 (Bottom Layer) |
|----------------------------------|-------------------|----------------------|
| Material type                    | Mohr-Coulomb      | Mohr-Coulomb         |
| Unit weight (kN/m <sup>3</sup> ) | 22                | 20                   |
| Bulk Modulus (MPa)               | 41.7              | 4.2                  |
| Shear Modulus (MPa)              | 19.2              | 1.9                  |
| Poisson's ratio                  | 0.3               | 0.3                  |
| Cohesion(kPa)                    | 1                 | 1                    |
| Angle of internal friction       | 45 <sup>0</sup>   | 35 <sup>0</sup>      |
| Dilation angle                   | 30 <sup>0</sup>   | 23 <sup>0</sup>      |

Models are simulated for the two layered soil system with unreinforced condition and load settlement profiles were plotted. Figure 4.14 shows the load settlement curves for the homogeneous soil system and two layered soil system, which inferred that the load carrying capacity has been increased about 4 times to that of homogeneous soil system. It can be concluded from these results that provision of stiff layer over weak layer will increase the load carrying capacity significantly. Considering the above results, a stiff layer of thickness 2 times the diameter of footing was used in later studies.

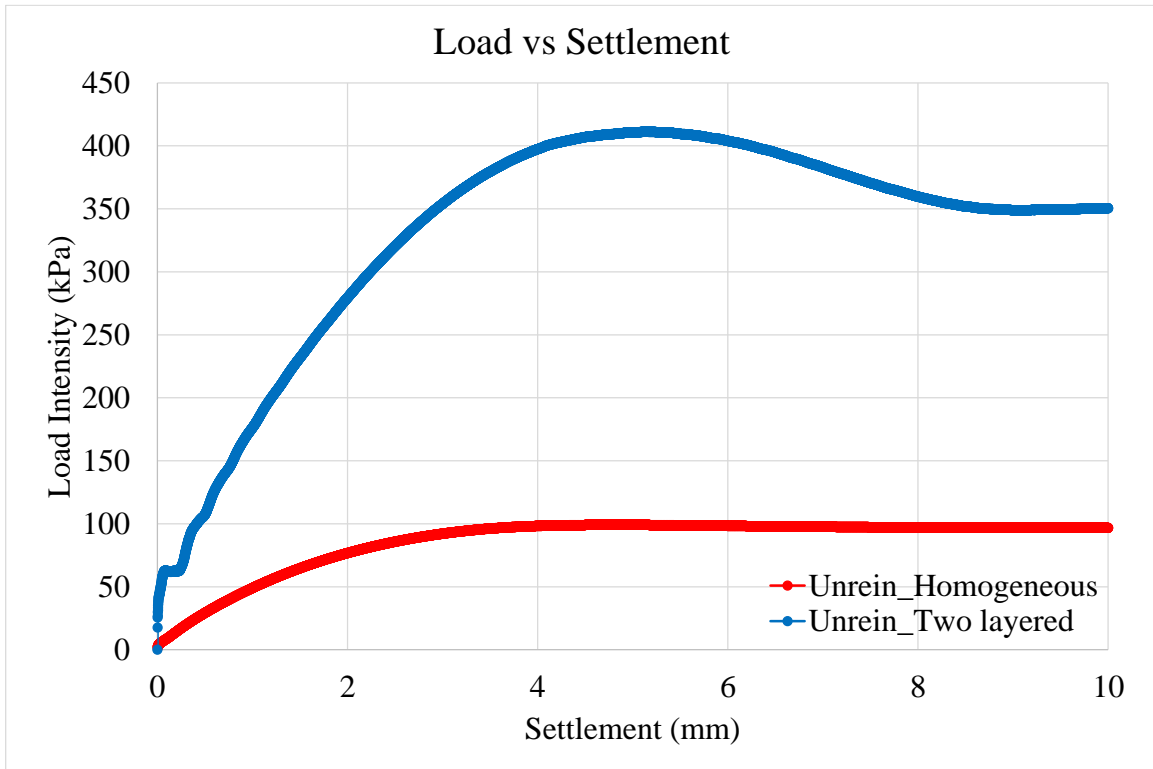


**Figure 4.14: Load-Settlement curves for studying the effect of stiff layer over weak layer in two layered soil system.**

#### **4.5.5 Two layered soil system – Single layer of reinforcement condition**

In this section the effect of reinforcement and its parameters such as initial depth of reinforcement and stiffness of reinforcement which will influence the improvement in load carrying capacity was studied. Study was conducted using a circular footing with diameter of 0.1m, which is resting on ground surface of semi-infinite two layered soil system.

##### **4.5.5.1 Effect of initial depth of reinforcement & Effect of reinforcement**

For the initial study in this section, the reinforcement parameter like initial depth of reinforcement was studied to find its effect on the improvement in load carrying capacity. Different initial depth of reinforcement values from  $0.1 \times B$  to  $0.5 \times B$  were considered to compare the variation in load carrying capacity. Figure 4.15 shows the typical layout of the model on two layered soil system with single layer of reinforcement. The material properties used in this study were same as the earlier studies. For this study, reinforcement of axial stiffness 20000 kN/m was used.



**Figure 4.15: (a) Schematic model of two layers soil system with single layer of reinforcement condition**

Analysis has been done with various simulations in which initial depth of reinforcement was varied. Load settlement profiles have been plotted for various initial depth of reinforcement values and compared with the unreinforced condition. Figure 4.16 shows the load carrying capacity behavior for various conditions. It can be observed that the reinforcement at an initial depth of  $0.1 \times B$  giving good improvement in load carrying capacity compared to other initial depth values. It means that increasing the initial depth of reinforcement, increases the depth of unreinforced zone between footing and reinforcement which leads to act as similar or close to the unreinforced condition. It can be concluded from this result is that  $0.1 \times B$  is the effective initial depth of reinforcement in improving the load carrying capacity.

It can also be inferred from the Figure 4.16 that the improvement with the reinforcement in two layered soil system was about only 10% compared to the unreinforced condition. The improvement in load carrying capacity with reinforcement was very significant in homogeneous case which is about 58%, while in the two layered soil system it was limited to only 10%. This is because in two layered soil system, the stiff layer in which reinforcement has placed playing a dominating role over reinforcement in increasing load carrying capacity.

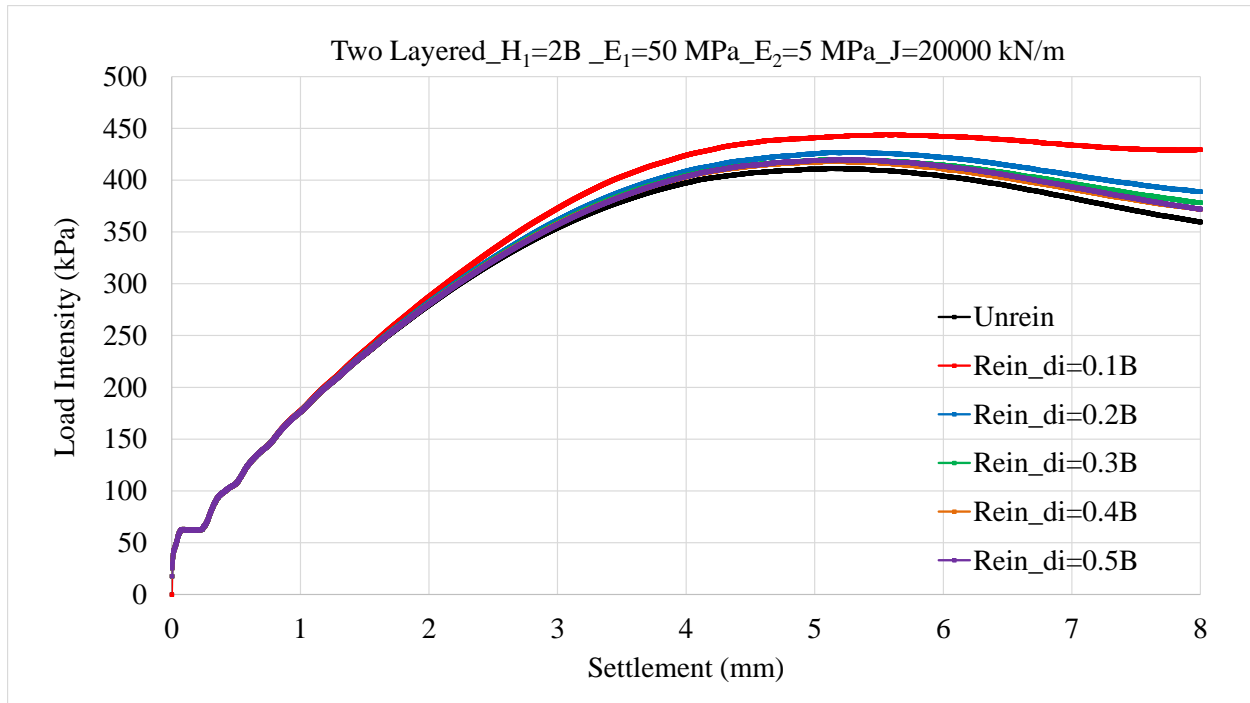


**Figure 4.16: Load-Settlement curves for studying the effect of initial depth of reinforcement in two layered soil system with single layer of reinforcement condition.**

#### 4.5.5.2 Effect of stiffness of top layer with single layer of reinforcement in two layered soil system

In this case the effect of stiffness of top layer was studied using three different stiffness values for top layer. Three different stiffness values of 10 MPa, 20 MPa and 50 MPa were considered to study the variation in load carrying capacity. Load settlement profiles for three different stiffness values for top layer in unreinforced and single layer of reinforced condition were plotted in Figure 4.17. It shows that, as the stiffness of top layer decreases the load carrying capacity also decreases in unreinforced condition, while the improvement with the reinforcement was increased as the stiffness of top layer decreased. The improvement in load carrying capacity from unreinforced condition to reinforced condition for three different stiffness values for top layer was listed in Table 4.7.

**Table 4.7: Improvement with reinforcement for various stiffness values for top layer in two layered soil system with single layer of reinforcement condition**

| Settlement (mm) | Load Intensity (kPa)    |      |                         |                         |      |                         |                         |      |                         |
|-----------------|-------------------------|------|-------------------------|-------------------------|------|-------------------------|-------------------------|------|-------------------------|
|                 | E <sub>1</sub> = 10 MPa |      | Improvement in load (%) | E <sub>1</sub> = 20 MPa |      | Improvement in load (%) | E <sub>1</sub> = 50 MPa |      | Improvement in load (%) |
|                 | Unrein                  | Rein |                         | Unrein                  | Rein |                         | Unrein                  | Rein |                         |
| 3               | 217                     | 240  | 10.60                   | 287                     | 314  | 9.41                    | 356                     | 374  | 5.06                    |
| 4               | 262                     | 298  | 13.74                   | 336                     | 375  | 11.61                   | 397                     | 424  | 6.80                    |
| 5               | 300                     | 351  | 17.00                   | 362                     | 411  | 13.54                   | 410                     | 441  | 7.56                    |
| 6               | 328                     | 392  | 19.51                   | 367                     | 423  | 15.26                   | 403                     | 442  | 9.68                    |
| 7               | 343                     | 423  | 23.32                   | 363                     | 433  | 19.28                   | 382                     | 434  | 13.61                   |
| 8               | 348                     | 442  | 27.01                   | 352                     | 445  | 26.42                   | 359                     | 430  | 19.78                   |

The percentage improvement with reinforcement was more in the case of less stiff material on top. It can be concluded that the better performance of reinforcement can be attained if the reinforcement was placed in less stiffer material. Though the improvement in load carrying capacity was almost same in the cases of  $E_1=10$  MPa and  $E_1=20$  MPa, the provision of top layer stiffness of 10 MPa will be cost effective.

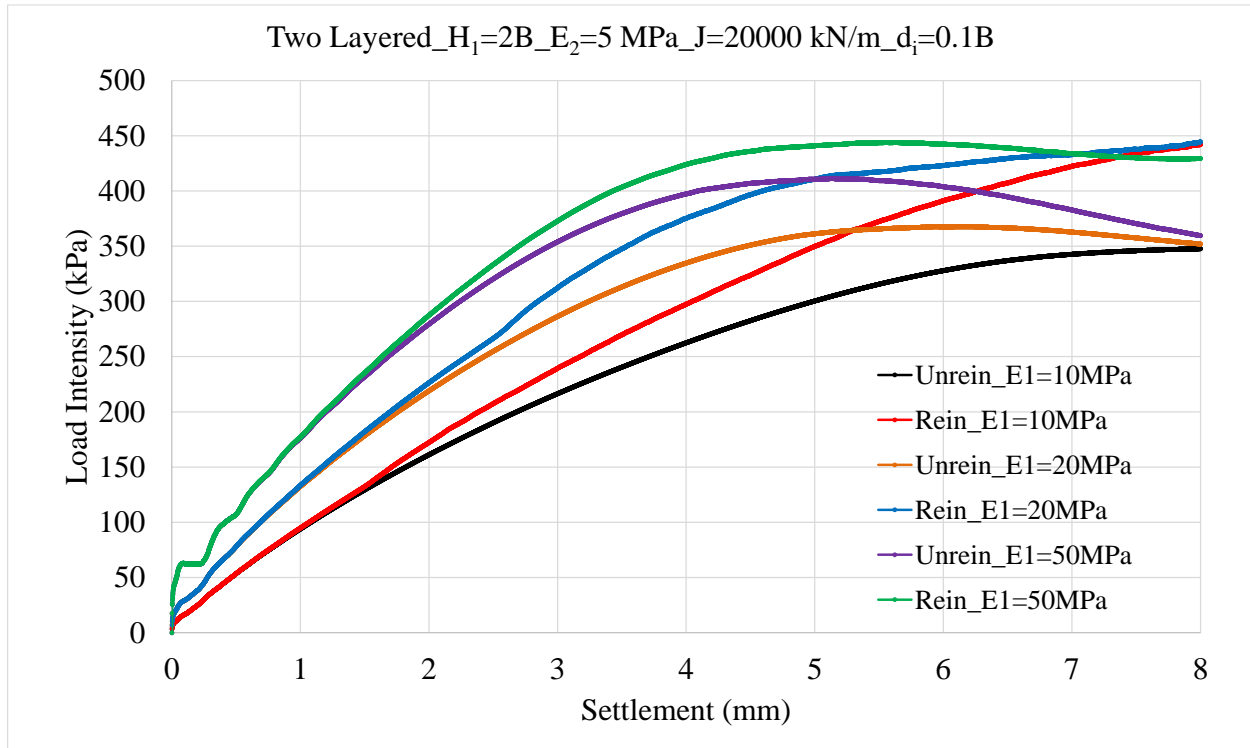
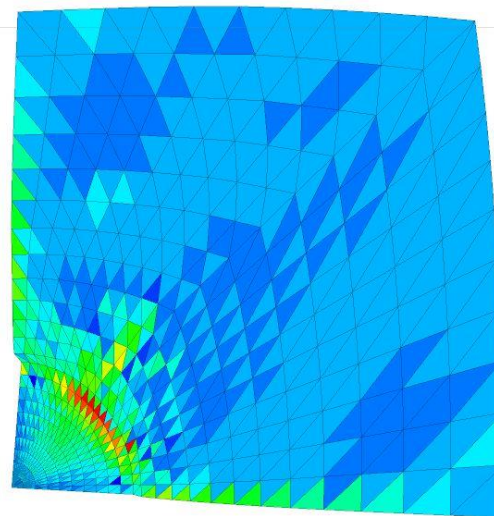
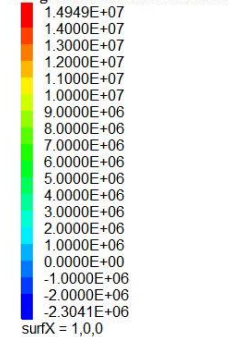


Figure 4.17: Load-Settlement curves for studying the effect of stiffness of top layer in two layered soil system with single layer of reinforcement condition.

**FLAC3D 5.01**  
©2015 Itasca Consulting Group, Inc.

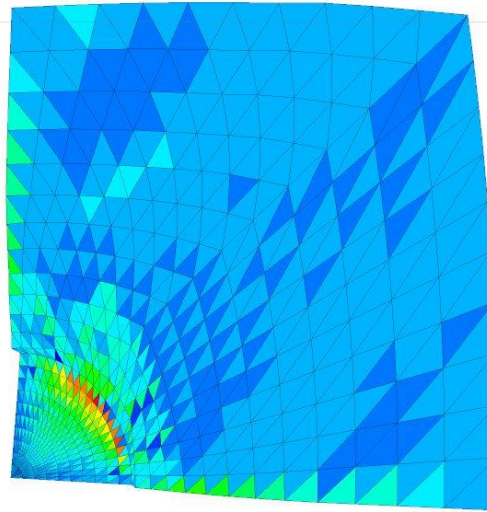
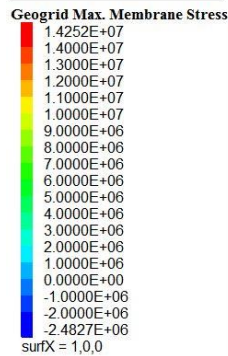
Geogrid Max. Membrane Stress



(a)  $E_1=10$  MPa

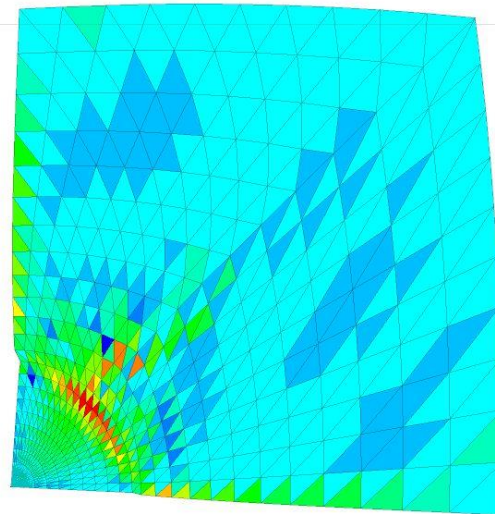
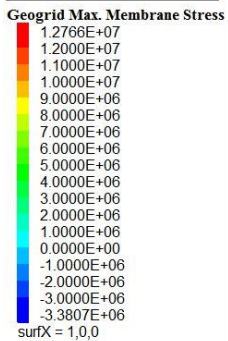


**FLAC3D 5.01**  
©2015 Itasca Consulting Group, Inc.



(b)  $E_1 = 20$  MPa

**FLAC3D 5.01**  
©2015 Itasca Consulting Group, Inc.



(c)  $E_1 = 50$  MPa

**Figure 4.18: Membrane stresses induced in the reinforcement for various stiffness values of top layer in two layered soil system with single layer of reinforcement condition**

The membrane stresses induced in the reinforced during the analysis with three different stiffness values for the top layer has shown in Figure 4.18. It shows that the maximum membrane stress induced in the case of less stiffer material i.e.  $E_1 = 10$  MPa. As stated earlier, this is because better utilization of tensile property of reinforcement can be attained when it placed in less stiffer material.

From this study it can be concluded that the effective initial depth of reinforcement was considered as 0.1 times the diameter of the footing and the optimum stiffness of top layer was considered as 10 MPa.

#### 4.5.6 Two layered soil system – Two layers of reinforcement condition

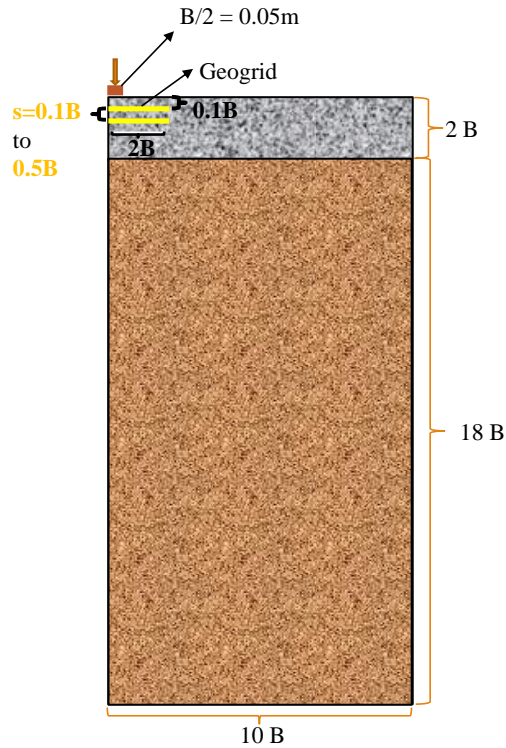
In this study, the case with the two layered soil system with two layers of reinforcement was considered. The objective in this study is to find the effective spacing between reinforcement layers and optimizing the reinforcement stiffness. The material properties for bottom layer are used same as that of earlier studies. The properties of top layer was modified as concluded from earlier study i.e.  $E_1=10$  MPa. The material properties for two soil materials are listed in Table 4.8.

Table 4.8: Material properties of two soils for the case of two layered soil system with two layers of reinforcement

| Parameter                        | Soil1 (Top Layer) | Soil2 (Bottom Layer) |
|----------------------------------|-------------------|----------------------|
| Material type                    | Mohr-Coulomb      | Mohr-Coulomb         |
| Unit weight (kN/m <sup>3</sup> ) | 22                | 20                   |
| Bulk Modulus (MPa)               | 8.3               | 4.2                  |
| Shear Modulus (MPa)              | 3.8               | 1.9                  |
| Poisson's ratio                  | 0.3               | 0.3                  |
| Cohesion(kPa)                    | 1                 | 1                    |
| Angle of internal friction       | 45 <sup>0</sup>   | 35 <sup>0</sup>      |
| Dilation angle                   | 30 <sup>0</sup>   | 23 <sup>0</sup>      |

##### 4.5.6.1 Effect of spacing between reinforcement layers

A set of simulations were conducted for studying the effect of spacing between reinforcement layers. Spacing between reinforcement layers varied from  $0.1 \times B$  to  $0.5 \times B$ . Figure 4.19 typical layout of the model on two layered soil system with two layers of reinforcement. The initial depth of reinforcement was used as 0.1 times the diameter of footing which had been concluded in earlier study. The axial stiffness of reinforcement as 20000 kN/m was considered in the study.



**Figure 4.19: Schematic model of two layers soil system with two layers of reinforcement condition**

Variation in load settlement curve with variation of spacing between reinforcement layers was shown in Figure 4.20. The plots were compared with the unreinforced condition and single layer of reinforcement condition. It states that the improvement in load carrying capacity with two layers of reinforcement was very marginal when compared to improvement with single layer of reinforcement. The spacing between reinforcement layers was effective in improving load carrying capacity was at  $0.3 \times B$ .

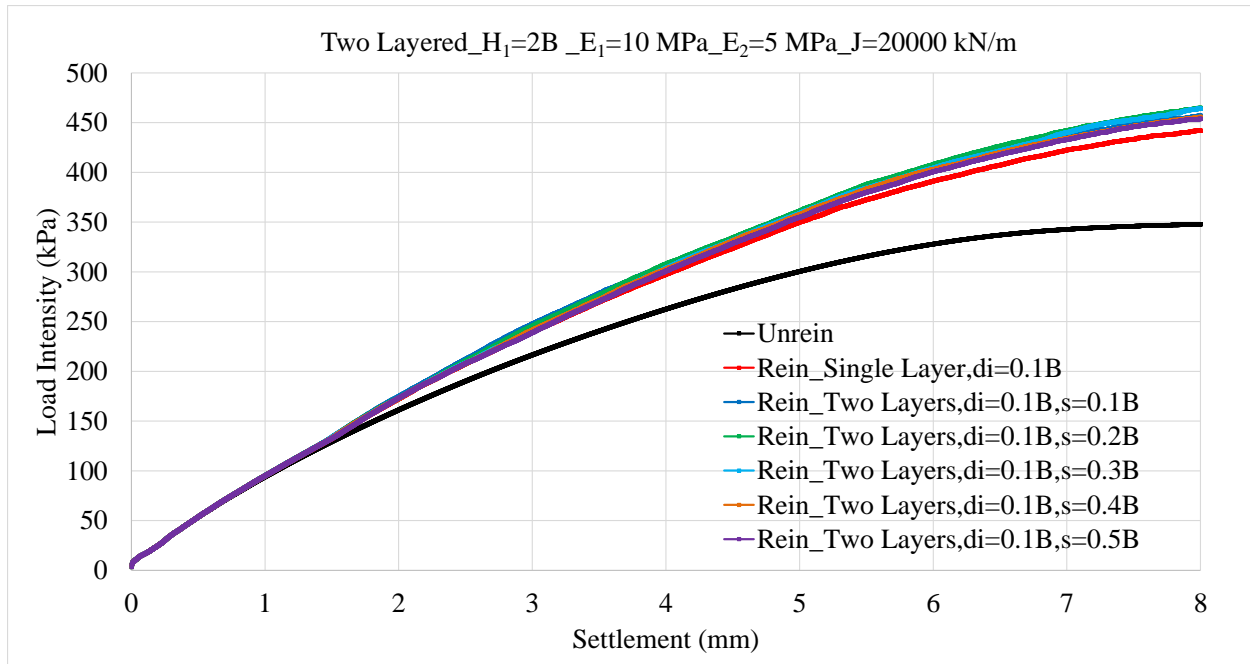


**Figure 4.20: Load-Settlement curves for studying the effect of spacing between reinforcement layers in two layered soil system with two layers of reinforcement condition.**

It can be concluded from this study that the provision of second layer of reinforcement doesn't contribute to the improvement of load carrying capacity significantly. But the second layer of reinforcement with space between reinforcements  $s=0.3B$  is giving marginal improvement over the single layer of reinforcement condition.

#### 4.5.6.2 Effect of stiffness of reinforcement

In this section, study was conducted to optimize the stiffness of reinforcement. For this study two stiffness values for the reinforcement was used. Load settlement plots for two different stiffness values i.e. 5000 kN/m and 20000 kN/m for reinforcement were plotted in Figure 4.21. Improvement in load carrying capacity was compared for this two stiffness values of reinforcement with unreinforced condition and single layer of reinforcement condition.

The plot shows that by reducing the stiffness of reinforcement to 4 times i.e. from 20000 kN/m to 5000 kN/m, the load carrying capacity was reduced by about 4% and 7% only in single layer of reinforcement condition and two layers of reinforcement condition respectively. It means that there is less variation in the load carrying capacity even if the stiffness of reinforcement reduced to 4 times. From the above results it can be concluded that reinforcement stiffness value of 5000 kN/m can be taken as optimum value.

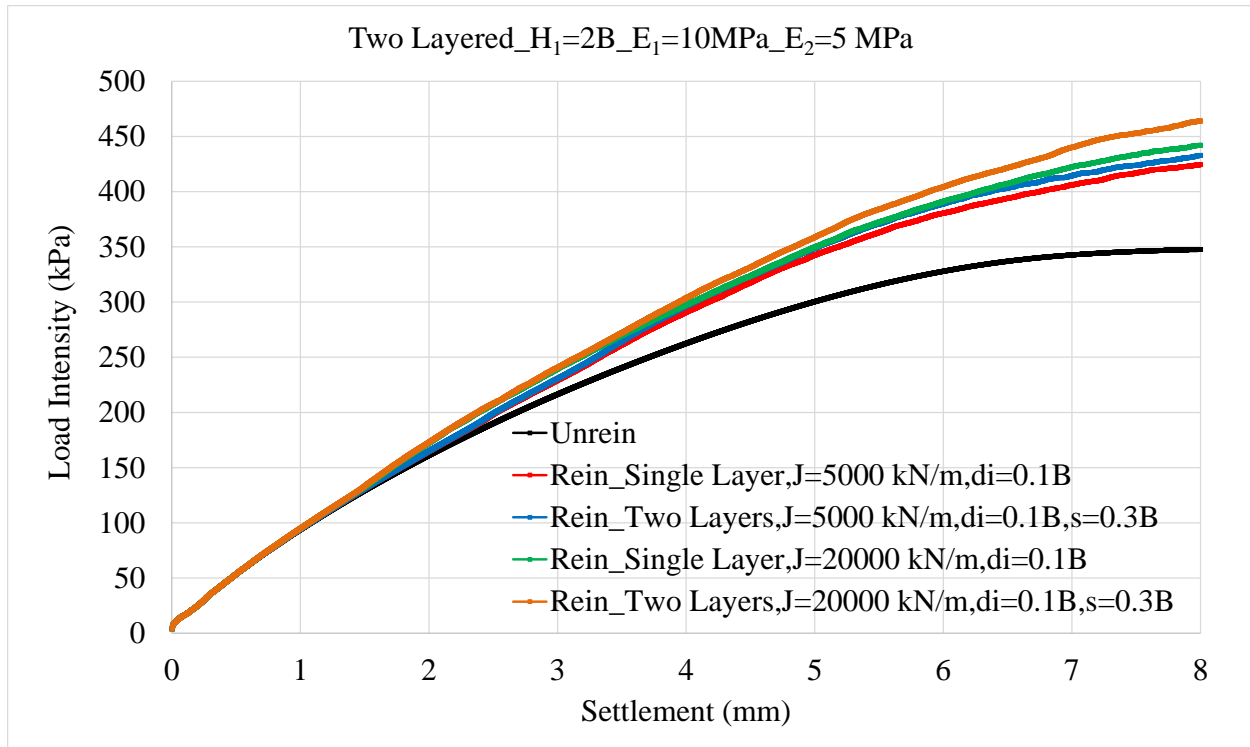


**Figure 4.21: Load-Settlement curves for studying the effect of stiffness of reinforcement in two layered soil system with two layers of reinforcement condition.**

## 4.6 Results and Discussions

### 4.6.1 Effect of stiffness of bottom layer

In this section, the effect of stiffness of bottom layer was studied by reducing it from 5MPa to 2.5 MPa. The material properties for the top layer were given same as the previous studies and reinforcement stiffness was taken as 5000 kN/m which was also concluded in previous studies. Properties for the bottom layer was varied according to two different elastic stiffness values.

Effect of variation in bottom layer stiffness was plotted in terms of load settlement profiles which is shown in Figure 4.22. Load settlement profiles were plotted for two different stiffness values of bottom layer and compared in unreinforced condition, reinforced condition with single layer and two layers of reinforcement. Plots shows that, by reducing the bottom layer stiffness to half, the load carrying capacity of footing was reduced about 8% in unreinforced condition and 10% in reinforced conditions. It concludes that there was a marginal effect of bottom layer stiffness on the load carrying capacity of footing.

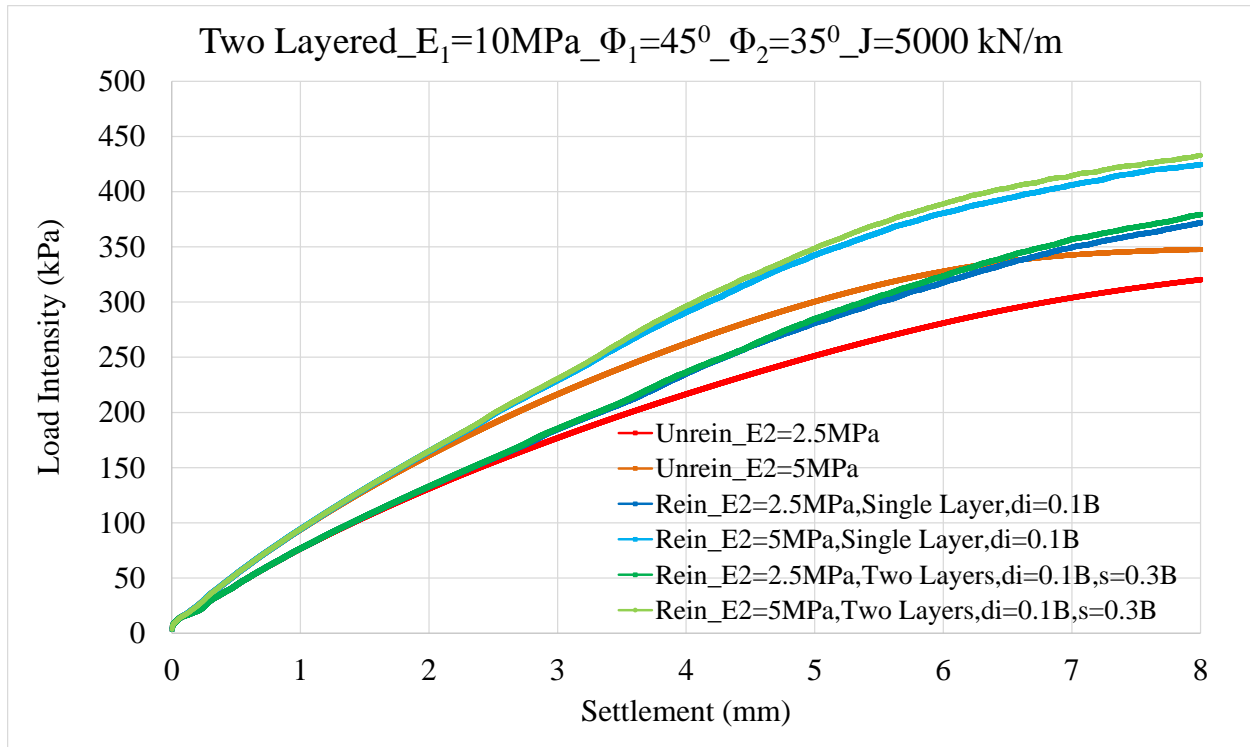


**Figure 4.22: Load-Settlement curves for studying the effect of bottom layer stiffness in two layered soil system**

#### **4.6.2 Effect of stiffness of top layer**

Similar to the previous studies, the effect of top layer was studied in this section by reducing its stiffness to half. Bottom layer properties are used as concluded from the previous study i.e.  $E_2=2.5\text{MPa}$ . Reinforcement properties are similar to the previous study. The stiffness of top layer was varied from  $E_1=10\text{MPa}$  to  $E_1=5\text{MPa}$ .

The variation in load settlement profiles were plotted for two different stiffness values of top layer. The results were compared for unreinforced and reinforced conditions. In each case, unreinforced, single layer reinforced and two layered reinforced conditions, the plots were compared for two stiffness values as shown in Figure 4.23. It can be observed that, by reducing the top layer stiffness to half, there was a considerable reduction in the load carrying capacity of the footing of about 18% and 20% in unreinforced condition and reinforced conditions respectively. It can be concluded that even by reducing the top layer stiffness to half, the reduction in load carrying capacity was considerably minimal.

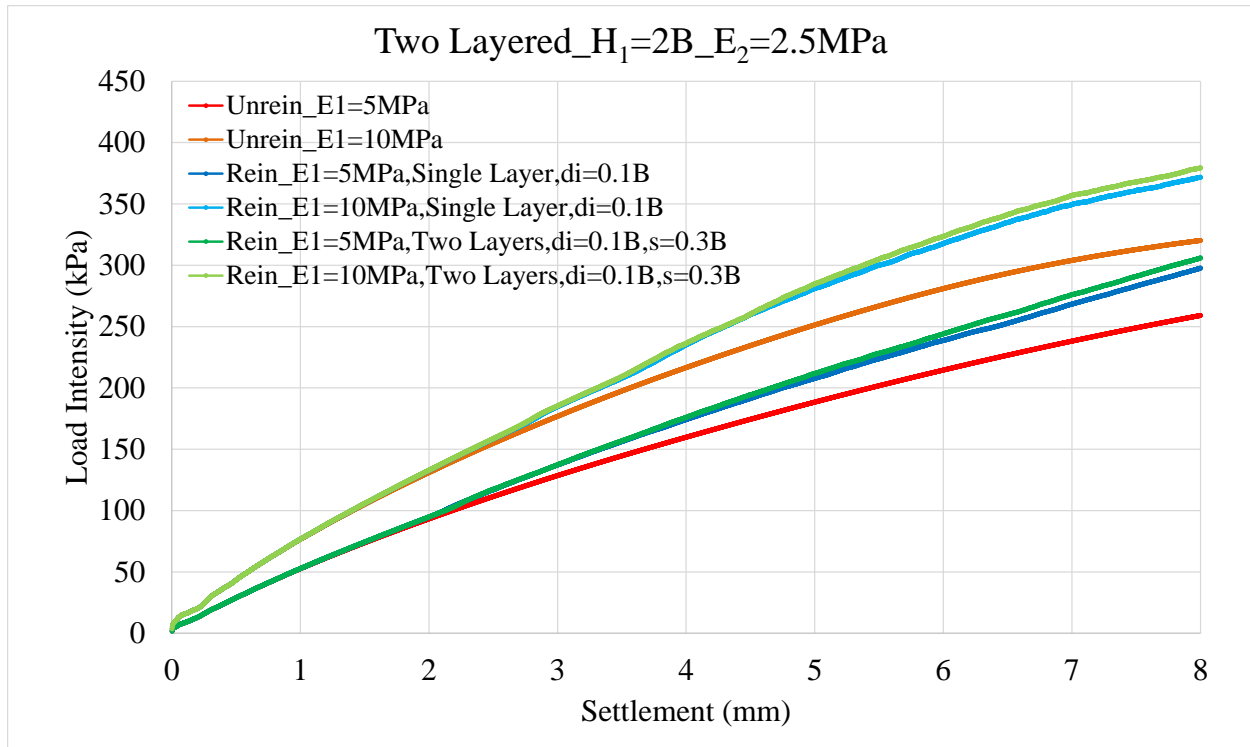


**Figure 4.23: Load-Settlement curves for studying the effect of top layer stiffness in two layered soil system**

#### **4.6.3 Effect of thickness of top layer**

This study was conducted on the variation of thickness of top layer. In the previous study, the thickness of top layer was used as 2 times the diameter of footing, but by reducing its thickness to half i.e. ( $H_1=1B$ ), the effect of top layer thickness on the load carrying capacity was studied. Figure 4.24 shows the schematic diagram of model with variation of thickness of two layers.

The load settlement curves were plotted for two case with variation of top layer thickness. Analysis has been done for different thickness of top layer in unreinforced and reinforced conditions.

Comparison plots for two thickness values are shown in Figure 4.25. The load carrying capacity has been reduced by about 27% in all the cases by reducing the top layer thickness to half. It is also observed that the case with top layer thickness as 2B is giving closure load carrying capacity compared with top layer thickness 1B with reinforcement. It can concluded that in a cost effective manner that using a case with top layer thickness equals to 1B with reinforcement gives the better load carrying capacity.

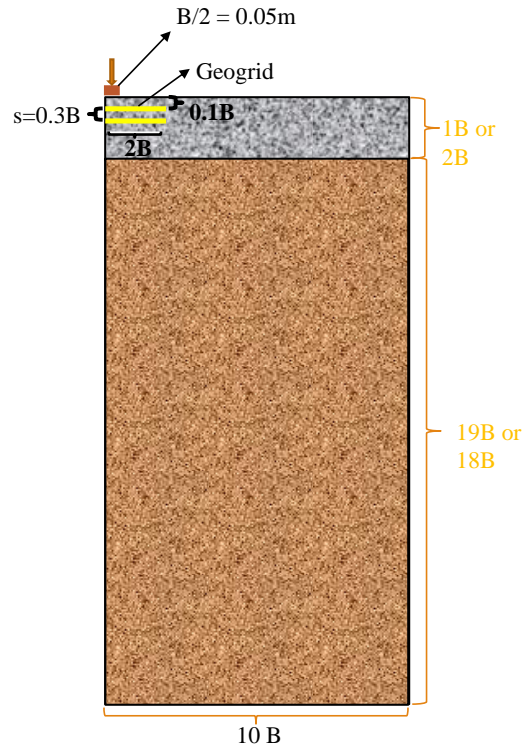


Figure 4.24: Schematic model of two layers soil system with variation of top layer thickness

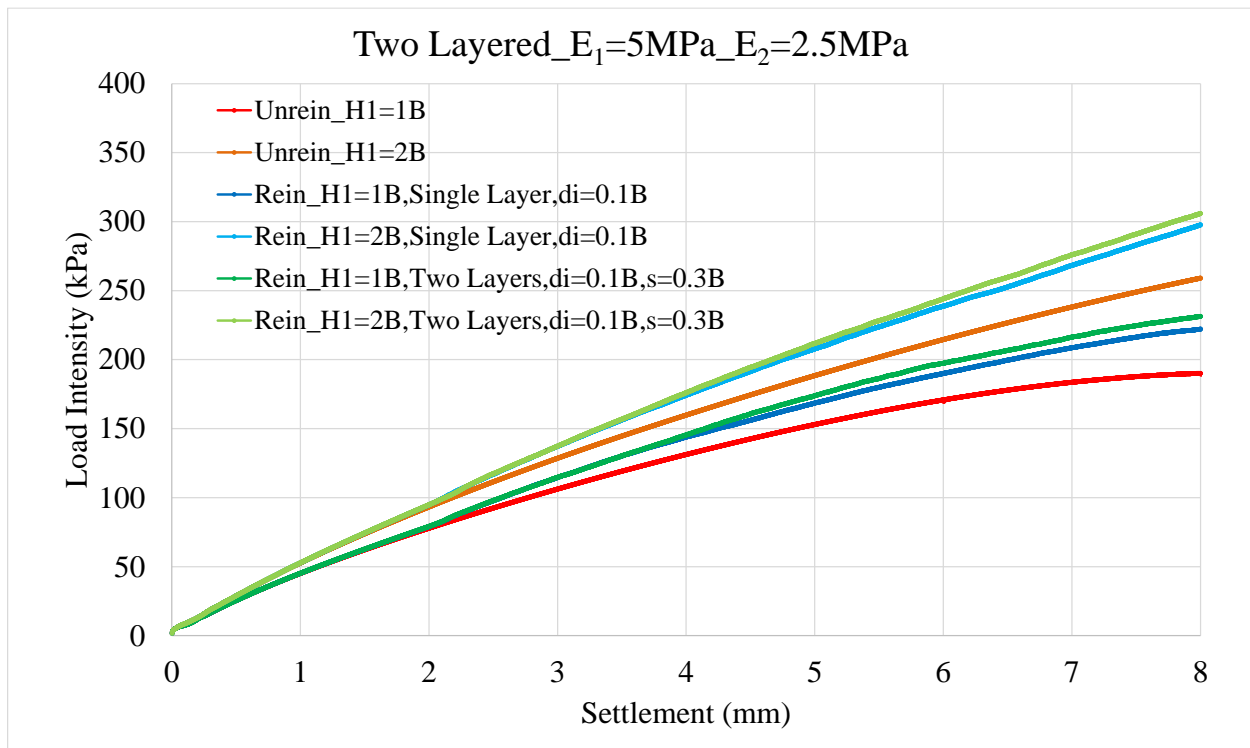


Figure 4.25: Load-Settlement curves for studying the effect of top layer thickness in two layered soil system



#### 4.6.4 Effect of angle of internal friction ( $\phi_2$ ) of bottom layer

In this study, the effect of angle of internal friction of bottom layer ( $\phi_2$ ) was discussed by using two different values as  $35^\circ$ ,  $25^\circ$ . For this study the material properties for two soils and reinforcement are similar from previous study except the variation in angle of internal friction angle for bottom layer. The dilatancy angle for the corresponding friction angle was taken as about  $2/3^{\text{rd}}$  to the friction angle.

The difference between two friction angles brought significant variation to the load settlement profiles in unreinforced and reinforced conditions. The load settlement profiles for two frictional angle are plotted for different conditions in Figure 4.26.

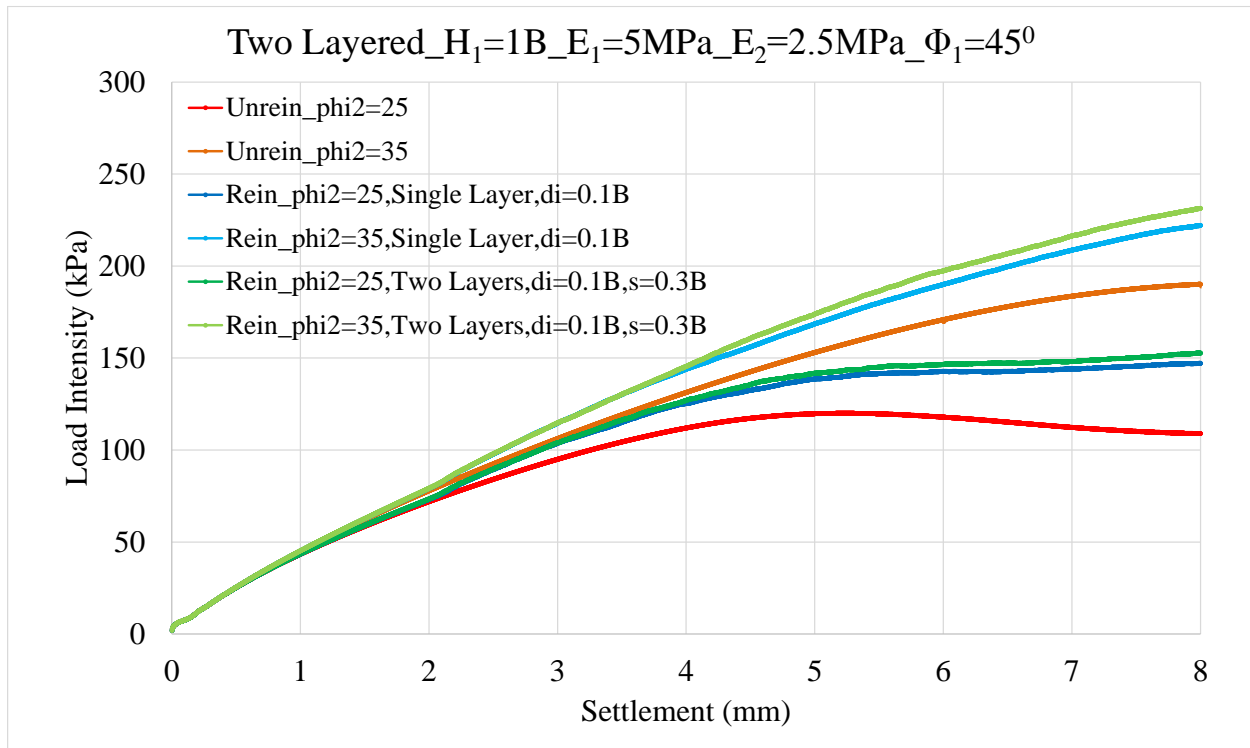


**Figure 4.26: Load-Settlement curves for studying the effect of angle of internal friction of bottom layer in two layered soil system**

The change in friction angle from  $35^\circ$  to  $25^\circ$ , reduced the load carrying capacity by about 42% and 35% in unreinforced and reinforced conditions respectively at 8 % of settlement. This shows that the angle of internal friction of bottom layer also have significant impact on the load carrying capacity of footing.

# Chapter 5

## Conclusions

Large scale experimental arrangement had been modelled in the laboratory to study the interaction between bridge abutment and proposed approach slabs with granular beds. The behavior of unreinforced and reinforced granular beds when subjected to wheel loads were studied by conducting large scale tests.

Conjectures of the experimental evaluation are summarized below:

- 1) The optimum thickness of granular bed ( $H_1$ ) was found to be 0.72 times the diameter of wheel load in the case of unreinforced soil.
- 2) The optimized length of the geogrid ( $L_g$ ) was found to be four times the diameter of wheel load at which the settlements have diminished by 35 % as compared to that of unreinforced case.
- 3) The optimum initial depth of geogrid ( $d_i$ ) from the top surface was found at 0.4 times the diameter of the wheel load with 35 % reduction in the settlement with respect to unreinforced granular bed.
- 4) The effect of edge distance ( $d_e$ ) of wheel load from the edge of an abutment had been studied. The critical distance of a wheel from the abutment was determined as 0.3 times the diameter of footing. From the results, it is clear that there is a significant decrement of settlements for reinforced granular beds with wheel load moving away from the abutment.
- 5) Reinforcing granular beds with anchors and nails was recommended as a special condition in reducing the settlements below wheel load.

Based on the numerical studies, the following conclusions can be made regarding the behavior of circular footings resting on semi-infinite homogeneous soil system and two layered soil system with multi layered reinforcement.

- 1) When the ratio of elastic modulus of two layers of soil i.e.  $E_1/E_2=10$  then the load carrying capacity of the footing increased by about four times in unreinforced condition.
- 2) The effect of reinforcement was found to be substantial in homogeneous case, as improvement in load carrying capacity was about 40%. Whereas, the improvement was limited to merely 10% in the case of two layered soil systems.
- 3) Increase in number of the reinforcement layers had shown a marginal effect in improving the load carrying capacity.
- 4) Effective initial depth of reinforcement below the footing and effective spacing between reinforcement layers were found to be at 0.1 times and 0.3 times to the diameter of footing respectively.
- 5) The ratio of the deformation modulus of the top layer to that of the bottom layer was found to be as a most influencing fraction in governing the load carrying capacity with  $E_1/E_2 = 2$ .
- 6) The internal friction angle of bottom layer also has a significant effect on the load carrying capacity of footing.

# References

- [1] M. R. Abdi, and M. A. Arjomand. Pullout tests conducted on clay reinforced with Geogrid encapsulated in thin layers of Sand. *Geotextiles and Geomembranes*, 29, (2011) 588-595.
- [2] M. T. Adams, and J. G. Collin. Large Model Spread Footing Load Tests on Geosynthetic Reinforced Soil Foundations. *J. Geotechnical and Geoenvironmental Engineering*, 123(1), (1997) 66-72.
- [3] R. E. Abendroth, L. F. Greimann, and M. D. LaViolette. An Integral Abutment Bridge with Precast Concrete Piles. IOWA Department of Transportation, Center for Transportation Research and Education Report, Ames, Iowa. Final Rep., IHRB Project TR-438, 2007.
- [4] N. Abu-Hejleh, D. Hanneman, D. J. White, and I. Ksouri. Flowfill and MSE Bridge Approaches: Performance, Cost and Recommendations for Improvements. Colorado Department of Transportation, Colorado, Report No. CDOTDTD-R-2006-2, 2006.
- [5] N. Abu-Hejleh, T. Wang, and J. G. Zornberg. Performance of Geosynthetic-Reinforced Walls Supporting Bridge and Approaching Roadway Structures. ASCE Geotechnical Special Publication No. 103, *Advances in Transportation and Geoenvironmental Systems Using Geosynthetics*, (2000) 218–243.
- [6] N. Abu-Hejleh, J. G. Zornberg, T. Wang, and J. Watcharamonthein. Design Assessment of Founders-Meadows GRS Abutment Structure. Proc., 82nd Annual TRB Meeting, 2003.
- [7] Anand J. Puppala, Ekarut Archeewa, Sireesh Saride, Soheil Nazarian and Laureano Hoyos. Recommendations for Design, Construction, and Maintenance of Bridge Approach Slabs. The University of Texas at Arlington, Arlington, Texas, Technical report, FHWA/TX-11/0-6022-2, 2012.
- [8] A. K. M. Anwarul Islam. On Reducing Bumps at Pavement-Bridge Interface. YSU Center for Transportation and Materials Engineering (CTME), Youngstown State University, Youngstown, 2010.
- [9] M. Bakeer, M. Shutt, J. Zhong, S. Das, and M. Morvant. Performance of Pile-Supported Bridge Approach Slabs. *J. Bridge Engineering*, ASCE, 10(2), (2005) 228-237.
- [10] R. D. Barksdale, and R. C. Bachus. Design and Construction of Stone Columns. Rep. No. FHWA/RD-83/026, Federal Highway Administration, Washington D.C, 1983.
- [11] R. F. Barron, J. Wright, C. Kramer, W. H. Andrew, H. Fung, and C. Liu. Cement Deep Soil Mixing Remediation of Sunset North Basin Dam. *Dam Safety 2006*, Association of Dam Safety Officials, 2006.

- [12] P. K. Basudhar, S. S. Saha, and K. Deb. Circular Footing Resting on Geotextile-Reinforced Sand Bed. *Geotextiles and Geomembranes*, 25(6), (2007) 377-384.
- [13] D. T. Bergado, T. R. Anderson, N. Miura, and A. S. Balasubramaniam. *Soft Ground Improvement in lowland and other environments*. ASCE, New York, 1996.
- [14] J. Binquet, and K. Lee. Bearing Capacity Tests on Reinforced Earth Slabs. *J. Geotechnical Engineering Division*, 101(12), (1975a) 1241-1255.
- [15] J. Binquet, and K. Lee. Bearing Capacity Analysis of Reinforced Earth Slabs. *J. Geotechnical Engineering Division*, 101(12), (1975b) 1257-1276.
- [16] A. H. Boushehrian, N. Hataf, and A. Ghahramani. Modeling of the Cyclic Behaviour of Shallow Foundations resting on Geomesh and Grid-Anchor Reinforced Sand. *Geotextiles and Geomembranes*, 29, (2011) 242-248.
- [17] M. Bozozuk. Bridge Foundations Move. *Transportation Research Record 678: Tolerable Movements of Bridge Foundations, Sand Drains, K-Test, Slopes, and Culverts*, Transportation Research Board, National Research Council, Washington D.C., (1978) 17–21.
- [18] J. L. Briaud. *Introduction to Soil Moduli*. Geotechnical News, BiTech Publishers Ltd, Richmond, B.C., Canada, 2001.
- [19] J. L. Briaud, R. W. James, and S. B. Hoffman. Settlement of Bridge approaches (the Bump at the end of bridge). *Transportation research Board, National Research council, Washington D.C., NCHRP Synthesis 234: 1997*.
- [20] S. F. Brown, J. Kwan, and N. H. Thom. Identifying the Key Parameters that influence Geogrid Reinforcement of Railway Ballast. *Geotextiles and Geomembranes*, 25(6), (2007) 326-335.
- [21] G. Burke. Current Methods of Sampling and Testing of Soil Cement and Their Limitations. *Proceedings of International Workshop on Deep Mixing Technology 2, National Deep Mixing Program, Oakland, 2001*.
- [22] W. Chung, and G. Cascante. Experimental and Numerical Study on Soil-Reinforcement Effects on the Low-Strain Stiffness and Bearing Capacity of Shallow Foundations. *Geotechnical and Geological Engineering*, 25, (2007) 265-281.
- [23] C. S. Cai, X. M. Shi, G. Z. Voyiadjis, and Z. J. Zhang. Structural Performance of Bridge Approach Slabs under Given Embankment Settlement. *J. Geotechnical and Geoenvironmental Engineering*, 10(4), (2005) 482-489.
- [24] M. R. Cooper, and A. N. Rose. Stone column support for an embankment on deep alluvial soils. *Proc of the Institution of Civil Engineers, Geotechnical Engineering*, 137(1), (1999) 15-25.

- [25] S. C. Das, R. Baker, J. Zhong, and M. Schutt. Assessment of mitigation embankment settlement with pile supported approach slabs. Louisiana Transportation and Research Center, Baton Rouge, 1990.
- [26] K. Deb, N. Sivakugan, S. Chandra, and P. K. Basudhar. Numerical Analysis of Multi-Layer Geosynthetic-Reinforced Granular Bed over Soft Fill. *Geotechnical and Geological Engineering*, 25, (2007) 639-646.
- [27] M. Duncan, and Chin-Yong Chang. Nonlinear analysis of stress and strain in soils. *Soil Mechanics and Foundation Division, Proceedings of ASCE*, (1970) 1629-1653.
- [28] B. Dupont, and D. Allen. Movements and Settlements of Highway Bridge Approaches. Rep. No. KTC-02-18/SPR-220-00-1F, Kentucky Transportation Center Report, Lexington, 2002.
- [29] T. V. Edgar, J. A. Puckett, and R. B. D'Spain. Effect of Geotextile on Lateral Pressure and Deformation in Highway Embankments. *Geotextiles and Geomembranes*, 8(4), (1989) 275-306.
- [30] C. Ghosh, and M. R. Madhav. Reinforced Granular Fill-Soft Soil System: Membrane Effect. *Geotextiles and Geomembranes*, 13, (1994a) 743-759.
- [31] C. Ghosh, and M. R. Madhav. Reinforced Granular Fill-Soft Soil System: Confinement Effect. *Geotextiles and Geomembranes*, 13, (1994b) 727-741.
- [32] B. O. Hardin, and V. P. Drnevich. Shear modulus and damping in soils: Design equations and curves. *Proc. ASCE: J. Soil Mechanics and Foundations Division*, 98(SM7), (1972) 667-692.
- [33] M. R. Hausmann. *Engineering Principles of Ground Modification*. McGraw-Hill Publishing Company, New York, 1990.
- [34] T. C. Hopkins. Settlement of Highway Bridge Approaches and Embankment Foundations. Rep. No. KYHPR-64-1 7; HPR-1 (4), Kentucky Transportation Center, Lexington, Kentucky, 1969.
- [35] T. C. Hopkins. Settlement of Highway Bridge Approaches and Embankment Foundations. Rep. No. KYHPR-64-1 7; HPR-1 (8), Kentucky Transportation Center, Lexington, Kentucky, 1973.
- [36] E. J. Hoppe, and J. P. Gomez. Field study of an integral backwall bridge. Rep. No. VTRC 97-R7, Virginia Transportation Research Council, Charlottesville, VA, 1996.
- [37] J. S. Horvath. Integral-Abutment Bridges: Geotechnical Problems and Solutions Using Geosynthetics and Ground Improvement. *IAJB 2005 - The 2005 FHWA Conference on Integral Abutment and joint less Bridges*, Baltimore, Maryland, USA, 2005.
- [38] J. Hsi, and J. Martin. Soft Ground Treatment and Performance, Yelgun to Chinderah Freeway, New South Wales, Australia. In *Ground Improvement-Case Histories*, Elsevier Geo-Engineering Book Series 3, 563-599, 2005.
- [39] J. P. His. Managing Difficult Ground-Case Studies. *Proceedings of First Sri Lankan Geotechnical Society International Conference on soil and Rock Engineering*, Colombo, 2007.

- [40] R. W. James, H. Zhang, and D. G. Zollinger. Observations of severe abutment backwall damage. Transportation Research Record 1319, Transportation Research Board, (1991) 55-61.
- [41] P. Jayawickrama, P. Nash, M. Leaverton, and D. Mishra. Water Intrusion in Base/Subgrade Materials at Bridge Ends. TxDOT Report, FHWA/TX-06/0-5096-1, Texas Tech University, Lubbock, Texas, 2005.
- [42] R. M. Koerner. Designing with Geosynthetics. 5th Ed., Prentice Hall, 2006.
- [43] R. L. Kondner, and J. S. Zelasko. A Hyperbolic Stress-Strain Formulation for Sands. Proceedings, 2nd Pan-American Conference on Soil Mechanics and Foundation Engineering. Brazil, (1963) 289-324.
- [44] S. L. Kramer, and P. Sajer. Bridge Approach Slab Effectiveness. Report No. WA-RD 227.1, Washington State Department of Transportation, Olympia, Washington, 1991.
- [45] A. Kumar, and B. S. Walia. Bearing Capacity of Square Footings on Reinforced Layered Soil. Geotechnical and Geological Engineering, 24, (2006) 1001-1008.
- [46] A. Kumar, and S. Saran. Closely Spaced Footings on Geogrid-Reinforced Sand. J. Geotechnical and Geoenvironmental Engineering, 129(7), (2003) 660-664.
- [47] A. Kumar, and S. Saran. Closely Spaced Rectangular Footings on Reinforced Sand. Geotechnical and Geological Engineering, 22, (2004) 497-524.
- [48] J. G. Laguros, M. M. Zaman, and I. U. Mahmood. Evaluation of Causes of Excessive Settlements of Pavements Behind Bridge Abutments and their Remedies; Phase II. (Executive Summary). Rep. No. FHWA/OK 89 (07), Oklahoma Department of Transportation, 1990.
- [49] L. R. Lenke. Settlement Issues-Bridge Approach Slabs. Rep. No. NM04MNT-02, New Mexico Department of Transportation, 2006.
- [50] Q. L. Lin, and I. H. Wong. Use of Deep Cement Mixing to Reduce Settlements at Bridge Approaches. J. Geotechnical and Geoenvironmental Engineering, ASCE, 125(4), (1999) 309.
- [51] M. R. Madhav, and P. P. Vitkar. Strip footing on a weak clay stabilized with a granular column or a pile. Canadian Geotechnical Journal, 15, (1978) 605-609.
- [52] M. R. Madhav, and F. B. Poorooshasb. A New Model for Geosynthetic Reinforced Soil. Computers and Geotechnics, 6, (1988) 277-290.
- [53] M. R. Madhav, and F. B. Poorooshasb. A Modified Pasternak Model for Reinforced Soil. Mathematical Computing and Modeling, 6, (1989) 277-290.
- [54] G. Madhavi Latha, Amit Somwanshi. Bearing capacity of square footings on geosynthetic reinforced sand. Geotextiles and Geomembranes, 27(4), (2009) 281-294.
- [55] J. K. Michell, and T. R. Huber. Performance of a Stone Column Foundation. J. Geotechnical Engineering, ASCE, 111(2), (1985) 205-223.

- [56] G. J. Monley, and J. T. Wu. Tensile Reinforced Effects on Bridge Approach Settlement. *J. Geotechnical Engineering*, 119(4), (1993) 749-763.
- [57] M. Mosallanezhad, N. Hataf, and A. Ghahramani. Experimental Study of Bearing Capacity of Granular Soils, Reinforced with Innovative Grid-Anchor System. *Geotechnical and Geological Engineering*, 26, (2008) 299-312.
- [58] H. Nassif. Finite Element Modeling of Bridge Approach and Transition Slabs. Rep. No. FHWA-NJ-2002-007, Department of Civil and Environmental Engineering, Center for Advanced Infrastructure & Transportation (CAIT), Rutgers, New Jersey, 2002.
- [59] D. P. Nicholson, and R. J. Jardine. Performance of vertical drains at Queenborough bypass. *Geotechnique*, 31(1), (1982) 67-90.
- [60] M. Oda, I. Koishikawa, and T. Higuchi. Experimental study of anisotropic shear strength of sand by plane strain tests. *Soils and Foundations*, 18(1), (1978) 25-38.
- [61] M. I. M. Pinto. Application of Geosynthetics for Soil reinforcement. *Proceedings of the ICE-Ground Improvement*, 7(2), (2003) 61-72.
- [62] A. Porbaha. State of the Art in Deep Mixing Technology, Part I: Basic Concepts and Overview of Technology. *Ground Improvement*, 2(2), (1998) 81-92.
- [63] A. J. Puppala, S. Saride, A. Ekarat, L. R. Hoyos, and S. Nazarian. Recommendations for Design, Construction, and Maintenance of Bridge approach Settlements. FHWA/Tx-09/6022-1, Technical Report, Texas Department of transportation, 185, 2009.
- [64] B. R. Phanikumar, Ram Prasad, and A. Singh. Compressive load response of geogrid-reinforced fine, medium and coarse sands. *Geotextiles and Geomembranes*, 27(3), (2008) 183-186.
- [65] S. W. Perkins, and E. R. Cortez. Evaluation of Base-Reinforced Pavements using a Heavy Vehicle Simulator. *Geosynthetic International*, 12(2), (2005) 86-98.
- [66] H. B. Raghavendra. Effect of Properties and Length of Reinforcement on Load Carrying Capacity of Reinforced Soil Beds. *Ground Improvement*, 8(3), (2004) 121-126.
- [67] H. Rathmayer. Deep Mixing Methods for Soft Subsoil Improvement in the Nordic Countries. *Proceedings of IS-Tokyo'96, The 2nd International Conference on Ground Improvement Geosystems*, Tokyo, (1996) 869-878.
- [68] J. Seo. The Bump at the End of the Bridge: An Investigation. Thesis (PhD), Texas, A&M University, College Station, Texas, 2003.
- [69] C. J. Serridge, and O. Synac. Ground Improvement Solutions for Motorway Widening Schemes and New Highway Embankment Construction over Soft Ground. *Ground Improvement Journal*, 11(4), (2007) 219-228.



- [70] S. K. Shukla. Application of Geosynthetics for Soil reinforcement. *Ground Improvement*, 8(4), (2003) 179-182.
- [71] S. Sireesh, T. G. Sitharam, and Sujit Kumar Dash. Model studies of embedded circular footing on geogrid-reinforced sand beds. *Geotextiles and Geomembranes*, 27(2), (2004) 89-98.
- [72] T. G. Sitharam, and S. Sireesh. Model Studies of Embedded Circular Footing on Geogrid-Reinforced Sand Beds. *Ground Improvement*, 8(2), (2004) 69-75.
- [73] T. D. Stark, S. M. Olson, and J. H. Long. Differential Movement at the Embankment/Structure Interface Mitigation and Rehabilitation. Rep. No. IABH1, FY 93, Illinois Department of Transportation, Springfield, Illinois, 1995.
- [74] H. E. Wahls. NCHRP Synthesis of Highway Practice No. 159: Design and Construction of Bridge Approaches. Transportation Research Board, National Research Council, Washington D.C., 1990.
- [75] J. L. Walkinshaw. Survey of Bridge Movements in the Western United States. Transportation Research Record 678: Tolerable Movements of Bridge Foundations, Sand Drains, K-Test, Slopes, and Culverts, Transportation Research Board, National Research Council, Washington, D.C., (1978) 6-12.
- [76] D. White, S. Sritharan, M. Suleiman, M. Mohamed, and C. Sudhar. Identification of the Best Practices for Design, Construction, and Repair of Bridge Approaches. CTRE. Project 02-118, Iowa State University, Ames, Iowa, 2005.
- [77] A. M. Wolde-Tinsae, S. M. Aggour, and S. A. Chini. Structural and Soil Provisions for Approaches to Bridges. Interim Report AW087-321-046, Maryland Department of Transportation, 1987.
- [78] M. S. Won, and Y.S. Kim. Internal Deformation Behaviour of Geosynthetic-reinforced Soil Walls. *Geotextiles and Geomembranes*, 25(1), (2007) 10-22.
- [79] H. K. W. Wong, and J. C. Small. Effect of Orientation of Bridge Slabs on Pavement Deformation. *J. Transportation Engineering*, 120(4), (1994) 590-602.
- [80] J. T. H. Wu, K. Z. Z. Lee, and K. Ketchart. A Review of Case Histories on GRS Bridge-Supporting Structures with Flexible Facing. Proc. 82nd Annual TRB Meeting, 2003.
- [81] J. T. H. Wu, K. Z. Z. Lee, B. S. Helwany, and K. Ketchart. Design and Construction Guidelines for Geosynthetic-Reinforced Soil Bridge Abutments with a Flexible Facing. Proc. NCHRP Report 556. Transportation Research Board, Washington D.C., 2006.
- [82] R. DeBorst, P. A. Vermeer. Possibilities and limitations of finite elements for limit analysis. *Geotechnique*, 34 (2), (1984) 199-210.
- [83] S. Frydman, H. J. Burd. Numerical studies of bearing capacity factor  $N_\gamma$ . *J. Geotechnical and Geoenvironmental Engineering*, ASCE, 123 (1), (1997) 20-29.

- [84] J. H. Yin, Y. J. Wang, A. P. S. Selvadurai. Influence of nonassociativity on the bearing capacity of strip footing. *J. Geotechnical and Geoenvironmental Engineering, ASCE*, 127 (11), (2001) 985-989.
- [85] H. L. Erickson, A. Drescher. Bearing capacity of circular footings. *J. Geotechnical and Geoenvironmental Engineering, ASCE*, 128 (1), (2002) 38-43.
- [86] J. Marti, P. Cundall. Mixed discretization procedure for accurate modelling of plastic collapse. *International Journal for Numerical and Analytical methods in Geomechanics*, 6, (1982) 129-139.